24

HAMBURGER WASSERBAU-SCHRIFTEN

Herausgegeben von Prof. Dr.-Ing. Peter Fröhle

2020

Frederik M. Treuel

Dynamic Draft of Extraordinary Large Vessels on the Lower Elbe Waterway

WASSERBAU
River and Coastal Engineering

Dynamic Draft of Extraordinary Large Vessels on the Lower Elbe Waterway

von

Frederik M. Treuel

Institut für Wasserbau, Technische Universität Hamburg

Hamburger Wasserbau-Schriften, Band 24

Herausgegeben von Prof. Dr.-Ing. Peter Fröhle

Bibliografische Information der Deutschen Nationalbibliothek

Die Deutsche Nationalbibliothek verzeichnet diese Publikation in der Deutschen Nationalbibliothek; detaillierte Daten sind im Internet über http://www.dnb.de abrufbar.

Impressum

Institut für Wasserbau
Denickestrasse 22
21073 Hamburg
Tel.: +49 40 42878-3761
Fax: +49 40 4273-10199
E-Mail: wasserbau.office@tuhh.de

1. Auflage, Dezember 2020

DOI: https://doi.org/10.15480/882.3080

Dynamic Draft of Extraordinary Large Vessels on the Lower Elbe Waterway

Vom Promotionsausschuss

der Technischen Universität Hamburg

zur Erlangung des akademischen Grades

Doktor-Ingenieur (Dr.-Ing.)

genehmigte Dissertation

von

Frederik M. Treuel

aus

Cuxhaven

2020

Aufzählung der Gutachter:

1. Gutachter: Prof. Dr.-Ing. Peter Fröhle
2. Gutachter: Prof. Dr.-Ing. Carlos Jahn

Tag der mündlichen Prüfung: 09. Januar 2020

Vorwort

Der Hafen war und ist Hamburgs Tor zur Welt. Ein nicht unerheblicher Anteil der Wirtschaftskraft der Metropolregion Hamburg hängt direkt oder indirekt vom Hamburger Hafen ab. Entsprechend wichtig ist eine leistungsfähige und möglichst uneingeschränkt nutzbare Hafeninfrastruktur. Ein wesentliches Element für die dauerhafte Nutzung der Hafeninfrastruktur ist die Hafenzufahrt, über die die Schiffe mit den Waren in den Hamburger Hafen gelangen. Weltweit spielt in den letzten Jahrzehnten die Containerisierung des Seeverkehrs eine besondere Rolle. Bedingt durch den anhaltenden Containerboom wurden die Abmessungen von Containerschiffen immer größer und nahmen insbesondere in den letzten beiden Dekaden zunehmend beschleunigt zu. Aktuelle Containerschiffe haben Kapazitäten von 20.000 TEU und mehr und zudem neue Schiffshüllenformen. Containerschiffe mit einer Länge von 400m und einer Breite von 60m sowie einem Tiefgang größer als 16m mehr sind keine Seltenheit mehr.

Die Elbe verbindet den Hamburger Hafen mit der Nordsee und damit mit den Weltmeeren und dient seit Jahrhunderten als Zufahrt zum Hamburger Hafen. Von der Ansteuerung in der Nordsee beträgt die Revierfahrt auf Nordsee und Elbe rd. 150 km und ist somit im internationalen Vergleich sehr lang. Zudem sind sowohl die Breite als auch die Tiefe der Fahrrinne begrenzt und beide Größen wurden in der Historie mehrfach angepasst, d.h. die Fahrrinne der Elbe wurde mehrfach vertieft und verbreitert. Dennoch können bereits seit Jahren Containerschiffe der jeweils aktuellen Generation die Elbe nicht mehr ohne Einschränkungen befahren.

Länge, Breite, Tiefgang und Schiffshüllenform haben einen signifikanten Einfluss auf das dynamische Bewegungsverhalten der Containerschiffe insbesondere in begrenztem Fahrwasser, welches in Hafenzufahrten im Allgemeinen gegeben ist. Aus dem dynamischen Bewegungsverhalten der Schiffe resultiert eine gegenüber der Einsinktiefe in Ruhe nicht unerheblich vergrößerte Schiffseintauchung, die die nutzbare Tiefe einer Hafenzufahrt vermindert. Daher ist es wichtig, dieses dynamische Bewegungsverhalten zu kennen und mit mathematischen Ansätzen beschreiben zu können. Bekannte modellbasierte Untersuchungen zum dynamischen Bewegungsverhalten sind auf Schiffsgrößen bis zu 12.000 TEU begrenzt. Messungen in der Natur an realen Schiffen auf realem tiefen- und breitenbegrenztem Fahrwasser umfassten bisher lediglich Schiffe mit einer Kapazität von rund 7.500 TEU.

Hier setzt die Arbeit von Herrn Treuel an. Er hat sich das Ziel gesetzt, mit seiner Arbeit dazu beizutragen, das grundlegende Verständnis des dynamischen Bewegungsverhaltens von Schiffen mit zumindest aus heutiger Sicht außergewöhnlich großen Abmessungen zu verbessern. Er behandelt dieses Thema exemplarisch auf der Grundlage von hochkomplexen Messungen an Schiffen, die auf der Elbe zwischen dem Hamburger Hafen und dem freien Fahrwasser der Nordsee durchgeführt wurden. Parallel wurden jeweils die hydrodynamischen Bedingungen in der Elbe und die wesentlichen physikalischen Parameter des Wassers aufgenommen. Diese Messungen wurden im Zuge des Vorhabens „Elbe-Squat“ durchgeführt, welches am Institut für Wasserbau in Kooperation mit einem Ingenieurbüro im Auftrag der Wasser- und Schifffahrtsverwaltung des Bundes durchgeführt wurde. Im Institut für Wasserbau hat Herr Dr. Treuel dieses Vorhaben federführend koordiniert und bearbeitet.

Der betragsmäßig größte Anteil am dynamischen Bewegungsverhalten bei Fahrt in begrenztem resultiert hierbei aus dem Squat, einer Größe, die das zusätzliche Einsinken eines Schiffes als Folge der bei Fahrt im begrenzten Fahrwasser besonders ausgeprägten Umströmung des Schiffskörpers beschreibt.

Im Ergebnis hat Herr Treuel eine sehr komprimierte Arbeit zur Beschreibung des Bewegungsverhalten von großen Schiffen auf begrenztem Fahrwasser vorgelegt, die die wesentlichen Einflüsse der aus den Umgebungsbedingungen und den Bedingungen der Schiffsbewegung auf die Schiffsdynamik mit Schwerpunkt auf Rollen, dynamische Tiefgangsänderungen und Squat umfasst und zudem erstmals Analysen zu Schiff-Schiff-Interaktionen enthält. Zudem wurden die Einflüsse von Hogging (Wölbung des Schiffs unter Auftrieb), Schiffstrimmung und Schiffsrollen auf den dynamischen Tiefgang analysiert und hierzu Modellansätze abgeleitet.

Ein weiteres und sehr wichtiges Ergebnis der Arbeit ist die im Rahmen des Vorhabens „Elbe-Squat“ aus den begleiteten Schiffspassagen akribisch erstellte und dokumentierte Datenbasis zum Bewegungsverhalten von großen Schiffen auf dem begrenzten Fahrwasser der Elbe. Dieser Datensatz stellt eine sehr gute und sehr gut dokumentierte Grundlage für weiterführende Untersuchungen dar.

Die Ergebnisse der Untersuchungen und der Arbeit sind zudem von großem praktischem Wert für zukünftige Planungen der Verkehre mit großen Schiffen auf tiefen- und breitenbegrenzten Fahrwassern. Herr Treuel hat im Ergebnis seiner Untersuchungen 10 praxisrelevante Empfehlungen abgeleitet, die er prägnant zusammenfasst.

Es freut mich persönlich sehr, dass Herr Dr. Treuel sein Dissertationsvorhaben auch nach seinem Weggang von der TU weiterbetrieben und abgeschlossen hat. Die vorliegende Arbeit liefert die Grundlage für eine verbesserte Vorhersage und Bewertung möglicher Abladetiefen von Schiffen auf der Elbe und wir sicher in der Praxis Beachtung und Anwendung finden.

Peter Fröhle

Leiter des Instituts für Wasserbau

Abstract

Vessel towards and from the Port of Hamburg travel in confined waters along their passage on the Lower Elbe sea-waterway. Such vessels experience dynamic draft increase due to water-related factors like density as well as channel- and ship-related factors like squat, trim and heel. In the area of conflict between economic value of maximum loading conditions and administrative draft regulations due to ship safety, the optimal determination of dynamic draft is of major interest. Much research interest has focused on pragmatic determination approaches over the last decades, but the progressive ship size development has outrun the latest results already.

Administrative draft regulations for the Lower Elbe passage apply PIANC (2014) for dynamic draft determination with an adjusted version of ICORELS squat determination. However, that approach is generally accepted, latest validations with specific data from field-investigations have been performed in 2003. Investigated ships, that travelled the Lower Elbe frequently by that time had capacities only around 5500 and 7500 TEU (MAUSHAKE & JOSWIG, 2004).

Recent ship size developments towards frequently travelling vessel units with capacities up to 20000 TEU stress out the gap between existing design approaches and present ship sizes. In case of the Lower Elbe sea-waterway, that leads to the necessity to investigate the dynamic draft behaviour of nowadays travelling vessel sizes directly in the field.

Aiming for a deeper understanding of draft influencing dynamics, this dissertation acquires, analyses and assesses the dynamic draft behaviour of extraordinary large vessels on the Lower Elbe waterway fundamentally. Furthermore, special focus is given on influences, which formerly have been of marginal interest, but now become of significance due to the actual ship sizes, e.g. impacts on draft due to ship-ship interaction.

With the central method of field-investigations, carried out between 2013 and 2016 on the Lower Elbe sea-waterway, this dissertation examines the generally accepted dynamic draft determination approaches. It determines necessary parameters and presents the measurement set up to acquire such parameters. After post-processing the gathered data, the dissertation analyses the measurement results and assesses the present draft determination process. Focal points are the assessment of applicability of different ship-squat determination approaches for present vessel sizes as well as the identification of unutilized safety margins within the draft determination process.

The results from field measurements confirm, that formerly existing safety margins within squat determinations decrease with increasing ship sizes. At ship sizes over 19000 TEU, that development even becomes critical concerning ship safety by channel design. Unutilized safety margins are discovered for present ship sizes at specific loading conditions, especially within the draft increasing impact of dynamic roll as well as in the combined influence of static trim and hogging.

Ship-ship interactions during the passage become of significant impact onto dynamic draft determinations with increasing ship dimensions. This dissertation extracts such interactions from the database, correlates influencing factors and provides recommendations to deal with ship-ship interactions within the dynamic draft determination process. Additionally, it provides recommendations aiming to prevent critical impact combinations.

Finally, special recommendations for the dynamic draft determination of extraordinary large vessels on the Lower Elbe waterway are given and further research needed towards a draft optimizing procedure is presented.

Zusammenfassung

Als deutsche Seeschifffahrtsstraße hat die Unter- und Außenelbe signifikante ökonomische Bedeutung. Die limitierten Gewässerabmessungen erfordern die Regulierung des dynamischen Tiefgangs von außergewöhnlich großen Fahrzeugen. Auf der Passage zwischen der deutschen Bucht und dem Hamburger Hafen erfahren die Schiffe die tiefgangsvergrößernden Auswirkungen des beschränkten Fahrwassers, welche sich in einer Veränderung des dynamischen Tiefgangs durch Einflüsse aus Wasserdichte, Squat sowie Trimm- und Rollbewegungen ergeben.

Die Berechnung des dynamischen Tiefgangs und folglich der zu unterhaltenden Wassertiefe erfolgt anhand der international anerkannten Richtlinien der Seeschifffahrtskommission (PIANC, 2014). Die pragmatischen Ansätze basieren nahezu vollständig auf qualitativen Erkenntnissen aus theoretischen Modellen. Quantitative empirische Erkenntnisse basieren ausschließlich auf modellbasierten Schlepptankversuchen, bei denen die Schiffsmodelle jedoch nur maximale Äquivalente zu Schiffskapazitäten um 12000 TEU im Prototyp abbilden. Validierende Messungen in der Natur liegen nicht vor oder sind, wie im Falle der Unterelbe, bereits aus dem Jahr 2003 und beschränken sich auf nicht mehr maßgebende Schiffe mit Kapazitäten von 7500 TEU. (MAUSHAKE & JOSWIG, 2004).

Mit der beschleunigten Größenentwicklung zu regelmäßig verkehrenden Schiffskapazitäten von bis zu 20000 TEU und vollkommen neuen Schiffshüllenformen, ergibt sich für die Unter- und Außenelbe die Notwendigkeit, das dynamische Fahrverhalten von außergewöhnlich großen Fahrzeugen grundlegend neu zu untersuchen und zu bewerten.

Mit dieser Arbeit soll das grundlegende Verständnis der dynamischen Tiefertauchung von außergewöhnlich großen Fahrzeugen gestärkt und wesentliche Einflussfaktoren auf den dynamischen Tiefgang auf der Grundlage von Messungen in der Natur erarbeitet werden. Ein besonderes Augenmerk liegt dabei auf tiefgangsvergrößernden Einflüssen aus z.B. Schiff-Schiff Interaktionen, welche erst die Größe heutiger Schiffe in signifikantem Maße hervorruft.

Im Rahmen dieser Dissertation wurden Messungen zur Erfassung des dynamischen Tiefgangs von außergewöhnlich großen Fahrzeugen auf der Unter- und Außenelbe durchgeführt. Die sensorische Erfassung des Schiffssquats und sämtlicher beeinflussenden Parameter stellt die zentrale Methodik dieser Arbeit dar. Die zu erfassenden Parameter werden erläutert, das gewählte Messsystem und die Durchführung der Messungen beschrieben. Erfasste Daten werden aufbereitet, berechnete Parameter plausibilisiert und die Ergebnisse präsentiert. Anhand der Ergebnisse wird der Prozess der Bemessung des dynamischen Tiefgangs bewertet und kritische Lastfallkombinationen erörtert.

In den Messergebnissen wird zum ersten Mal deutlich, dass mit zunehmender Schiffsgröße die systemische Sicherheit der bisherigen Bemessungspraxis abnimmt. Ab Schiffsgrößen von 19000 TEU müssen die Ergebnisse der allgemein anerkannten Bemessungsansätze für Schiffsquat sogar als kritisch eingeordnet werden. Ebenso zeigt sich, dass Schiffsbegegnungen mit zunehmenden Schiffsgrößen auch zunehmende Bedeutung bei der Tiefgangsbemessung bekommen und kritische Lastfallkombinationen regulierend beeinflusst werden können.

Bislang ungenutzte Sicherheitsreserven werden bei der Bemessung von Krängungs- und Rollbewegungen im Einfluss des Kielradius sowie im Einfluss des Zusammenwirkens von Trimm und Hogging auf die Tiefgangszunahme identifiziert. Abschließend werden konkrete Empfehlungen zur Anwendung der neuen Erkenntnisse für die Bemessungspraxis auf Unter- und Außenelbe gegeben und weitergehende Möglichkeiten zur Erforschung einer schiffsspezifischen Bemessung benannt.

Table of Content

1 Introduction

There is a considerable interest in evaluating the present dynamic draft determination approaches for vessels travelling in confined waters to balance the area of conflict between the economic need for maximum loading conditions and the necessity of administrative draft limitations for safe marine traffic. A valid draft determination for channel design requires a solid basis of data from the field as well as an advanced knowledge of hydrostatic and hydrodynamic processes of a ship in confined waters.

To this end, PIANC summarizes findings on draft allowance determination in the *Harbour Approach Channel Guidelines.* The most recent determination guidelines of PIANC (2014) recapitulate improved approaches from ICORELS (1980), BARRAS & DERRET (2012) and ULICZKA & KONDZIELLA (2006). For the stage of channel design PIANC re-introduced the 1985 approach of totalizing draft-increasing influences from water, ship and channel-related factors plus additional safety margins. Final draft summarizes static fresh water draft and trim as well as additional amplification from density, heel and squat.

Channel design and draft determination for the Lower Elbe sea-waterway as approach channel towards the Port of Hamburg is still performed using that approach. However, such approach is generally accepted, all findings and results are based on either theoretical considerations or empirical model tests. Almost none determination approach is based on specific data from investigations in the field. Moreover, all PIANC model tests were carried out with maximum ship size equivalents of 12000 TEU, whereas actual travelling ship sizes on the Elbe River sea-waterway range between 12000 and 20000 TEU.

German Federal Waterway Engineering and Research Institute (BAW) recommends field investigation to observe interactions between ship and waterway on the Lower Elbe. Measurements in the field were necessary for channel design validations (KOESTERS, et al., 2017). While ship squat on the Elbe passage is still estimated in line with PIANC using the *International Commission on the Reception of Extraordinary Large Ships (ICORELS)* design approach, last approval of the squat estimation approach by results from field investigations was performed in 2003. Investigated ship sizes were between 5500 TEU and 7500 TEU vessels by that time (MAUSHAKE & JOSWIG, 2004).

Recent ship size development towards units with 20000 TEU brings up the question if the channel design approach used for the Lower Elbe fairway is still valid for such vessel generations. Considering the gross value of tonnage, draft allowance determination demands a detailed design approach that leads to maximum draft utilization levels on the one hand and guaranteed safety for ships and life on the other hand. An economic, resilient and safe design leads to the necessity of a solid data basis for channel design and a most accurate design approach.

The purpose of this dissertation is to fundamentally analyze and assess the dynamic draft behaviour of extraordinary large vessels on the Lower Elbe waterway. Special focus is given on new influences, e.g. ship-ship interactions, which lately became of significance due to the latest ship size development.

With the central method of investigations in the field, this work establishes an extensive data basis of draft influencing parameters from ship, waterway and ship handling. The overall aim is to facilitate the analysis and the assessment of nearly all dynamic draft influencing parameters on the Lower Elbe sea-waterway for the vessel sizes of the actually travelling fleet.

Between 2012 and 2016 the author of this dissertation conducted field investigations on dynamic draft behavior of extraordinary large vessel on the Lower Elbe waterway for the *Institute of River and Coastal Engineering of the Hamburg University of Technology*. Such investigation aimed to discover the status quo of dynamic ship behavior and to gather all necessary data for design approach validation. The measurement campaigns were performed successfully in cooperation with *Consulting Engineers von Lieberman Hamburg*, *BAW* and *Waterway and Shipping Office (WSA).*[1]

Within the first section, this dissertation provides a definition of ship movements as well as a description of the squat effect. It presents general boundary conditions and the status quo of current channel design approaches. Furthermore, it explains dynamic draft governing factors like vessel characteristics, waterway configurations and combined factors and presents the development towards the most important squat determination approaches.

The following section depicts the significance of the Lower Elbe as approach channel for the Port of Hamburg and. The section describes the status quo of the Lower Elbe channel design and presents the results of previous investigations on squat and dynamic draft on the Lower Elbe. Due to recent developments in ships' sizes and traffic numbers, the section emphasizes the necessity of actual field-investigations for design approach validations.

The dissertation describes the design of the field measurement and the measurement set up. Sensor composition and settings are explained and the performance of the field measurement is presented. The section describes the data acquisition and data handling, which finally leads to an extensive data base of draft influencing components.

Within the main part, this dissertation determines and analyses channel- and ship-related factors from the field investigations. The work assesses hydrostatic influences and interactions of draft, trim, hogging and heel as well as hydrodynamic influences from speed through water and under keel clearance.

Results are presented and discussed in detail. The influence of several parameter combinations is examined. E.g., generally accepted squat determination approaches from ICORELS, BARRAS and SCHMIECHEN are performed with measured parameters from the field. Section 6.4 presents the results and compares them with real squat data from the field. The results from the comparison of theoretical squat approaches and measured squat values discover that with increasing ship sizes, safety margins within the squat determination approaches decrease to a critical extend.

Furthermore, the extensive data base makes it possible to analyze ship-to-ship interactions. For the first time boundary conditions of ship-ship interaction, e.g. overall speed, distance and accumulated blockage, which lead to significant additional draft increase, are assessed.

The last section provides a conclusion as well as condensed recommendations to optimize the future determination of the dynamic draft of extraordinary large vessels on the Elbe River waterway. Finally, it presents research demand towards a ship and load specific individual design that maximizes draft utilization and respects the determination process in a pragmatic and safe way.

[1] ALBERS T., REITER B., TREUEL F. (2016): Erfassung und Analyse des dynamischen Fahrverhaltens von größen- und tiefgangsrelevanten Fahrzeugen auf Unter- und Außenelbe, Project Report, unpublished (German)

2 State of research on dynamic draft governing components

A travelling vessel experiences dynamic motions around lateral, longitudinal and vertical axis due to waves, wind and maneuvers. Dynamic draft with influences from pitch, roll and yawing effects differs from fresh water draft. Furthermore, effects from the water body itself, e.g. density, influence the draft as well.

Vessels, sailing in laterally and vertically confined waters, interact with the banks of the waterway and the bottom of the fairway. While ship waves induce stress on the waterway bank, the confined underwater cross-section leads to additional draft increasing effects like squat. Finally, ship-to-ship interaction have additional impact on the dynamic draft (Figure 2.1)

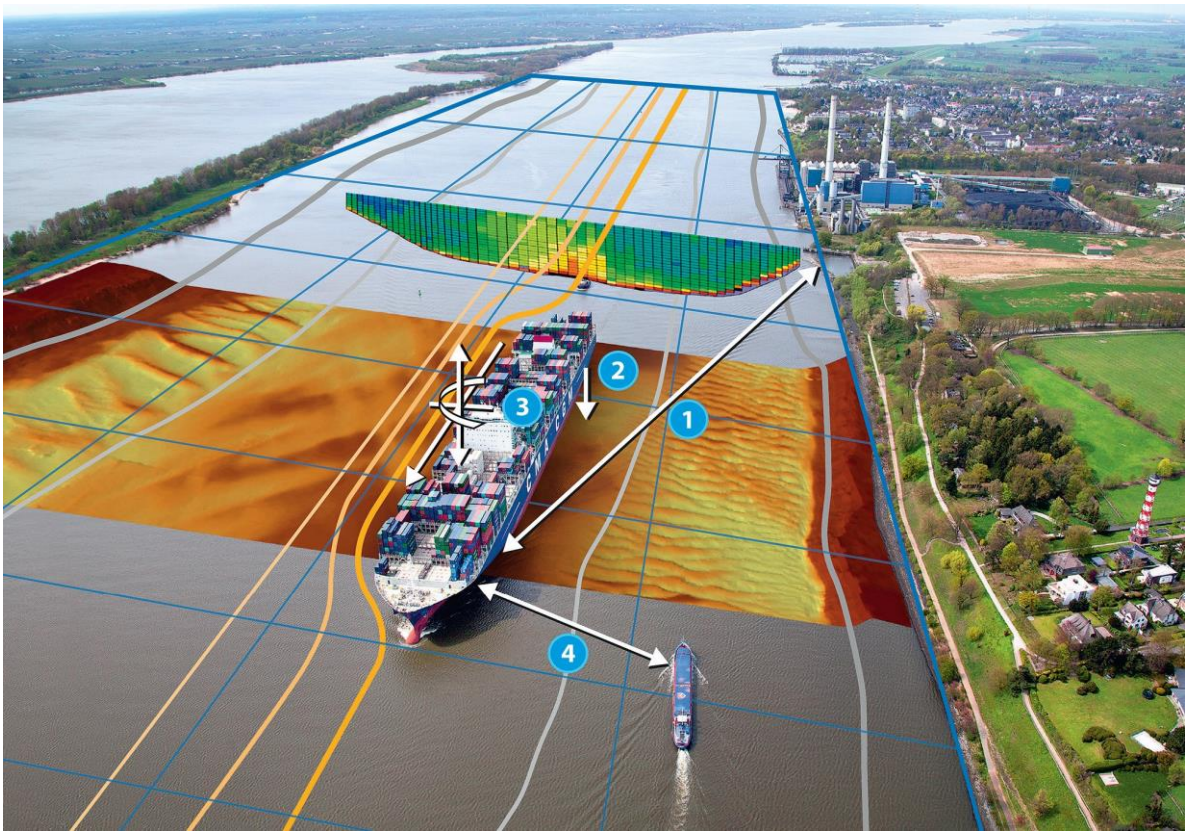

Figure 2.1: Ship-waterway interactions with bank (1) and bottom (2), ship motions (3) and ship-ship interaction (4) of a travelling ship in confined waters (KOESTERS, et al., 2017)

The flexible hull of a ship experiences static distorting forces from the force of gravity as well as from the force of buoyancy. Dynamic motions emerge from nautical maneuvers and water related effects e.g. squat and waves. Almost all motions and distortions influence the static and dynamic draft of the ship. On the Lower Elbe waterway static and dynamic draft is mainly influenced by loading conditions, turning maneuvers and speed alterations as well as water related influences. In this regard, wind shading effects by land diminishes the influences of waves. However, due to the laterally and vertically restricted waterway, squat-effect has significant influence on the draft.

Loading conditions evoke a rotation around the lateral and the longitudinal axis. Hydrostatic rotation around the longitudinal axis is called heel. Due to the large width of the vessel's underwater body, heel influences static draft at the outer edge of the hull, which is called off-centric draft (Figure 2.2).

Hydrostatic motion around the lateral axis is called trim, which leads to influences on static draft at the fore- and aft-perpendicular at bow and stern. Heel and trim are static occurrences. Equivalent dynamic motions around lateral and longitudinal axis happen to travelling ships due to maneuvers. Dynamic motion around the lateral axis is called pitch, dynamic motion around the longitudinal axis is called roll.

From the theoretical perspective, impacts from heel and roll as well as from trim and pitch can be examined separately. From the practical perspective, the single impacts form an absolute draft value, which, for this work, is of utmost interest. Thus, this work will examine the single influences wherever it is possible, but will handle heel and roll as well as trim and pitch as combined influences on the dynamic draft.

Next to static and dynamic motions from maneuvers and loading conditions, the laterally and vertically restricted waterway leads to additional vertical sinkage of the vessel in combination with additional trimming moment. The combination from sinkage and trim is called squat (Figure 2.3).

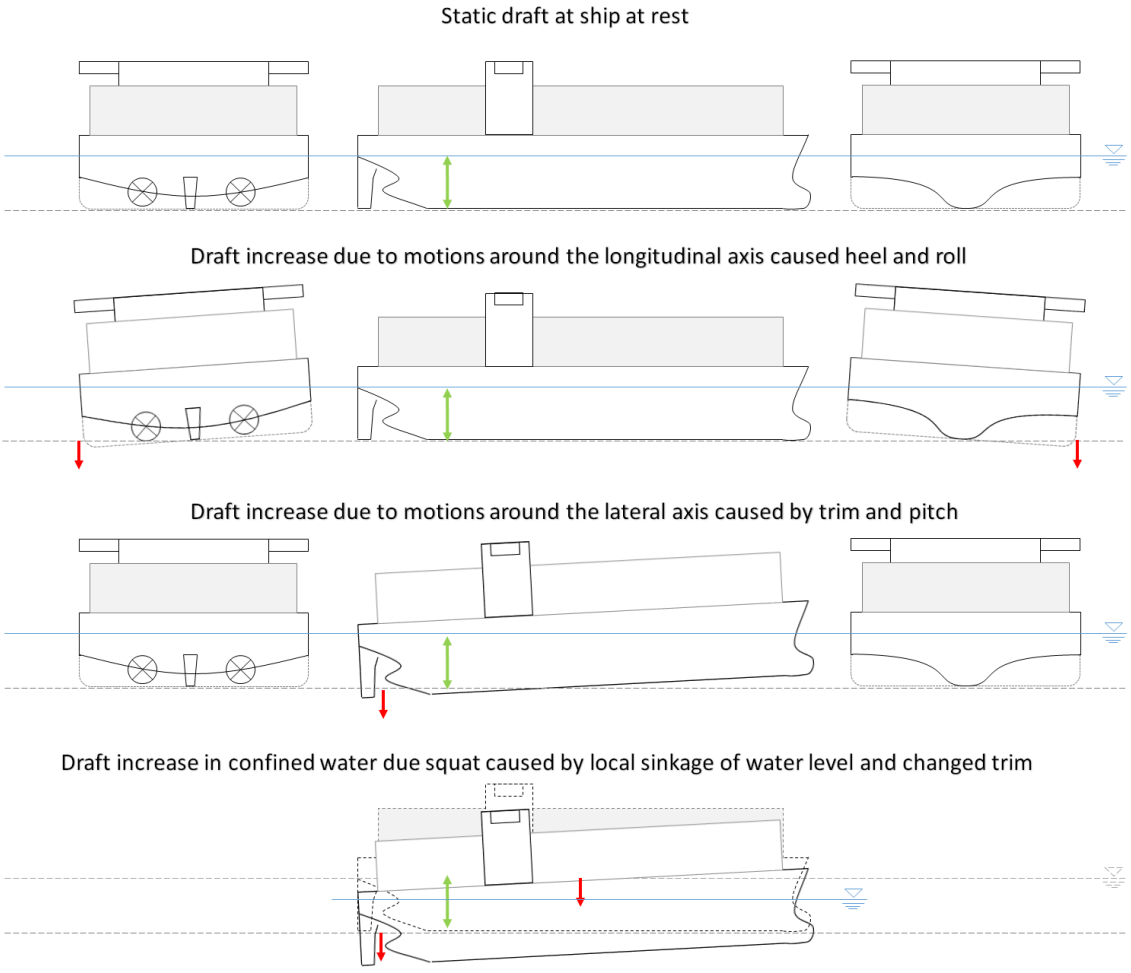

Figure 2.2: Draft increasing ship motions

Within the latest version of channel design guidelines, *World Association for Waterborne Transport Infrastructure (PIANC)* recommends the cumulative summation of water level factors, ship related factors and bottom related factors to determine channel design depth, which is the depth between reference water level and channel dredge level (Figure 2.3).

In general, reference water level is equal to nautical chart zero. However, in case of tidal activities, vessels may use the tidal elevation during passage to maximize nautical depth. Thus, reference level

plus tidal offset with an additional fixed safety margin for unfavorable conditions becomes design water level. Tidal offset and safety margin build the water level factors.

To determine net under keel clearance (NUKC), ship related factors consist of the static ship draft plus vertical draft changes due to change in density, draft changes due to dynamic heel motions, squat effects and draft changes due to wave response. With an additional safety margin, static draft and all factors mentioned build the gross under keel clearance (GUKC). Reference level plus ship related factors determine the nominal channel bed level. Bottom related factors consist of safety margins for sounding uncertainties, bottom changes between dredging runs and the dredging execution tolerance.

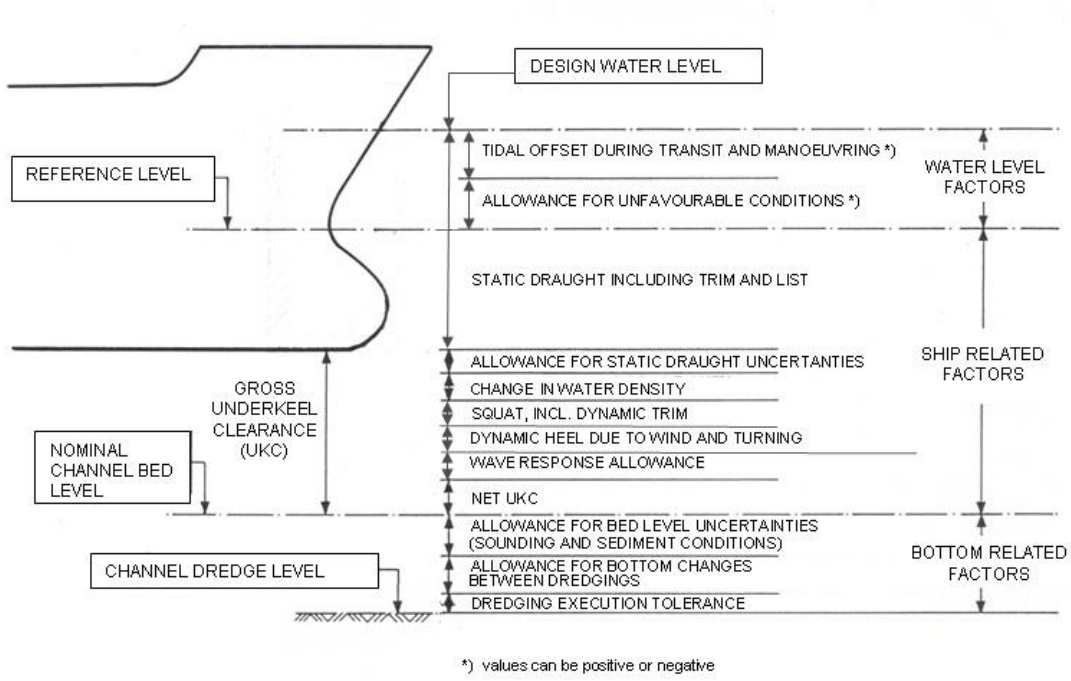

Figure 2.3: Channel design factors (PIANC, 2014)

While nowadays water level factors and bottom related factors are optimized due to advanced numerical forecast modelling as well as very accurate sonar sensors and dredging techniques, ship related factors are still rough estimations.

Dynamic draft calculations due to dynamic heel, for instance, neglect keel radius as well as the position of the maximum underwater cross-section of the ship. Influences due to density are roughly considered within a density safety margin. Dynamic trim phenomena due to density induced shift in buoyancy and floatation are generally unknown or neglected. Squat effects, the main driver on dynamic draft, are either estimated by approaches that originate from physical theory or originate empirically from scaled towing tank investigations in ship model basins. The results of such derivations and model-based approaches are then upgraded by fixed safety margins, to obtain secure values from the safety perspective. Simultaneously, the economical perspective for maximum draft utilization is unconsidered within the draft determination process.

The following section examines determination approaches for ship related factors. It starts with a definition of squat and summarizes generally accepted squat estimation approaches. Furthermore, it presents established approaches to determine influences of density, heel and ship-ship interactions.

The overview of the determination process makes it obvious, that for such a complex passage as the Lower Elbe waterway, the determination methods need to be adapted to the specific boundaries, that origin from vessel and waterway. The section leads up to the methodical background for field investigations on the Lower Elbe waterway.

2.1 Dynamic sinkage due to squat

The underwater body of the traveling vessel pushes water ahead and displaces a particular volume of the fluid. The body surrounding water flows into the lateral and vertical direction and must return around the sides of the ship and its keel. In analogy to the Venturi Effect, the relative flow velocity increases. The changes in flow pattern around the hull lead to changes in pressure distribution in comparison to the hydrostatic pressure. In order to level out the increase in kinematic energy the potential energy reacts in a water level depression according to the Bernoulli Effect. The ship follows the sinkage of that depression with a decrease of the under keel clearance (UKC). The asymmetry in hydrodynamic pressure distribution causes a trimming moment and additionally UKC variations at bow or stern. The downward displacement of a moving vessel due to the simultaneous combination of sinkage and dynamic trim change compared to the UKC of the vessel at-rest is called ship squat. In open waters, the squat effect is negligible but in shallow and lateral confined waters, the effect reduces the UKC significantly. (MILLWARD, 1996)

Latest investigations state, that for slender body type vessels e.g. container ships, initial trim influences the position of maximum squat occurrence (BRIGGS, 2006). The position of occurrence generally depends on form of the hull and the initial trim of the ship at-rest. If initially trimmed by bow, the maximum squat will occur at the bow. If initially trimmed by stern, the maximum squat will occur at the stern. Full-form ships such as supertankers turn towards the bow and experience maximum squat there. Fine-form ships such as containerships and cruise ships turn towards the stern and maximum squat will occur at the stern. The direction of the initial trim will remain. The initial trim at-rest will not level out due to squat underway.

2.1.1 Definition of squat and governing factors

Vessel characteristics

Ship characteristics, which govern squat are the vessel's operational speed relative to water, the configuration of the ship's hull and the ship's cross-section amidships.

Operational speed $V_S\ (kn\ or\ m/s)$ is the travelling speed through water with tidal and fluvial currents taken into account. Basic dimensions of a ship include the length between forward and aft perpendiculars $L_{PP}\ (m)$, the beam $B\ (m)$ and the draft $T\ (m)$. Block coefficient $C_B\ (-)$ represents the shape of the hull and characterizes the form of the ship relative to an equivalent rectangular volume represented by the basic dimensions. C_B can be determined from the ship's displacement volume if the basic dimensions are known. Block coefficient numbers range from around 0.8 for full-form vessels to 0.45 for fine-form ships. Displacement volume $\nabla(m^3)$ is defined as:

$$\nabla = C_B L_{PP} B T \qquad 2.1$$

Amidships cross-section $A_S\ (m^2)$ is the product from the keel radius, the beam and draft of the ship. Keel radius reduces the rectangular area from beam and draft. It is defined as a constant of 0.98. Amidships cross-section is defined as:

$$A_S = 0.98BT \tag{2.2}$$

Water plane coefficient C_{WP} $(-)$ describes the form of the hull by the ratio of the water plane area A_{WP} (m^2) at zero water level in relation to ship`s length and beam:

$$C_{WP} = \frac{A_{WP}}{L_{PP}B} \approx \frac{1}{3}(2C_B + 1) \tag{2.3}$$

Waterway configurations

Waterway dimensions influence the relative flow velocity around the ship's hull. With respect to squat, PIANC categorizes three main configurations of cross-sections for rivers and port approach channels (PIANC, 2014). The type of cross-section is characterized by the proximity of channel sides and bottom as well as ship's draft T (m). Waterway related factors are channel depth h (m), trench height h_T (m), width W (m) and bank slope run factor n $(-)$. Cross-sections with ratios of channel depth to ship draft h/T > 1.5-2.0 are considered as relatively deep-water boundaries where squat is negligible. For lower ratios, PIANC categorizes channels into unrestricted, restricted and canal types (Figure 2.4).

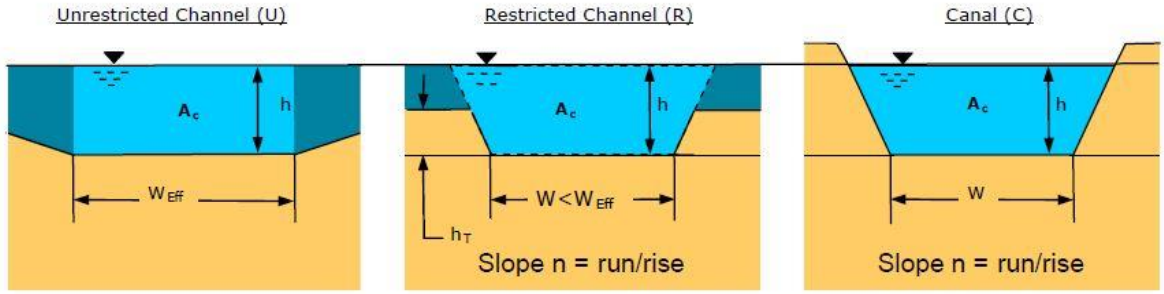

Figure 2.4: Channel types (PIANC, 1997)

Channel types are stereotyped by assumption of symmetric and well-defined cross-sections. Channel width W (m) , channel depth h (m) and bank slope run factor n $(-)$ determine the wetted area A_C (m^2) that influences the flow velocity distribution

$$A_C = Wh + nh^2 \tag{2.4}$$

Unrestricted channels have relatively wide and open bodies, e.g. shallow offshore areas and channel entrances. Even if h/T ratio might be small, channel width is large, so that channel sides have no influence on the flow distribution around the hull. Effective width W_{eff} (m) and a slope run factor of 0 determine the rectangular wetted area. Due to BRIGGS, et al. (2013) effective width W_{eff} (m) functions as an artificial side boundary that limits lateral water body influence on the flow distribution. Effective width depends on block coefficient C_B $(-)$ and beam B (m) of vessel. PIANC (2014) defines W_{eff} as:

$$W_{eff} = \left[\frac{7.04}{C_B{}^{0.85}}\right] B \tag{2.5}$$

for supertankers with C_B 0.76 – 0.85 effective width is 8.1 – 8.9 $* B$

for general cargo vesels with C_B 0.71 – 0.79 effective width is 8.6 – 9.4 $* B$

for containerships with C_B 0.61 – 0.71 effective width is 9.4 – 10.7 $* B$

Restricted channel is a hybrid between unrestricted channel and canal type with minor width than W_{eff} (m) and an underwater trench h_T (m). The underwater trench restrains and influences the flow distribution around the hull while the water column above the trench allows free water flow like in unrestricted channels. The wetted area is a rhomboid of the trench width and the extension of trench side slopes to the water surface. Restricted channel is the typical channel type of dredged rivers and artificial channels with maintained and enforced bottom level.

Canal type is a channel with emerged banks and idealized slopes from the bottom to the surface e.g. relatively narrow rivers with revetments. The wetted area of the cross-section is restrained to the rhomboid of channel width, bank slope and water depth.

Real world channels like natural and maintained rivers can be exposed to tidal influences and are usually a combination of all three channel types. For squat calculations, channel type and corresponding cross section should be taken into account. Some of the squat estimation formulas are even limited to a certain channel type due to their empirical origin.

Combined vessel and waterway factors

Squat prediction approaches require several dimensionless ratios from vessel characteristics, waterway configurations and combinations of both factors. The ratios represent boundary conditions to which validity and applicability of empirical approaches are constrained e.g. depth to draft ratio R_{hT} $(-)$ length to depth ratio R_{Lh} $(-)$ and trench height to depth ratio R_{Th} $(-)$. Directly applied to determine squat are the ratios between ship to waterway cross-section. They are represented by the blockage factor S $(-)$ and the depth Froude number F_{nh} $(-)$, which is a measure of ship`s resistance in shallow water.

Water depth to draft ratio R_{hT} is defined as:

$$R_{hT} = \frac{h}{T} \qquad 2.6$$

Vessel length between perpendiculars L_{PP} (m) to draft ratio R_{LT} is given by:

$$R_{LT} = \frac{L_{PP}}{T} \qquad 2.7$$

Trench height to water depth ratio R_{hTh} is given by:

$$R_{hTh} = \frac{h_T}{h} \qquad 2.8$$

The blockage factor S $(-)$ determines channel restriction by the underwater mid-ship cross-section of the vessel. It is the fraction from the ship`s cross-section A_S and the channel cross-section A_C:

$$S = \frac{A_S}{A_C} \tag{2.9}$$

Next to gravitational acceleration, water depth and channel profile, the blockage factor is the basis within the derivation of critical ship speed. At critical speed, the ship generated wave pattern changes and the water return pattern around the ship switches from laminar to turbulent. The wave resistance at bow increases dramatically and a ship would needs sufficient power to overcome such resistance. The maximum resistance is defined at the velocity of wave propagation in shallow water $V_C\ (m/s)$. Wave propagation velocity can be determined by the square root from gravitational acceleration $g\ (m/s^2)$ and channel depth $h\ (m)$. Dimensionless depth Froude number $F_{nh}\ (-)$ is defined as the fraction from vessel speed $V_S\ (m/s)$ and maximum wave propagation velocity:

$$F_{nh} = \frac{V_S}{\sqrt{gh}} \tag{2.10}$$

Region of effective speed barriers is given by Froude numbers between $0.85 < F_{nh} < 1.1$. Most full form ships are not able to reach depth Froude numbers over $0.6 - 0.7$ due to insufficient power. All squat estimation approaches deal at sub-critical speed and most of them at $F_{nh} < 0.7$.

2.1.2 Squat estimation approaches

The commonly applied methods for squat prediction are theoretical approaches, empirical formulae and numerical methods. In 1997, the Joint PIANC-IAPH Working Group II-30 listed 11 squat estimation formulae from theoretical derivations over empirical findings to graphical solutions. During the last decades numerical methods e.g. the squat prediction program of BECK, NEWMAN & TUCK (BNT) developed and during the last years, numerical modeling tools evolved.

Theoretical approach on slender body theory

TUCK derived in 1963 a theoretical formula to calculate hydrostatic dynamic sinkage and dynamic trim using slender body potential theory in shallow waters. The following theoretical findings build the basis of ship squat estimation.

In 1898, MICHELL compared the linearized aerodynamic flow patterns past a thin airfoil to a thin vertical-sided obstruction over the full water column with infinite width (MICHELL, 1898). He showed that the small disturbance velocity potential $\Phi\ (x, y)$ satisfies the shallow water theory with

$$\beta\Phi_{xx} + \Phi_{yy} = 0 \tag{2.11}$$

$$\text{where } \beta = 1 - {F_{nh}}^2 \text{ and } F_{nh} = \frac{V}{\sqrt{gh}}$$

With the ship's submerged cross-section A_S (m²) at station x, TUCK solved that equation by using the estimation that the ship behaves within the horizontal plane (x, y) like a thin airfoil (TUCK, 1966). The thickness of the airfoil is obtained by averaging the cross-section over the water depth to $A_{S,x}/h$.

Furthermore, velocity disturbance $\nabla\Phi$ vanishes in subcritical flow ($\beta < 0$) and the equation can be solved by using the body boundary condition

$$\Phi_y(x, 0_\pm) = \pm\frac{VA'_S}{2h} \tag{2.12}$$

For fully subcritical flow, the solution has a singularity as $\beta \to 0$ *or* $F_{nh} \to 0$ and with the local beam $B(x)$ at station (x), the upward (negative) force is given by

$$F = \frac{\rho V^2}{2\pi\sqrt{1 - F_{nh}^2}} \int\int dx\, d\xi\; B'(x) A'_S(\xi) \log|x - \xi| \tag{2.13}$$

TUCK performed a dimensionless analysis for a fore-aft symmetric ship with length L_{PP}. With $V = \int A_S(x)dx$ as the displacement volume $\nabla(m^3)$ the hydrostatic sinkage $S\ (m)$ results in

$$S = C_S \frac{\nabla}{L_{PP}^2} \frac{F_{nh}^2}{\sqrt{1 - F_{nh}^2}} \tag{2.14}$$

The non-dimensional coefficient C_S depends only weakly on the ship's hull (TUCK & TAYLOR, 1970). With the waterplane area $A_{WP} = \int B(x)dx$ it is an almost universal constant given by

$$C_S = -\frac{L_{PP}^2}{2\pi A_{WP}\,\nabla} \int\int dx\, d\xi\; B'(x) A'_S(\xi) \log|x - \xi| = 1.4 \tag{2.15}$$

C_S was calculated for a variety of hulls and was found to range between 1.3 and 1.5.The suggested value was approximated to 1.46 or, for sake of simplicity, 1.5. (PIANC, 1997) and (GOURLAY & TUCK, 2001)

From the hydrodynamic sinkage, the dynamic trim angle θ can be derived with C_θ as the dynamic trim coefficient by:

$$\theta = C_\theta \frac{\nabla}{L_{PP}^2} \frac{F_{nh}^2}{\sqrt{1 - F_{nh}^2}} \tag{2.16}$$

With the Longitudinal Centre of Flotation (LCF) and the second moment of waterplane area $I_{LCF} = \int (x - LCF)^2\, B(x)dx$ the trim coefficient can be calculated by:

$$C_\theta = -\frac{L_{PP}^3}{2\pi I_{LCF}\,\nabla} \int\int \frac{dS}{d\xi} \frac{(x - LCF)B(x)}{x - \xi}\, dx d\xi \tag{2.17}$$

The dynamic trim coefficient depends strongly on the fore-aft symmetry of the ship's hull. For modern container vessels, the coefficient is either positive or negative. For modern bulks, it is

positive and finally it is zero for total fore aft symmetry (GOURLAY & TUCK, 2001). Experts generalized the coefficients for different hulls and made them available for the use of mariners (WEHAUSEN & LAITONE, 1960).

Empirical approaches

TUCK & TAYLOR (1970) empirically adjusted the theoretical approach by results from model tests. They simplified the dynamic sinkage calculation under the estimation of shallow water with infinite width to the following approximation:

$$S = 1.5 \frac{\nabla}{L_{PP}^2} \frac{V^2}{gh} \qquad 2.18$$

HOOFT (1974) combined TUCK's formulae 2.14 and 2.16. With $C_S = 1.46$ and $C_\theta = 1.0$ his empirical formula is:

$$S = 1.46 \frac{\nabla}{L_{PP}^2} \frac{F_{nh}^2}{\sqrt{1 - F_{nh}^2}} + 0.5 L_{PP} \sin\left(\frac{\nabla}{L_{PP}^2} \frac{F_{nh}^2}{\sqrt{1 - F_{nh}^2}} \right) \qquad 2.19$$

HUUSKA (1976) found a combined sinkage and trim coefficient to 2.4 for unrestricted waterways. For restricted channels and canals, he introduced the channel geometry by the blockage factor K_S. His estimation for the bow sinkage is:

$$S_b = 2.4 K_S \frac{\nabla}{L_{PP}^2} \frac{F_{nh}^2}{\sqrt{1 - F_{nh}^2}} \qquad 2.20$$

$$\mathrm{K}_S = 7.45\, s_1 + 0.76 \quad for\ s_1 > 0.03$$
$$\mathrm{K}_S = 1 \quad for\ s_1 > 0.03$$
$$\mathrm{s}_1 = (A_S/A_C) K_1$$

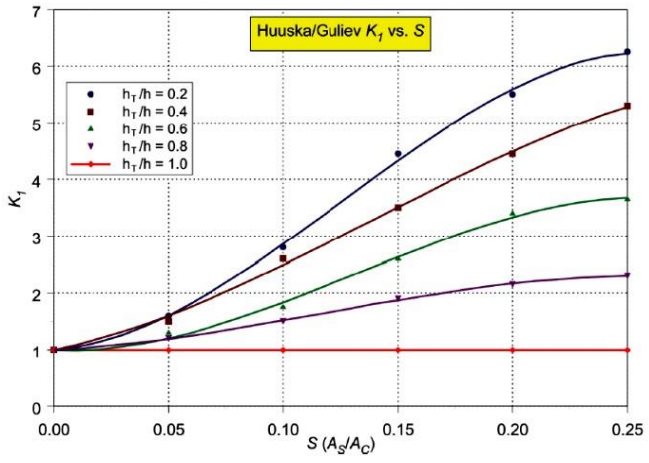

Figure 2.5: Blockage correction factor (GULIEV, 1971)

The International Commission on the Reception of Extraordinary Large Ships (ICORELS, 1980) finally combined TUCK's fundamental theoretical approach on slender body potential theory in shallow water with the empirical adjustments of HOOFT and HUUSKER and recommended the use of the simplified estimation:

$$S_b = 2.4 \frac{\nabla}{L_{PP}^2} \frac{F_{nh}^2}{\sqrt{1 - F_{nh}^2}} \qquad 2.21$$

MILLWARD performed lateral restricted water model tests with ships of different hulls with block coefficients of $0.44 < C_B < 0.83$ and length to water depth ratios of $6 < L/h < 12$ in 1990 (MILLWARD, 1990). In 1992, he revised his own empirical approach from 1990 and suggested an approach for bow squat based on his findings and TUCK's theoretical model (MILLWARD, 1992):

$$S_b = \left(61.7\, C_B \frac{T}{L} - 0.6\right) \frac{F_{nh}^2}{\sqrt{1 - F_{nh}^2}} \frac{L}{100} \qquad 2.22$$

Independent from theoretical derivations, BARRAS (1981) came to a new empirical approach. From full scale and model test with ship block coefficients between $0.5 < C_B < 0.9$ and depth to draft ratios between $1.1 < h/T < 1.5$ (BARRAS, 1979), he proposed the estimation of bow squat:

$$S_b = \frac{1}{30} C_B S_2^2 V^{2.08} \qquad 2.23$$

$$with\ \mathrm{S}_2 = \frac{A_S}{A_C - A_S}$$
$$and\ \mathrm{V}_S\ in\ (kts)$$

RÖMISCH (1989) performed extensive model test based on critical ship speed within water depth to draft ratios of $1.19 < h/T < 2.25$ and proposed a formula for maximum squat

$$S_{max} = C_V C_F K_{\Delta T} T \qquad 2.24$$

$$where\ \mathrm{C}_V = 8\left(\frac{V_S}{V_{cr}}\right)^2 \left[\left(\frac{V_S}{V_{cr}} - 0.5\right)^4 + 0.0625\right]$$
$$with\ V_{cr}\ from\ \text{RÖMISCH (1989)}$$
$$\mathrm{K}_{\Delta T} = 0.155 \sqrt{h/T}$$
$$\mathrm{C}_F = \left(\frac{10 C_B B}{L}\right)^2\ for\ bow\ squat$$
$$\mathrm{C}_F = \left(\frac{10 C_B B}{L}\right)^2\ for\ bow\ squat$$

ANKUDINOW proposed the latest empirical approach in 1996, where he predicts average sinkage and trim in shallow water under the influences of ship hull, propeller and draft:

$$S_M = \left(1 - K_P^S\right)(PA\,R\_Hulls)\left(\frac{PA\,R_+H}{T}\right)(PA\,R\_F_{nh})(PA\,R\_CH2) \\ -F_{nh}^{10}[0.005(1 - C_B)]\frac{L}{B}\frac{1}{1 - 0.95F_{nh}^{10}} \qquad 2.25$$

$$TRIM = -2.5(PA\,R\_Hulls)\left[\frac{(PA\,R\_H)}{T}\right](PA\,R\_F_{nh})(PA\,R\_CH2)K\_Trim \\ -0.005F_{nh}^{10}[(1 - C_B)]\frac{L}{B}\frac{PA\,R_+H/T}{1 - 0.95F_{nh}^{10}} \qquad 2.26$$

K_P^S is the coefficient for the propeller effects, $PA\,R\_Hulls$ for hull effects, $PA\,R\_H/T$ and $PA\,R_+H/T$ for depth-draft ratio effects. $PA\,R\_CH1$ and $PA\,R\_CH2$ are effects of the channel geometry and $PA\,R\_F_{nH}$ effects of the depth Froude number. K_Trim is synthetically derived from effects of propeller, transom stern and initial trim, taken from ANKUDINOV (1996). (ZHOU, et al., 2013)

In order to derive a very simple squat estimation approach, SCHMIECHEN (1997) performed a dimensional analysis. He defines squat in relation to water depth as a function of depth Froude number and the relation between draft and water depth:

$$\frac{s}{h} = f(F_{nh} * T/h)$$

$$with\ s = z_{Gauge} - z_{Ship} \\ h = z_{Gauge} - z_{bed} \\ V = V_{Ship} - V_{Water} \\ F_{nh} = \frac{V}{\sqrt{gh}} \qquad 2.27$$

Based upon TUCK (1966), SCHMIECHEN derived the relation between squat and draft to

$$\frac{s}{T} = C_2\frac{F_{nh}^2}{\sqrt{1 - F_{nh}^2}} \\ with\ C_2 = 2.4\,C_B\frac{B}{L} \qquad 2.28$$

ANKUDINOV (1996) performed hydraulic model investigations with the HERALD OF FREE ENTERPRISE. He found a cubic squat growth based on depth Froude number. Based on the findings, SCHMIECHEN used a simple cubic approximation for the TUCK-parameter:

$$\frac{F_{nh}^2}{\sqrt{1-F_{nh}^2}} = 2F_{nh}^3 \qquad 2.29$$

For depth Froude number of 0.7 SCHMIECHEN derives the following squat estimation approach:

$$\frac{s}{T} = C_3 F_{nh}^3$$

$$with\ C_3 = 4.8\ C_B \frac{B}{L} \qquad 2.30$$

SCHMIECHEN finally defines a practical estimation of squat for an average design ship to

$$s = \frac{1}{3} T F_{nh}^3 \qquad 2.31$$

Tested squat estimation approaches for the Lower Elbe waterway

BAW hindcasted squat on the Lower Elbe waterway using hydrological boundary conditions from the field measurements of 2003 and 2004. BAW entered such boundary conditions into the practical SCHMIECHEN approach (Equation 2.31) as well as into the ICORELS approach (Equation 2.21).

Finally, BAW adjusted the ICORELS approach and recommended its use for container ships with $C_B < 0.7$:

$$S = 2.0 * \frac{\nabla}{L_{PP}^2} \frac{F_{nh}^2}{\sqrt{1-F_{nh}^2}} \qquad 2.32$$

Using simplified presumptions e.g. on soil topography, average ship lengths and beams, ICORELS approach with pre-factor of 2.0 described the measured bow squat sufficiently well. For higher Froude numbers, SCHMIECHEN approach provided conformity with the measured bow squat values as well. Neither approach was able to provide sufficiently good trim values on the extreme bow trimming of the 5500 TEU vessels (ULICZKA & KONDZIELLA, 2006). Due to the hindcast determinations, BAW confirmed ICORELS pre-factor of 2.0, already used for the design of the Lower Elbe fairway, as well as SCHMIECHEN approach for higher depth Froude numbers, to be valid for further estimations.

Numerical Methods for squat prediction

BECK, NEWMAN & TUCK (1975) developed a numerical squat prediction program (BNT) based on potential flow modeling. The expanded work of TUCK on slender body theory included a finite width dredged channel with vertical walls and a certain depth within an infinitely wide outer-channel. BNT models the ship's hull within 21 equally spaced underwater cross-sections along the ship between the fore and aft perpendicular. For a given length, beam and draft the ship's hull can be characterized by information from the stability book. Such information contain displacement volume, location of the Longitudinal Centre of Buoyancy (LCB), waterplane area and location of the

Longitudinal Centre of Flotation (LCF) (GOURLAY, 2010). With the resulting underwater area in combination with data e.g. speed and water depth it is possible to calculate dynamic pressure by differentiating the velocity potential along the hull, obtained from the depth Froude number at each section. The BNT model is included within the Channel Analysis and Design Evaluation Tool (CADET) by the US Navy to determine the dredge depth for port approach channels. (BRIGGS, et al., 2013)

Numerical models based on linearized terms by slender-body theory neglect non-linear terms as well as speed ranges outside subcritical speed. In order to solve such higher terms as well as to model larger vessels at relatively high speed, the application of Computational Fluid Dynamics (CFD) developed over the last years.

JACHOWSKI (2008) started to use commercially available Reynolds Averaged Navier-Stokes Equation (RANSE) based numerical software to predict squat in shallow water for the KRISO container ship (KCS) model. PRAKASH & CHANDRA (2013) investigated the resistance of a ship in shallow water at five subcritical, one critical and one supercritical speed level by applying the commercial ANSYS RANSE solver. WORTLEY (2013) modeled the Duisburg Test Case (DTC) of EL MOCTAR, et al. (2012) with OpenFOAM as RANSE solver. CASTIGLIONE (2014) used the CFDSHIPS-Iowa RANSE solver of DELFT 372 to model the behavior of a catamaran at different hull symmetries, speeds and water depths. TEZDOGAN (2016) employed the Star-CCM+ RANS solver of CD-ADAPCO to investigate the DTC within an asymmetric canal. TERZIEV (2018) performed a study to compare empirical, analytical and unsteady RANSE methods on the DTC at all channel types and a range of speeds. The results show a good agreement between slender body theory, empirical formulae and CFD at low speed range. At high-speed ranges, the study shows the expected effects of neglecting viscous and non-linear terms by slender body theory in disagreements of the results with CFD results. (TERZIEV, et al., 2018).

All numerical squat estimations are limited to specific boundary conditions of the basic test cases. None of the models became a generally accepted determination method so far.

Hydraulic modelling at BAW-DH

At BAW, hydraulic model tests were undertaken to investigate the behavior of PPM container ships in laterally restricted and unrestricted waterways. Another focal point of research was the interaction of ships with dunes on the waterway bed in various configurations. Tests were conducted in a model scale of 1:40 in the shallow water tank of BAW with 100 m length, 35 m width and 0.7 m water depth.

Design ships were JUMBO ($L_{PP} = 320\text{m}, B = 40\text{m}, T = 14.5\text{m}, C_B = 0.740$ at UKC of 1 and 2m) and MEGA-JUMBO ($L_{PP} = 360\text{m}, B = 55\text{m}, T = 15.5\text{m}, C_B = 0.677$ at UKC of 1m, 1.5m and 2m). The model tests were performed with speed levels between 8 kts and 16 kts. Ships were self-propelled and guided by a taut wire over a distance of 90 m. Squat was measured by a ship based laser geometric method with precision of $\Delta s < 1\text{ mm}$ in the model and therefore $\Delta s < 0.04\text{ m}$ in prototype. Three systematic studies were performed to investigate squat and trim of the ships in:

- laterally unrestricted shallow water
- laterally unrestricted water with underwater dunes on a firm bed and
- laterally restricted shallow water.

For the JUMBO model in unrestricted water over a flat bed, squat values at the bow exceeded squat values at the stern. At a speed of 13.9 kts, stern squat is around 0.65 m while bow squat is generally higher at 0.82 m (ULICZKA & KONDZIELLA, 2006). For the MEGA-JUMBO in unrestricted shallow water, the model led to speed depending bow squat values between 0.25 m at 9 kts and to 1 m at 15.3 kts. Stern squat values were around 50% higher with resulting 0.4 m at 9 kts and 1.5 m at 15.3 kts (PIANC, 2014).

Systematic investigations on the influences of underwater dunes within unrestricted water came to the results, that underwater bed structures like dunes increase form roughness of the bed. Assuming the nautical bottom at the top of the dunes, the structures led to locally increased waterway cross-sections. Either way, dunes increase the energy dissipation of the water flow underneath the ship and result into reduced squat values at bow and stern. This was found to be equal for regular and irregular located dunes. Within special ratios of dune frequency and ship length, the ship was triggered to start pitching behavior, which led to a 0.16 m higher bow and stern squat values than in other dune configurations. But even during pitching, a decreased squat overall was found in consequence of the presents of underwater structure. (ULICZKA & KONDZIELLA, 2006).

During the last set-up, the influence of the ratio of channel to ship cross-section onto squat was modeled. Channel width and bank steepness were varied systematically. BAW came to the findings, that squat values at bow and stern were much higher than in unrestricted water. Squat increased with the increase in waterway restriction. Figure 2.6 shows the stern squat to 1.5 m at 15 kts for the MEGA-JUMBO and a channel to ship cross-section ratio of 25 with a slope steepness rise-run factor of 3. For a cross-section ratio of 10 and a slope steepness of 4, stern squat increased by 0.1 m.

The last set-up was varied with the ship going symmetrically, centric in the middle of the fairway as well asymmetric, off-centric location in the fairway to discover bank effects for asymmetric locations. Surprisingly, BAW discovered that with off-centric location and therefore the lower passing distance and the partial cross-section ratio has an insignificant impact on squat values (Figure 2.6).

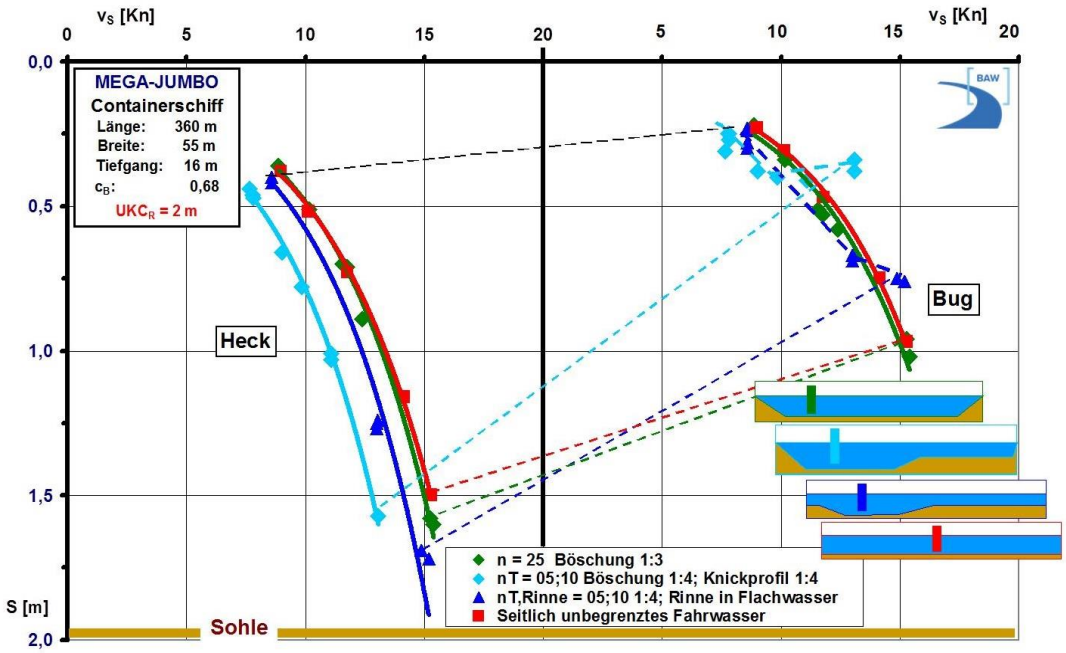

Figure 2.6: Influence of cross-section ratio and off-centric course on bow and stern squat for a PPM ships (KOESTERS, et al., 2017)

2.2 Additional sinkage due to ship-ship interactions

When two ships encounter each other head-on or overtake each other within the same fairway, the ship hulls interact. The interaction becomes visible in maneuverability in terms of changing yaw moments as well as changing trim moments during the process. Not directly visible effect is additional squat because of the changes in trim and additional sinkage during the interaction.

Flow pattern around the travelling ship result in a certain distribution of pressure and a certain wave system around the hull. Bow and stern areas experience high pressure, parts along the side of the hull and below keel experience low pressure. Such pressure distribution of two ships interfere during encountering and overtaking maneuvers. (DAND, 1981)

During ship-ship head-on encountering, high-pressure areas of both bows interact right before ship bows reach a parallel position in the fairway. Bow-bow pressure interference leads to repulsion and consequently to yaw moments away from each other. Interference of bow wave systems leads to positive trim moments and trim towards stern. When midship sections get closer to parallel courses, low-pressure areas along the side of the vessel interact and cause notable increased yaw moments towards the encountering vessel. Due to squat related water depression, both ships pitch into the wave trough caused by the other ship during that phase. Encountering ships trim distinctly by bow with maximum trim when bows are parallel to the encounter's midship section. Passing that point, trim moment change and ships begin to trim towards stern again. High-pressure areas at bow and stern interact and ships yaw away from each other.

Overtaking vessels experience the same interferences, but with slightly different effects in a different order. While high-pressure bow and stern areas are close to parallel courses, both ships discover trim moments towards stern as well as bow and stern yaw away from each other. When ships get close to parallel midship sections, both ships pitch into water depressions and trim by bow. Afterwards they trim again towards stern, when bow and stern areas are parallel to each other.

Despite the order of events, changed trim values during encountering or overtaking maneuvers increase the draft of both ships. Individual squat effects also interfere with each other and cause additional effects of sinkage for both vessels. ELOOT verified such effects (ELOOT, et al., 2011).

ELOOT performed ship-ship interaction model tests, RANSE calculations and field-based measurements in 2011. For data comparison, independent of ship length and duration of the interaction, the encountering or overtaking process was defined within a dimensionless timeframe, the Relative Longitudinal Position (RLP) (Figure 2.7). Parallel midship sections are defined as central point of the process with $RLP = 0$. For encountering maneuvers, parallel bow-bow positions and for overtaking maneuvers, parallel bow-stern positions are defined as $RLP = -1$. $RLP = 1$ defines the end of the process with parallel stern-stern or in case of overtaking maneuvers, parallel bow-stern positions (ELOOT, et al., 2011). Figure 2.7 shows the sinkage at different speed during the head-on encountering model test with a 291 m long container ship and a 310 m long bulk carrier, both at 12.5 m draft at 17.1 m UKC.

ELOOT came to the conclusion that additional squat due to ship-ship interaction is of minor relevance as long UKC of both ships is larger than 20% of ship's draft. If UKC is smaller than that amount, additional sinkage during passing can reach values between 50 and 100% of the squat before the interaction. (ELOOT, et al., 2011)

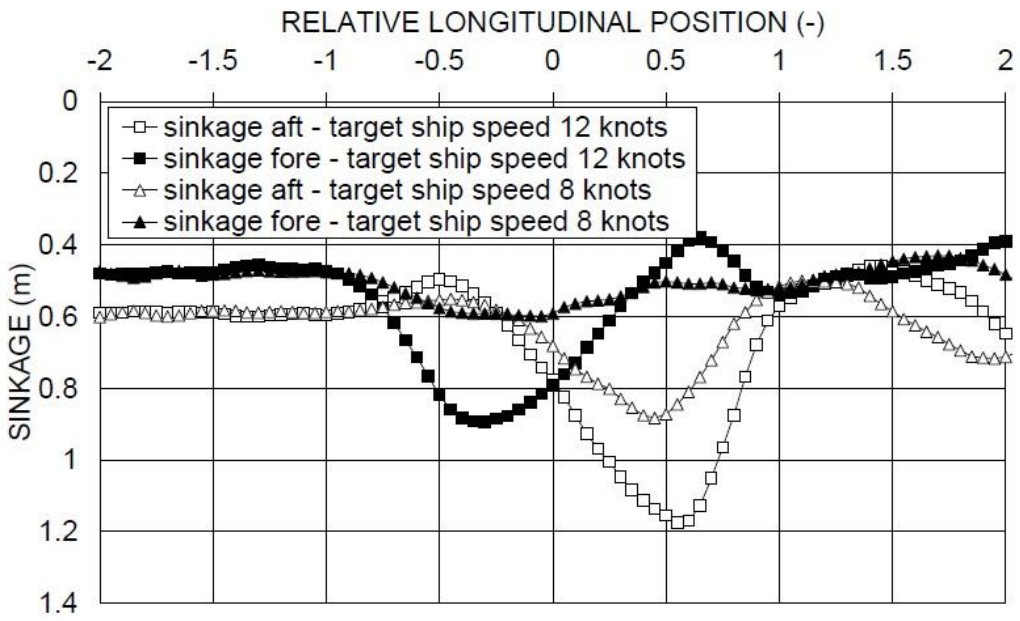

Figure 2.7: Sinkage at AP and FP during ship-ship interaction model tests (ELOOT, et al., 2011)

2.3 Impact of density

Archimedes' Principle states, that in fluid immersed bodies appear to discover a loss in mass equal to the mass of the displaced fluid. The immersed body reaches hydrostatic state, when the sum of vertical forces equals zero. In that state, downward gravity forces equal the upward force of buoyancy.

Gravity force of a vessel is defined as the product of overall mass, the displacement (Depl.) and gravitational acceleration:

$$\mathrm{F}_G = g * Depl \tag{2.33}$$

Force of buoyancy is defined as the product of density, gravitational acceleration and the underwater volume of the ship:

$$\mathrm{F}_B = \rho * g * \nabla \tag{2.34}$$

When both forces are equal, gravitational acceleration becomes negligible and underwater volume equals the fraction of overall mass and density:

$$\frac{Depl}{\rho} = \nabla \tag{2.35}$$

Therefore, density variation lead to variations of displacement, which consequently result in draft variations due to the change in density.

In case of estuaries like the Lower Elbe, inbound and outbound vessels experience a change in density from seawater to freshwater and vice versa, which causes a change in draft. Seawater density is usually assumed to 1025 kg/m³, freshwater density is assumed to 1000 kg/m³. At channel design stage, influence of density on draft is determined pragmatically by the use of the relative density, which is the ratio between seawater and freshwater density.

$$\nabla_{FW} = \nabla_{SW} \frac{\rho_{FW}}{\rho_{SW}} \qquad 2.36$$

According to equation 2.36, relative density with a difference in mass of 25 kg/m³ leads to maximum change in draft of 2.5% under the assumption of a cubic underwater volume of the ship with ship dimensions length, beam and draft.

2.4 Off-centric draft increase due to heel and roll

If a ship discovers an inclination around the longitudinal axis due to heel or roll, off-centric draft increase can occur at the sides of the underwater body. If the underwater cross-section of a ship is assumed rectangular with dimensions of beam and draft, an inclination due to heel or roll results in a draft at the side of the hull that exceeds draft of the centerline (Figure 2.8)

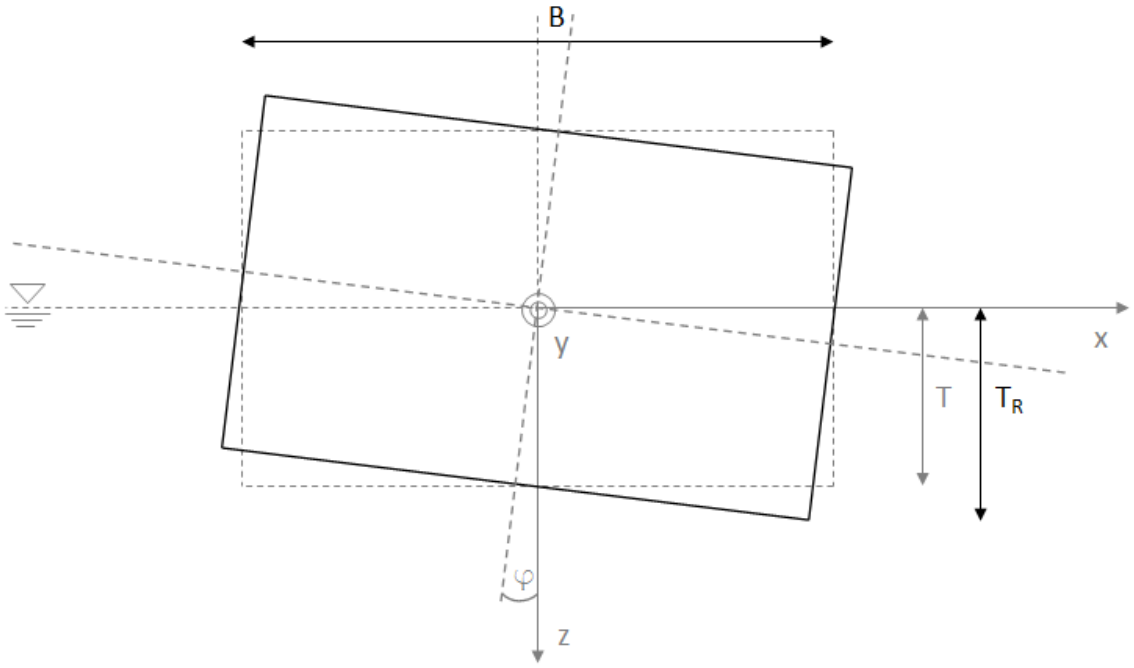

Figure 2.8: Additional draft due to heel and roll inclination

Off-centric draft can be calculated with the centerline draft and the heel or roll angle (BARRAS & DERRET, 2012). Such approach determines off-centric draft pragmatically but neglects keel radius of the ship and therefore overestimates off-centric draft.

$$\mathrm{T}_R = \frac{B}{2} * \sin\varphi + T * \cos\varphi \qquad 2.37$$

3 Status quo of the dynamic draft regulation on the Lower Elbe

This chapter gives an overview on the present state of the Lower Elbe waterway between port of Hamburg (at Elbe-km 620) and buoy E11 (at Elbe-km 750). It explains the present channel design parameters for the section of interest and shows the latest ship size developments on that section. Aiming for a database, which allows comparing real squat data with determinations from the IROREL squat estimation approach for channel design and tidal schedule calculations, section 3.4 reasons that field investigations need to be conducted.

3.1 Present state of the Lower Elbe waterway

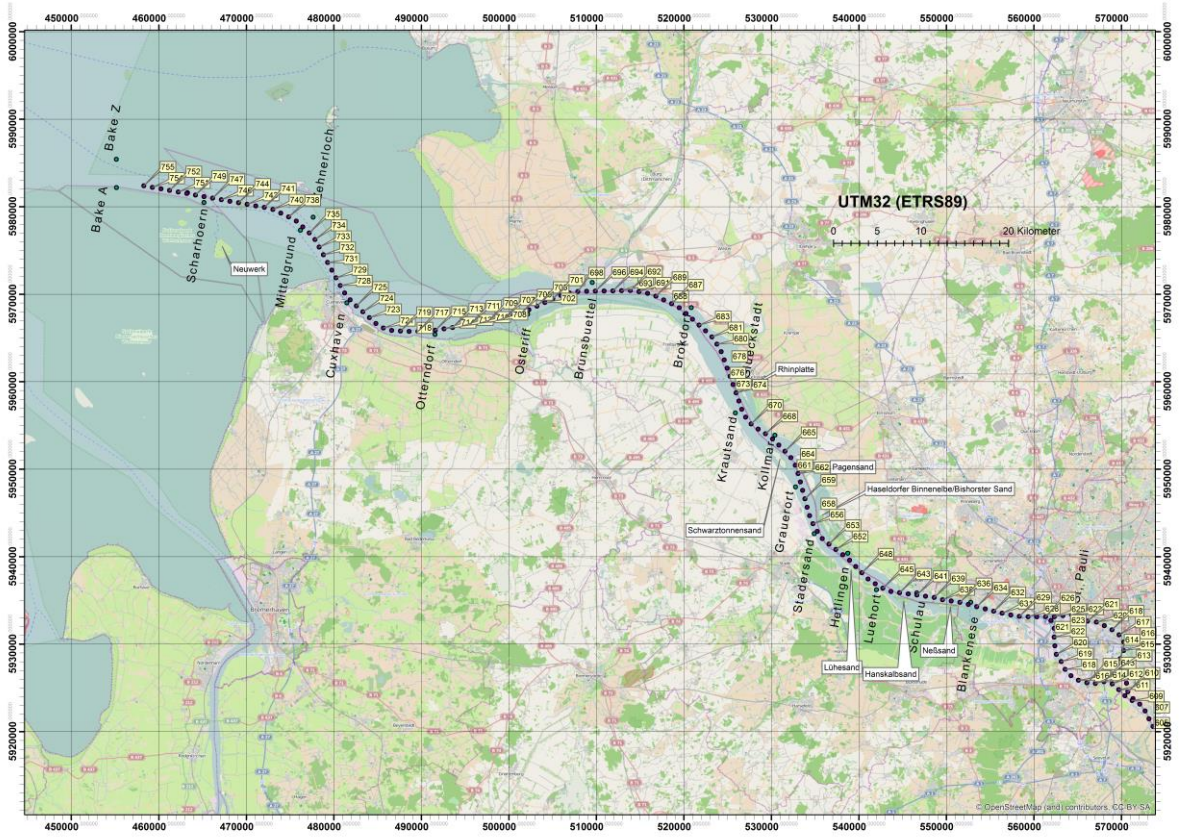

Figure 3.1[2]: Section of field-based measurements on the Lower Elbe waterway with kilometrage

Figure 3.1 shows the German Elbe River kilometrage between Lower Elbe waterway entrance and Hamburg Port. Most significant part in terms of channel design is the fairway section between Container Terminal Altenwerder (CTA) at Elbe-km 620 and buoy E11 next to Scharhoern Island at Elbe-km 750.

Fairway width is 400 m between Elbe-km 750-680, 300 m between Elbe-km 680-645 and 180-250 m within the Hamburg Port section. Maintained design water depth beneath sea level (German NHN) is 16.98 m at Elbe-km 750 (Scharhoern) and 16.70 m at Elbe-km 620 (CTA). Over a 65 km long shallow section between Elbe-km 713 (Otterndorf) and Elbe-km 648 (Luehesand Island) maintained water

[2]Elbe-squat project report 2016 (in German, unpublished). In collaboration with Consulting Engineers von Lieberman, Germany. Map based on OpenStreetMap contributors.

depth is only 16 m below NHN. Minimum depth of 15.80 m below NHN, which equals 12.90 m beneath chart datum (SKN), is located at Elbe-km 680 (Glueckstadt).

The Lower Elbe is influenced by tide and salinity on this section. Tidal range is 2.95 m at Cuxhaven gauge station and 3.65 m at St. Pauli gauge station. Salinity is between 25-30 PSU at Elbe-km 750 and declines to 0 PSU at Elbe-km 660.

Panamax (PM) container vessels with beams < 32.30 m may enter the fairway to Hamburg Port independent from tide with freshwater draft up to 12.80 m. Post-Panamax vessels with beams > 32.30 m may enter independently from tidal elevation with freshwater drafts up to 12.40 m. Vessels with higher drafts are allowed to enter the passage only in dependence of the tidal situation.

In- and outbound vessels with beams > 32.30 m (post-panamax container ship size) need to use the tidal elevation to overcome the shallow section of the fairway. Inbound vessels go with the crest of the tidal wave, outbound vessels start at Hamburg at a time slot, which allows the vessels to meet the tidal high water peak at the shallowest fairway section around Glueckstadt (Figure 5.2 and Figure 5.3).

Outbound vessels with freshwater draft up to 13.80 m may leave Hamburg Port tide-depending. They have a time slot to start of around 30-80 min. Inbound vessels can enter the passage in dependence of the tide with a maximum freshwater draft of 14.50 m.

For vessels with length over all > 340 m or beams > 45.0 m there are specific regulations. Table 3.1 shows maximum freshwater drafts (FWD) for inbound vessels in relation to length over all and beam.

Table 3.1: Maximum freshwater draft allowance of PPM inbound vessels

Length over all	Beam	Max. FWD (tide independent)	Max. FWD (tide dependent)
> 340 m	> 45.0 m	12.70 m	15.10 m
> 360 m	> 47.5 m	12.60 m	14.90 m
> 370 m	> 50.0 m	12.40 m	14.70 m
> 380 m	> 52.5 m	12.20 m	14.50 m
> 390 m	> 55.0 m	12.00 m	14.30 m
> 410 m	> 57.5 m	11.80 m	14.10 m

3.2 Latest channel design factors

Lower Elbe channel design of 2006 base upon water, ship and bottom related factors with respect to PIANC design guidelines (Figure 2.3). Design vessel is a container vessel with overall length of 300 m, beam of 32.50 m and seawater draft of 14.50 m. Channel design parameters are listed in Table 3.2.

Allowance for unfavorable conditions ΔW_{MLT} is determined for deviations from mean low tide level caused by eastern wind directions with respect of an occurrence probability of 80%.

Change of draft due to change in water density Δt_D is determined by:

$$\Delta T_D = T_{SW}\left(\frac{\rho_{SW}}{\rho_{FW}} - 1\right) \qquad 3.1$$

Squat including dynamic trim is calculated based on the BAW adjusted ICORELS approach (equation 2.32):

$$\Delta T_S = 2.0 * \frac{\nabla}{L_{PP}^2} \frac{F_{nh}^2}{\sqrt{1 - F_{nh}^2}}$$

Additional off-centric draft due to dynamic heel ΔT_K was calculated for a heel/roll angle of 1.5°. The calculation is based on equation 2.37 under consideration of the keel radius R:

$$\Delta T_R = \frac{B - R}{2} * \sin\varphi + T * \cos\varphi \qquad 3.2$$

Table 3.2: Design values for Lower Elbe channel depth[3]

Parameter	Definition	value
ΔW_{MLT}	Allowance of unfavorable deviations from low water	0.35 m
ΔW_U	Uncertainty in water level forecast	0.10 m
ΔT_D	Draft increase due to density	0.32 m
ΔT_S	Draft increase due to squat	1.40 m
ΔT_R	Draft increase due to roll	0.46 m
ΔT_M	Uncertainty in draft meter reading	0.10 m
ΔT_W	Vertical motion due to waves	0.00 m
Δh_S	Uncertainty in bottom soundings	0.25 m
$NUKC$	Net under keel clearance according to PIANC for sand	0.30 m

3.3 Former field-based squat investigations on the Lower Elbe waterway

In 2003 and 2004 German Federal Waterway Engineering and Research Institute (BAW) performed squat measurement on the Lower Elbe waterway. BAW accompanied 12 journeys of post-panamax container vessels (PPM) on the 120 km long passage between Hamburg Port at Elbe-km 624 and the North Sea at Elbe-km 735.

Eight journeys were undertaken with 7500 TEU vessels of the HAMBURG EXPRESS class owned by HAPAG-LLOYD shipping company. Four journeys were conducted with 5500 TEU vessels of YANG MING shipping. Ship characteristics were $L_{PP} = 320.4\text{m}, B = 42.8\text{m}, T = 10.8 - 12.6\text{m}, C_B = 0.62 - 0.65$ for 7500 TEU ships and $L_{PP} = 274.7\text{m}, B = 40\text{m}, T = 11.4 - 13.2\text{m}, C_B = 0.56 - 0.59$ at the 5500 TEU class.

[3] PROJEKTBÜRO FAHRRINNENANPASSUNG, 2006: B.2 Erläuterungsbericht: Beschreibung des Vorhabens, Technische Planung. German

The vessels were identically equipped with two autonomous Precise Differential Global Positioning System (PDGPS) antennae at the bow and two PDGPS antennae at the bridge in the rear part of the vessel. BAW-DH used Trimble 4700 and 5700 antennae with a frequency of 1 Hz.

The water level at the vessel position was determined from stationary water gauges from the Waterway and Shipping Office (WSA) as well as the Hamburg Port Authority (HPA) along the passage. The interpolation between gauging stations was validated by additional PDGPS measurements performed from an accompanying, very fast going research vessel.

The research vessel went ahead the container ship and acquired additional stationary data e.g. currents, water temperature and conductivity at six defined dross-sections along the passage using ADCP and CTD-probes. The measurements at the cross-sections were conducted immediately before the containership passed the cross-section. Next to maneuvering data from the Voyage Data Recorder (VDR), e.g. rudder angle and rate of turn (ROT), head-on passing situations and pilot change situations were recorded and documented.

After each measurement campaign, the antenna position data was post-processed by applying virtual reference stations based on SAPOS correction data to increase horizontal and vertical position accuracy to < 0.04m. From the intersection of the single antenna positions all vessel movements e.g. heel, were calculated and additional maneuvering data e.g. heading, course and speed, was derived.

Squat was determined by the difference between antenna height above water level at rest and the antenna height above water level in motion. Water depth was calculated from the water level and the underwater topography derived from a digital terrain model with additional actual nautical soundings from WSA and HPA. Under keel clearance (UKC) resulted from the difference between draft plus squat and the water depth at each station. Additional data from ADCP and CTD probes made it possible to determine velocity and density of each station. Therefore, vessel speed is speed through water (Stw) and squat data is density adjusted. Determination precision for squat data was estimated to $\Delta s = \pm 0.05\ \mathrm{m}$, for UKC to $\Delta UKC < \pm 0.2\ \mathrm{m}$, for speed $\Delta V_S = \pm 0.08\ \mathrm{kn}$ and for heel $\Delta\theta = \pm 0.07°$ (MAUSHAKE & JOSWIG, 2004).

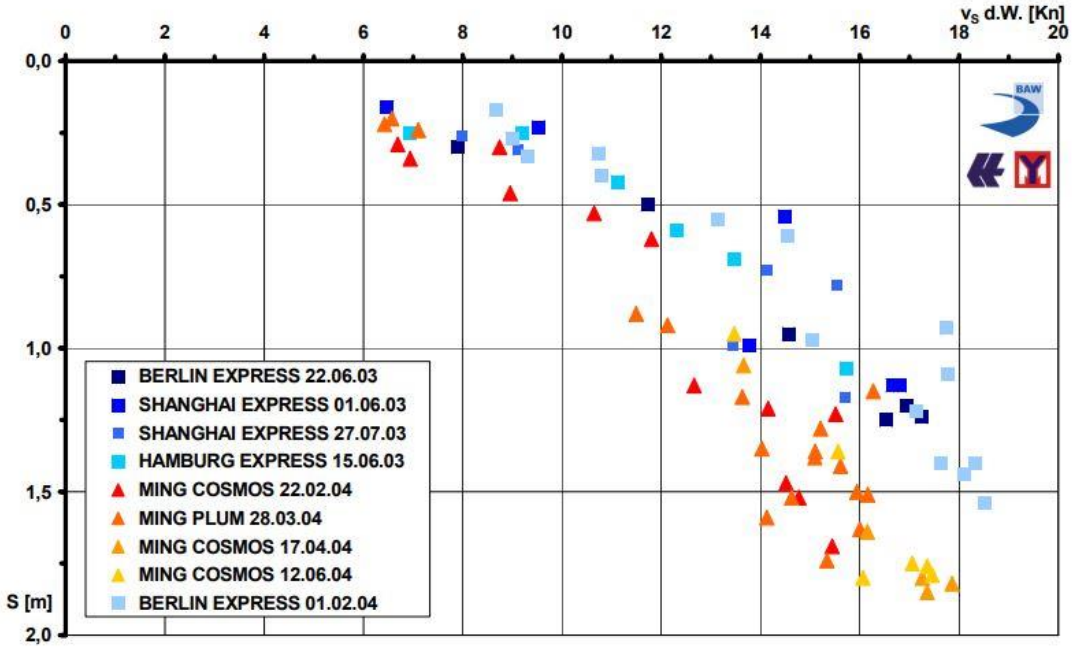

Figure 3.2: Results of squat measurements on the Elbe waterway (ULICZKA & KONDZIELLA, 2006)

Figure 3.2 shows results of such measurements in the field on the Elbe waterway. At vessel speeds between 6 kn and 19 kn, the results show bow squat values between 0.2 m and 1.6 m for the 7500 TEU class and bow squat values between 0.2 m and 1.8 m for the 5500 TEU class.

Spread of squat between both classes was due to different hull forms and different waterway to ship cross-section ratios at different UKC. It is stated, that a notable buoyancy increase at the fore body of the 5500 TEU class does only occur from immersion depth over 16 m. At 12 m, the transom stern immerses and trims the bow downwards. In consequence, the vertical motion of the bow is higher at the 5500 TEU class than at 7500 TEU class with weaker trim and equally high buoyancy (ULICZKA & KONDZIELLA, 2006).

Analysis of 125 head-on encountering situations came to an additional increase in squat due to ship-ship interaction. Additional squat applies equally to bow and stern squat. Within 50% of all interaction, additional squat was below 0.16 m. In 90% it was below 0.33 m. Maximum additional squat over all was measured to 0.44 m (ULICZKA, 2009).

3.4 Necessity for extensive field-based dynamic draft measurements

ULICZKA & KONDZIELLA assessed the abovementioned field-based results, performed complementary hindcast simulations as well as additionally model-based investigations in 2006. They approved the applicability of the BAW adjusted squat estimation approach (Equation 2.32). All results and estimation approaches have been based on the datasets of the investigated ship sizes with maximum of length at 320 m and maximum beam at 43 m within the field-based investigations.

Since the last field-based investigations in 2004, container ship sizes increased extremely (Figure 3.3). While 2004 container ships of 7500 TEU have been of significant relevance on the Lower Elbe waterway, ship sizes between 10000-140000 TEU became standard on the Lower Elbe passage in 2013. Latest statistics of 2017 show the trend of even larger ship sizes with ships of 14000-19000 TEU capacities to become the new standard vessel size for the Lower Elbe passage (Figure 3.4). Latest news even expect 25000 TEU carriers with lengths of 435m to be the next step of size development.[4]

Knowledge on dynamic draft behavior of such extraordinary large ships under draft regulations on the abovementioned passage of the shallow and narrow Lower Elbe fairway is of utmost significance. Future channel design and present tidal schedule program calculations need reliable and extensive datasets for dynamic draft assessment and ship maneuverability.

Therefore, it is necessary to gain an overview on the present state of dynamic draft behavior of all extraordinary and ultra large container vessels, which use the Lower Elbe fairway on a regular basis. The extraordinary ship size development, the wide range of required design data and the large temporal interval since the last field-based investigations lead to the necessity of new and extensive field-based investigation on the Lower Elbe waterway. Only the method of field-based investigations can assess the present state of dynamic draft behavior reliably and provide the necessary wide-ranging database.

[4] THB – Täglicher Hafenbericht, 04.04.2019, S.1, 71. Jahrgang, Ausgabe #67, DVV Media Group GmbH (German)

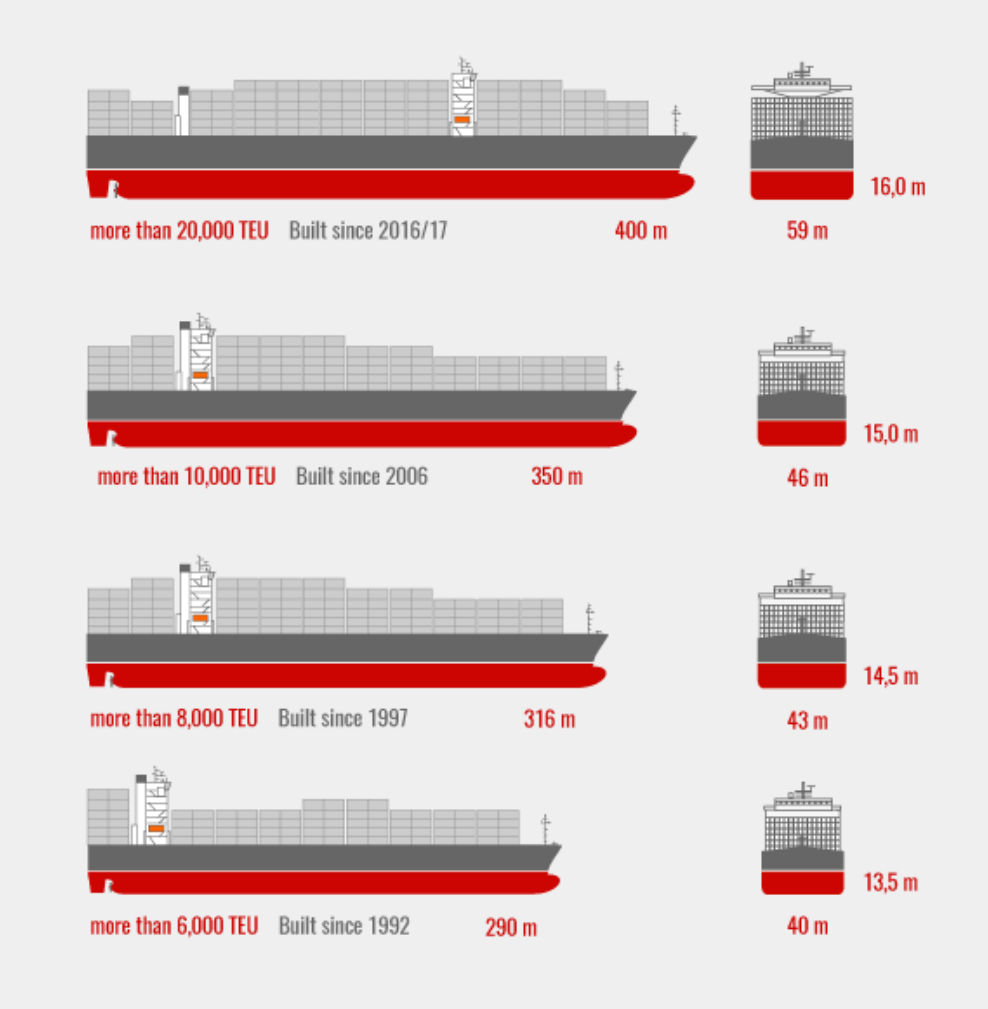

Figure 3.3: Ship size development within the last 20 years[5]

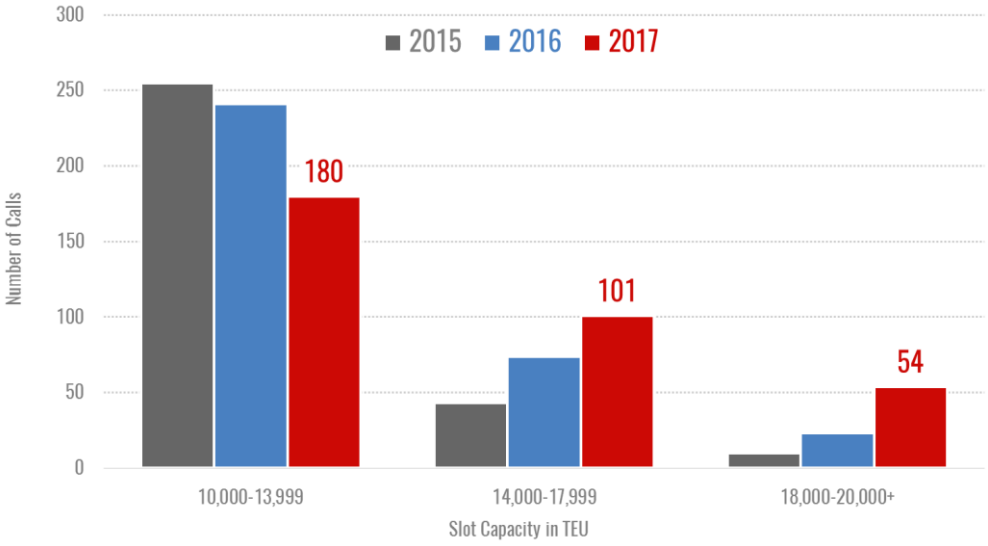

Figure 3.4: Ship capacity development 2015-2017[6]

[5] PORT OF HAMBURG MARKETING, 2016: Charts of yearly press conference 2016
[6] PORT OF HAMBURG MARKETING, 2017: Charts of half-year press conference 2017

4 Field-based investigations – Requirements, set up and execution

Section 3.4 reasons the necessity of field-based measurements to acquire dynamic draft data of the actual vessel fleet. This section lists the required hydraulic and hydrodynamic parameters and provides a description of acquisition methods and applicable sensors.

Assessment of the vessel fleet on the Lower Elbe passage within the years 2013 and 2016 lists seven extraordinary large ship classes that sail the Elbe passage on a regular basis. Ship sizes range from Panamax, over Post- and New-Panamax to Ultra Large Container Vessels (ULCV). In addition to container ships, extraordinary large bulk carriers (Capesize) need to be taken into account.

To gain a reliable database, a minimum number of three measurements campaigns should be performed for each of the seven vessel categories. The campaigns should investigate at least two inbound (IB) approaches and one outbound (OB) approach per ship category.

Table 4.1 shows the matrix of vessel sizes to investigate and the number of measurement campaigns. The total number of necessary measurement campaigns results in 21 runs in total.

Table 4.1: Matrix of investigation campaigns [7]

Ship class	Ship size	TEU	LOA	Beam	Min. FWD	Runs
C294	Panamax	4600	294.0 m	32.25 m	> 11,80 m	2 x IB, 1x OB
C335	Post-Panamax	8750	335.0 m	42.80 m	> 11.70 m	2 x IB, 1x OB
C347	New Panamax	11040	347.5 m	45.20 m	> 11.60 m	2 x IB, 1x OB
C366	ULCV	13830	365.5 m	51.20 m	> 11.20 m	2 x IB, 1x OB
C396	ULCV	16020	396.0 m	53.60 m	> 11.20 m	2 x IB, 1x OB
C400	ULCV	19000	399.7 m	58.60 m	> 11.20 m	2 x IB, 1x OB
BULK	Capesize	-	300.0 m	50 m	> 13.00 m	2 x IB, 1x OB

4.1 Required parameters for dynamic draft determination

Ship-based field investigations need to identify the investigated design vessel by name, ship type and specific voyage data. Ship configurations like length, beam and specific arrangements have to be known. Specific voyage data like draft, loading, time of berth/unberth need to be documented.

To determine real squat, horizontal and vertical position of the design vessel needs to be recorded at multiple positions on the vessel's surface with high frequency and high resolution. Vessel movements like trim and heel can be determined from vertical distances of such positions. Real squat can be determined from the vertical difference at each position between position height at rest and position height underway. All calculations need to base upon the static lateral and vertical positions of the ship at rest. Ship at rest means a vessel in a static, unmoored situation without propulsion and influences of tug forces. Exact timeslot of that situation needs be documented.

[7] PROJEKTBÜRO FAHRRINNENANPASSUNG, 2006: B.2 Erläuterungsbericht: Beschreibung des Vorhabens, Technische Planung. German

Table 4.2: Overview of necessary parameters for squat determination

Category	**Parameter description**
Vessel identity	Vessel name
	Ship type
Voyage data	Loading condition
	Time of berth, unberth
	Mooring situation
Ship configurations and hydrostatics	Length, beam, height
	Body plan
	Draft at rest, fore, mid, aft perpendicular
	Block coefficient
	Configurations for TPC, LCG, LCB and MCT
Ship dynamics	Lateral and vertical position
	Trim, heel
	Heading, course over ground
	Speed over ground
Fairway-based parameters	Water level
	Water depth
	Water density
	Current velocity, direction
	Channel topography
	Channel cross-sections
Maneuverability parameters	Revolutions
	Ruder position
	Rate of turn
	Wind direction, speed
Ship-ship interaction	Encountering, overtaking situation
	Name, ship type
	Length, beam, draft
	Course, speed

Draft is the vertical immersion and therefore distance between water level and ship's keel. Water level has to be known as well as the vertical dimensions of the ship's hull. Draft has to be documented for the position at the fore and aft perpendiculars as well as the perpendicular amidships. Determination of dynamic draft is based on draft at rest.

Static and dynamic draft during Elbe passage is influenced by density. To determine water density, water temperature and salinity have to be recorded. Change of draft due to density depends on displacement, density and specific tons per centimeter immersion (TPC). Change of trim due to density depends on displacement, density and the location of the Longitudinal Centre of Gravity (LCG), the Longitudinal Centre of Buoyancy (LCB) and the Moment to Change Trim (MCT).

Under-keel clearance is the distance between dynamic draft and channel bed. Water depth is the vertical distance between water level and channel bed topography.

One additional factor for squat estimation is speed of the design vessel travelling through water. In dependence from velocity direction and vessel course over ground, speed through water is the sum of vessel speed over ground and current velocity.

Additional maneuvering data like revolutions, rate-of-turn and ruder position should be recorded. Meteorological data and specifically wind direction and speed should be recorded as well.

For ship-ship interactions e.g. encountering and overtaking, the approaching vessels need to be identified and ship configurations like length, beam and draft need to be recorded. Encountering time, vessel speed, distance and course over ground need to be determined.

Table 4.2 summarizes all necessary parameters mentioned.

4.2 Conventions on parameter acquisition

4.2.1 Conventions for parameter acquisition

The field investigations aim for a real squat data base with a high data density and high parameter accuracy. To fulfill such goal, it is necessary to formulate requirements and conventions for the parameter acquisition.

In order to derive consistent data from various sources and sensors, all position data is required to be converted into the national coordinate system and leveled to NHN.

Figure 4.1 illustrates furthermore the convention of positive and negative trim and heel. Table 4.3 specifies the conversion parameter.

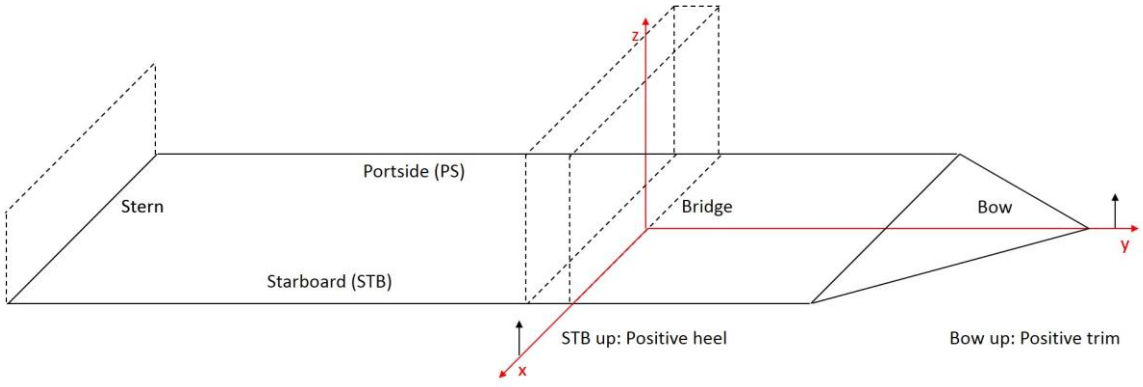

Figure 4.1: Convention for positive trim and heel

Table 4.3: National coordinate system requirements

Geodetic reference system	ETRS89
Ellipsoid	GRS80
Geoid	Normal height null (NHN)
Projection	Universal Transverse Mercator (UTM)
Zone	32 North
Central meridian	9° East

4.2.2 Required frequencies for parameters and sensors

Primary determination parameters need to fulfill a minimum in frequency and parameter accuracy. Within the results, real squat determination data should provide a high data frequency and accuracy. Thus, a minimum frequency of 1 Hz and an accuracy of ±0.1 m should be obtained over the full section of measurements. From such requirements, frequencies and accuracies are derived for lower degree parameters like trim and heel. Basic parameters like lateral and vertical position need to be acquired with a frequency of 2 Hz and an even higher accuracy. From the position data, parameters like course over ground and heading are determined. Required frequencies and accuracies are governed by the position frequency and accuracy.

A higher frequency within the primary data facilitates filtering and smoothing. To prevent a substantial loss of frequency within the final determination due to filtering and smoothing, also real squat should be acquired with a minimum frequency of 2 Hz.

Table 4.4 lists the basic parameters with required frequencies and accuracies. From that requirements, measuring frequencies are derived for all sensors, which are listed in Table 4.5.

Table 4.4: Overview on required parameter frequencies and accuracies for squat determination

Parameter	**Frequency**	**Accuracy**
Squat	2 Hz	≤0.1 m
Lateral position	2 Hz	≤0.05 m
Vertical position	2 Hz	≤0.05 m
Heading	2 Hz	≤0.08°
Corse over ground	2 Hz	≤0.4°
Trim	1 Hz	≤0.01°
Heel	1 Hz	≤0.09°
Draft at rest	1 Hz	≤0.09 m
Change of draft due to change of density	1 Hz	≤0.01 m
Water level	0.5 Hz	≤0.06 m

Table 4.5: Required frequencies for sensor system deployment

Tide gauges	1/60 Hz, interpolated to 1 Hz
GNSS antennae	2 Hz
Radar gauges	1 Hz
VDR	System-dependent, interpolated to 1 Hz
AIS	System-dependent, interpolated to 1Hz
Video cameras	1/10 Hz, single shot
CTD	1 Hz
DVL	1 Hz

4.3 Parameter acquisition methods

4.3.1 Parameter acquisition using documentations

Voyage data sheet:

The vessel is identified by the voyage data sheet on board of the vessel. The sheet contains vessel name, ship type as well as loading situation and draft situation.

Documentations:

The measurement team on board of the vessel performs additional draft-readings at fore, mid and aft perpendicular. The team documents the berthing situation and identifies the time-slot of vessel at rest without propulsion or tug forces.

General Arrangement:

Vessel length, beam and height as well as the complete body plan is copied from the General Arrangement Plan (GA).

Stability Booklet:

All hydrostatic parameters are copied and documented from the Stability Booklet (SB). SB contains all information about the vessel behavior at rest and underway e.g. displacement in dependence of draft and trim situation, block coefficient in dependence from draft and trim as well as information about TPC, MCT and positions of LCG, LCB, LCF.

4.3.2 Parameter acquisition using external data bases

Tide gauging stations:

German Federal Waterways and Shipping Administration (WSV) and Hamburg Port Authority (HPA) run more than 20 gauging station along the Lower Elbe waterway. Figure 4.2 shows name and location of the stations. WSV and HPA provide actual gauging data for each measurement campaign. Gauging data is post-processed, short-time fluctuations due to waves and sinkage due to vessel passage are corrected. Water level between gauging stations is spatiotemporally interpolated using

spline interpolation. Data is transferred from gauging zero (PN) into normal height null (NHN). Vessel position is projected on the spline and a continuous time series for water level at vessel position is determined for each measurement campaign.

Figure 4.2: Water gauging stations at Lower Elbe waterway

Navigational soundings:

For navigation operations and waterway maintenance, German Federal Waterways and Shipping Administration (WSV) and Hamburg Port Authority (HPA) run continuous soundings along the Elbe fairway systematically. For each measurement campaign, the actual data set was provided and transferred into a Digital Terrain Model (DTM) referenced on NHN. The vessel's water plane area is projected on the topography and the channel bed height spatially averaged. A continuous time series for channel bed height at each vessel position is determined. In combination with the water level time series, a continuous water depth time series is determined. Furthermore, the DTM makes it possible to generate waterway cross-sections along the vessel track.

4.3.3 Parameter acquisition using sensor systems

Global Navigation Satellite System (GNSS):

In order to determine ship position, vessel speed, course over ground, heading and ship movements at each time, the positioning technique based on GNSS is used. GNSS is a reference system for navigation using USA's NAVSTAR Global Positioning System (GPS) and Russia's Global'naya Navigatsionnaya Sputnikovaya Sistema (GLONASS) satellite technologies. Satellites are the space segment of the GNSS. They are spread in six orbital planes on circular orbits and run at an altitude of about 20200 km above Earth surface. They are inclined by > 50° with respect to the equator and run with orbital periods of approximately 11 hours 58 minutes. Every satellite broadcasts a signal, based

on an internal atomic clock with a stability of 10^{-13}, containing information on the satellite orbits, orbit perturbations, GNSS time, satellite clock, ionospheric parameters and system status. The signal is transmitted on two carrier frequencies within the microwave region between 1000 and 2000 megahertz, so called L-band. GPS and GLONASS receivers are user segment of the GNSS. A receiver reconstructs the carrier frequency and extracts codes and navigation messages. The receiver performs a Doppler- shift measurement by comparing the received signal with a generated reference signal. The receiver determines his position in relation to the satellite via the Doppler shift. Using the signals of at least three satellites, the receiver determines its position.

MAUSHAKE & JOSWIG (2004) recorded the horizontal and vertical positions of four receivers, fitted on the vessels surface at bow and stern. Synchronously, they recorded the vertical height of the water level using gauging stations along the Lower Elbe. Afterwards, they calculated the vertical distance between recorded positions and water levels at each point of time. Squat was determined by the vertical difference between the distance from water level to vessel surface, when ship was at rest, and the distance between water level and vessel surface, when ship was traveling. Vessel motions due to trim and heel were determined from vertical distances between the receiver positions.

The same technique is used to determine the parameters trim, heel and squat. Six GNSS receivers are installed on the design vessel's surface (Figure 4.6), logging constantly their positions. Afterwards the GNSS data is intersected with high precision real-time positioning data (HEPS) from land-based stations of the Satellite Positioning Service of the German National Survey (SAPOS). Such post-processing gains high precision of ± 0.05 m in horizontal and vertical position.

Radar gauges:

Draft at rest is obtained via visual single point readings of the perpendiculars on the vessel's hull. In order to obtain a method to constantly measure and store draft data, an indirect measuring technique is established. Radar gauges are fitted on the main deck at the outer edge of the vessel's hull (Figure 4.7). Horizontal and vertical position of the radar gauges are levelled within the ship's coordinate system. The gauges are oriented downwards, rectangular to the water surface. Using microwave technology, the gauges constantly meter and store the distance to the water surface. In combination with the GA, distance between gauge position and keel is determined. From that distance the distance between gauge and water level is subtracted and draft, distance between water level and keel, is determined.

Voyage Data Recorder (VDR):

The International Maritime Organization (IMO) and the International Convention for Safety of Life at Sea (SOLAS) require a VDR system on board of the design vessels. VDR is a data recording system that follows the requirements of IMO and SOLAS by collecting, compressing and storing data from various sensors on board of the vessel. It consists of a data collection unit (DCU) and a data recording unit (DRU). DCU collects continuously all vital data for ship operation and stores the data on the DRU within an external tamper-proof protective capsule. CDU is fitted in the wheelhouse under the bridge where all sensor data intersect. DRU is fitted on the most accessible spot on the deck above the navigation deck. The external floatable capsule withstands impacts, pressure and heat. In case of a marine incident e.g. sinking of the vessel, the capsule can be rescued and data can be recovered and replayed for investigational reasons by owner and authorities. According to IMO regulations, sensor data of the last 48 hours has to be stored. VDR compresses the sensor data according to the standards of the National Marine Electronics Association (NMEA 0183), which makes it possible to convert it into sensor depending time series and gain maneuverability parameters. NMEA data is

readout from VDR storage unit. Bridge communication and video data is not readout due to privacy protection. Table 4.6 contains relevant VDR parameter and their NMEA coding.

Table 4.6: Overview on relevant VDR parameters and related NMEA sentences

Parameter	**Sensor**	**Talker ID**	**NMEA sentence**
Time and position	GPS	GP	GGA
Speed over ground	GPS	GP	VTG
Speed through water	GPS	GP	VBW
Rudder angle, order and response	Rudder Angle Sensor	II	RSA
Revolutions, order and response	Shaft meter	-	PAVBADC
Heading	North Seek Gyro	HE	HDT
Rate-of-turn	Radar	RA	ROT
Wind speed and direction	Radar	RA	MWD
Depth under keel	Echo Sounder	SD	DPT

Automatic Identification System (AIS):

The International Maritime Organization (IMO) and the International Convention for Safety of Life at Sea (SOLAS) issue the requirement of an AIS class-A system on board of regulated vessels with a gross tonnage of more than 300. AIS is an automated system that provides and exchanges navigational information for navigational aid and vessel tracking services between suitably equipped vessels and shore stations. AIS broadcasts on two designated marine very high frequency radio (VHF) channels. AIS equipment on board is a transceiver equipped with a GNSS antenna and a VHF antenna. The transmitter broadcasts unique vessel information and navigational status via distinct VHF messages. Vessel name, size, type, cargo and draft information as well as position, course and speed status. The receiver collects the broadcasted data from ships within a defined radius around the vessel. Using NMEA standards, the received data can be replayed within the Electronic Chart Display and Information System (ECDIS). AIS class-A uses the transmission protocol called Self Organizing Time Division Multiple Access (SOTDMA). While underway, a vessel transits every 2 to 10 seconds identity, position, speed over ground, course over ground, true heading, rate-of-turn, navigation status and time stamp. Collecting the AIS data with a transceiver with integrated storage unit makes it possible to store all information about encountering and overtaking vessels (Figure 4.8).

Video cameras:

Additionally to AIS and documentation, video cameras are installed at the bow and the stern of the design vessel (Figure 4.8). The cameras record single shot pictures with a medium frequency. Pictures and exif metadata are stored on internal storage cards. Afterwards metadata is processed and a time stamp is integrated into the picture. Processed pictures are edited to a movie with running time stamp. The movies enable to identify mooring situation, encounters and overtakers.

CTD-probe:

Accurate measurements of density can only be performed in laboratories. An in situ measurement is not possible. For information on density distribution along the section of measurements, an indirect method with a conductivity, temperature and depth (CTD) probe is used (). The probe is a cluster of three single sensors. One sensor measures hydrostatic pressure. With air pressure adjustment, the water depth is derived. The other sensors measure temperature and salinity via electrical conductivity. The sensors are fitted within a cylindrical metal case. The CTD probe is fitted outside a research vessel and lowered down to an almost constant depth between 1-2 m. Data is transferred online via cable to a research PC. With that PC, the sensors are triggered and the data was visualized and stored on the PC, using specific probe deployment software. Data is post-processed and potential density determined. With depth, temperature and salinity, potential water density can be determined via UNESCO equation of state formula. Potential density meets in situ density using a polynomial fit. Especially in shallow water depths at low pressure, potential density matches in situ density with high precision. Combined with GNSS data, a potential density time series is obtained for each vessel location during the measurement campaign.

Doppler Velocity Log (DVL):

Although IMO regulations require a speed log on board of the design vessels, such speed logs are often not fully functional. Furthermore, the sampling rate is often low and velocity direction is neither displayed nor logged. To obtain current velocity and direction at the design vessels position, in situ measurements were performed with a Doppler-Velocity Log (DVL). The DVL is an active sonar with four beams, which are piezoelectric transducers to transmit and receive sound signals. A DVL contains an electronic amplifier and a receiver. Travelling time is obtained from an internal clock and an internal compass determines heading. A pitch and role sensor determines motions and orientation. A temperature sensor is used to estimate the sound velocity at the instrument position. The DVL sends out acoustic pings, which are reflected by particular matter, transported with the current. In order to determine the Doppler frequency shifting, an analog-to-digital converter and a digital signal processor are required to sample the returning signal. With the Doppler-frequency shift, velocity can be determined by calculating the relative distance to the reflection point. Velocity is measured in horizontal and vertical direction. If the channel bottom is in a reachable distance, the so called bottom tracking allows a calculation of the relative position of the instrument. The DVL is able to determine velocity and current direction in several layers depending on sensor type and deployment. The DVL is fitted outside of a research vessel in a specific water depth between 1-2m (Figure 4.12). The downward-looking DVL is connected to a PC with a cable. The DVL is triggered and deployed with the PC. The incoming data is visualized and stored on the PC. Data is post processed afterwards and in combination with GNSS sensors, a continuous time series of current velocity is determined. With the speed over ground time series, the speed of the design vessel, travelling through water, is obtained.

4.4 Sensor systems set up and deployment

4.4.1 Sensor systems on design and research vessel

The variety of sensor systems, makes it necessary to split the sensors into two systems. One system was based on the design vessel itself and one system is based on a research vessel (Figure 4.3)

Figure 4.3: Research vessel

Sensor system on the design vessel

Design vessel based system contains the VDR, two radar gauges, six GPS and GLONASS antennae as well as two video cameras. Design vessel set up contains two video cameras (VC) at the bow and the stern, two radar gauges (RG) at the bow and at the stern and GNSS antennae (GNSS). Figure 4.4 shows the sensor set up on the design vessel.

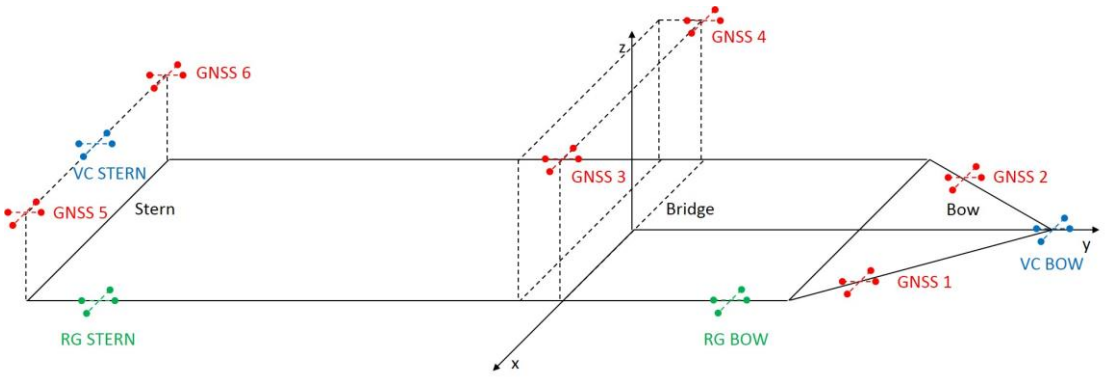

Figure 4.4: Sensor system set up on design vessel

GNSS antennae are located at the bow, at the navigation deck and at the stern with one antenna at starboard (STB) and one antenna portside (PS) at each position. All devices have internal batteries and data storage cards. All battery capacities are dimensioned in such a way, that they provide power for at least 10 hours each. All sensors are mounted on device carrier clamp systems. Such

clamp systems are designed in a way to be installed and uninstalled without damaging the vessel. The clamp layout allows a single person to carry and mount the clamp on the coaming or the railing within a very short amount of time. The device is fitted onto the clamp after installation.

Sensor system on the research vessel

Water-tangent sensors like the CTD-probe and the DVL are installed on an accompanying research vessel, which is designed to go ahead the design vessel all along the Elbe passage. It is equipped with two additional GLONASS antennae, to log the vessel position, course and heading to intersect the data of the research vessel onto the position of the design vessel.

Research vessel set up contains two GNSS antennae, a CTD probe with PC connection and a DVL with PC connection (Figure 4.9). Figure 4.5 shows the sensor set up on the research vessel. The GNSS antennae are installed at the bow and the stern of the research vessel along the longitudinal center line. GNSS are mounted on special carrier poles fixed to the deck.

CTD probe is mounted on a cantilever arm at the starboard side of the vessel. The CTD probe is lowered down to a water depth of 1.5 m and held at a constant depth. CDT probe is connected to a PC with a waterproof cable.

DVL is mounted on a carrier pole and lowered down through a duct and fixed at a water depth of 1.5 m. DVL is connected to a second PC via waterproof cable. GNSS antenna at the bow is connected to the DVL PC via cable and GNSS antenna at the stern is connected via cable with the CTD PC.

GNSS antennae are equipped with battery packs and storage cards. PC, DVL and CTD are powered over on-board power supply. Data from CTD and DVL is stored on the PC.

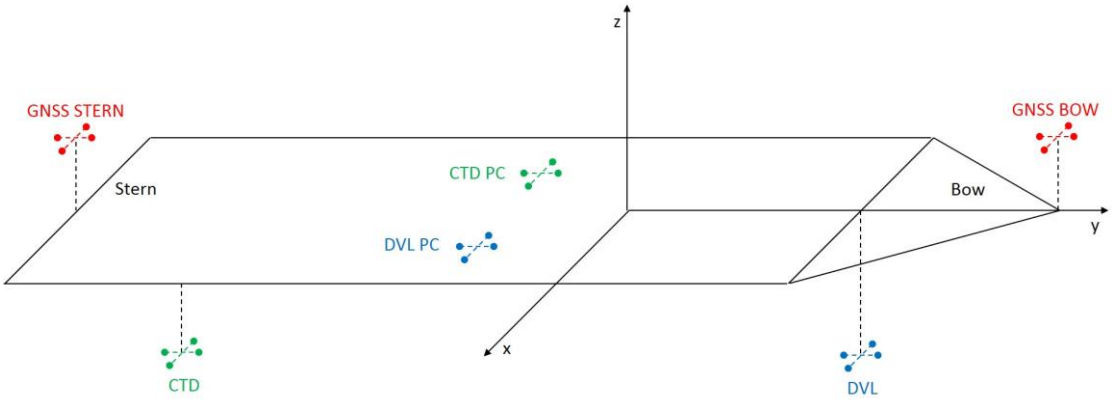

Figure 4.5: Sensor system set up on research vessel

4.4.2 Design vessel based sensor deployment

Deployment of GNSS receivers:

The GNSS sensor system on board the design vessel contains six receivers with antennae. Four receivers are LEICA receivers with GS14 antennae, able to work with GPS and GLONASS. The receivers are fitted within the antennae. Receiver and antenna are powered by an external 9 Ah battery pack. Maximum sampling rate is 2 Hz.

Data storage is an internal 16 GB storage card. Two TRIMBLE receivers with TRM ZEPHYR GEOD antennae, able to work with GPS only, are installed additionally. Receivers are connected to the

antennae via cable. An external battery pack powers the receivers and antennae. Receivers sample data with a rate of 1 Hz. The data is stored in an internal storage in the receivers.

The antennae are installed upward looking at the bow, the bridge wing and the stern of the design vessel. One antenna is installed starboard (STB) at the bow and one antenna portside (PS) at the bow. The antennae are mounted on self-developed stainless steel clamps on the bulwark.

Two antennae are installed on the navigation deck outside the bridge on the bridge wing. One antenna at PS, one at STB. In dependence of a roof, the antennae are mounted on stainless steel clamps on the railing or on antenna-poles, connected to the frame of the roof.

Two antennae are installed PS and STB at the stern on the highest possible deck. Antenna are mounted with stainless steel clamps on floodlight housings or on antenna-poles connected to the railing. Safety leashes secure the sensors to the railing.

Figure 4.6 exemplarily shows the different installation varieties of antennae at bridge wings and stern. Nomenclature specifies bow STB position to GNSS 1, PS position to GNSS 2. Bridge wing STB is position GNSS 3 and bridge wing at PS is GNSS4. At the stern GNSS 5 position is at STB and GNSS 6 position is at stern PS.

Figure 4.6: GNSS antennae on bridge (l.) and at stern (r.)

Deployment of radar gauges:

Two VEGAPULS 68 radar gauges are installed on the design vessel. Radar gauges work with a sampling rate of 700 ms and a storage rate of 1 Hz. Data is stored on an internal loop storage with a capacity of 12 hrs. An internal battery pack powers each system. The gauges are installed seaside and downward looking at the bow and the stern of the vessel. Figure 4.7 shows the stern radar gauge and the bubble tube level.

Each gauge is mounted on a stainless steel clamp connected to the railing at the stern or the bulwark at the bow. Sampling technology of the gauge requires a distance of around 0.8 m from the ship's hull. Therefore, the gauge itself is mounted on a spherical head on a cantilever arm that is connected to the clamp. During installation, the gauges are leveled rectangular to the water using the spherical head and a bubble tube. A safety leash secures the sensor to the railing. Nomenclature specifies radar gauge at the bow to RG BOW and stern gauge to RG STERN.

Figure 4.7: Stern radar gauge (l.) and bubble tube level at bow (r.)

Deployment of video cameras:

Two GO PRO HERO 3 cameras are installed at the bow and the stern on the longitudinal center line of the design vessel (Figure 4.8). Video cameras are connected to external battery packs. The cameras sample pictures with 0.1 Hz. Pictures are stored on internal 32 GB storage cards. Camera at the bow is mounted to a magnetic base, which is located on the bulwark at the bow. Camera at the stern is mounted to the railing. Nomenclature sets cameras to VC BOW and VC STERN.

Figure 4.8: Video cameras at bow (l.) and stern (r.)

Data extraction of Voyage Data Recorder:

Each design vessel is equipped with a VDR with a similar operating principle. Functionality and connectivity are dependent from crew and manufacturer. E.g. DEBEG 4300 and DEBEG 4350 by SAM ELECTRONICS has connectivity with an Ethernet cable. Data is restored using a special replay software. Data of IS VDR G4 by INTERSCHALT is extracted using a replay software on the bridge computer. Data of VR-3000 by FURUNO is stored on an online logging PC, connected to the VDR. JCY-1900 by JRC has USB ports at the bridge panel and prepares data transfer of the last 24 hrs via transfer button.

4.4.3 Research vessel based sensor deployment

Deployment of GLONASS receivers:

Two GNSS receivers are installed on board of the research vessel (Figure 4.11). Both receivers are within LEICA GS 14 antennae, powered by external 9 Ah battery packs. Receivers sample with 2 Hz and store on internal 16 GB storage cards. Both antennae are installed on the longitudinal center line of the research vessel. One at the bow (GNSS BOW) and one at the stern (GNSS STERN). Both antennae are connected via RS232 cables with two LOGIC INSTRUMENTS B300 PCs. PCs are powered by on-board supply (Figure 4.9).

Deployment of CDT probe:

SEA & SUN TECHNOLOGIES (SST) 48M CTD-probe is mounted to a cantilever arm at the starboard side (Figure 4.10). A cable connects the CTD with one PC. NMEA sentences for time and position are sent from GNSS via cable to the PC. CTD probe is synchronized by that GNSS signal. CTD is pulled through the water at a constant depth of around 1.5 m. Probe is triggered and deployed with the STANDART DATA ACQUISITION software by SST. Data is sampled with 1 Hz using the continuous mode of the probe. Data is stored on the internal probe storage and on the PC as well.

Deployment of Data Velocity Log:

The TELEDYNE RDI WORKHORSE NAVIGATOR DVL is mounted downward looking to a stainless steel pole (Figure 4.12). The pole is lowered down into the water through a duct in the center of the bow of the research vessel. DVL is pulled through the water at a constant depth of 1.5 m below water level.

DVL is connected to a PC by cable. Sampling rate was 1 Hz and data was stored on the PC. DVL is triggered and deployed with TELEDYNE RDI WinADCP software.

Deployment of AIS:

SIMRAD AI50 AIS transponder is fitted onto the panel of the research vessel. VHF and GPS antenna are mounted on the cabin roof. AIS is powered with on-board supply. The device samples AIS data within a 5 mile radius and stores the data with a 1 Hz sampling rate on an internal 8 GB storage card (Figure 4.9).

Figure 4.9: Research vessel AIS (l.) and measurement PCs (r.)

Figure 4.10: Cantilever arm for CTD probe at STB side of the research vessel

Figure 4.11: GLONASS antennae at bow (l.) and stern (r.) of the research vessel

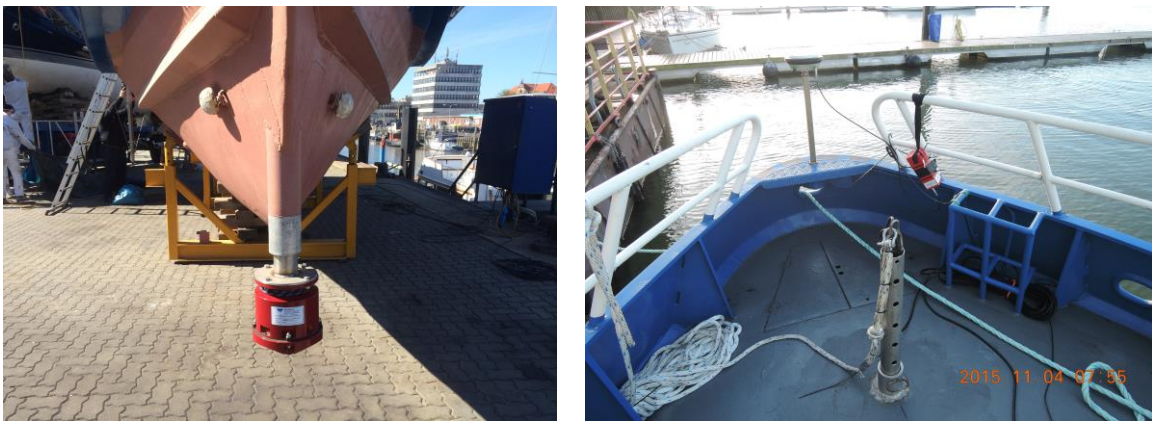

Figure 4.12: Mounted DVL (l.) and steel pole through bow duct (r.)

4.5 Methodology for determination of reference positions

4.5.1 Determination of single positions from GNSS antennae

Single point positions are based on GNSS data from the LEICA and the TRIMBLE antennae and receivers. LEICA data is downloaded within the internal SMARTWORX raw data format and transferred into the post processing software using antenna reference file GS14 PILLAR with 0 m offset. TRIMBLE raw data is downloaded and converted into the receiver independent exchange format (RINEX). RINEX data is transferred into the software and referenced with TRM41249 NONE antenna file with 0 m offset. LEICA data frequency is 2 Hz, TRIMBLE data frequency 1 Hz.

LEICA Geo Office Professional Software is used with project coordinate system settings based on Table 4.3 using the European Terrestrial Reference System ETRS89 with the GRS89 ellipsoid and the GCG2011 geoid. Antennae raw data is post processed with geodetic post-processing positioning service (GPPS) data from the Satellite Positioning Service (SAPOS) of the German National Survey. GPPS data is ordered with maximum frequency of 1 Hz from 5 different SAPOS station along the vessel track based in Hamburg, Lower-Saxony and Schleswig-Holstein.

The distance between GNSS 1 antenna position and reference station is determined along the vessel track. Reference data is ordered from the closest station to the vessel with a data overlap of 10 minutes at the intersection area between two reference stations. Table 4.7 gives an overview about the general reference sections and their boundaries, which varied between in- or outbound vessel track.

Table 4.7: Sections of GPPS data reference stations

Station	Location	ID	Section	Easting boundary	Northing boundary
CUX	Cuxhaven	0641	Buoy E6	452.659	5.984.092
			CUX-CAD	495.703	5.966.436
CAD	Cadenberge	0664	CAD-CUX	495.703	5.966.436
			CAD-ITZ	517.355	5.969.382
ITZ	Itzehoe	0708	ITZ-CAD	517.355	5.969.382
			ITZ-STD	531.759	5.951.651
STD	Stade	0662	STD-ITZ	531.759	5.951.651
			STD-HHW	543.689	5.935.910
HHW	Hamburg West	0836	HHW-STD	543.689	5.935.910
			Berthing Point	562.191	5.928.681

GPPS raw data is ordered and downloaded from SAPOS server in RINEX format and transferred into LEICA Geo Office Pro software. GPPS data is set as control points for raw data intersection. Maximum base length is determined between control points and limited to a maximum length of 30 km. Elevation angle settings for post processing are 10° for the positions at bow and stern, positions GNSS 1, 2, 5, 6 and 5° for the bridge wing positions GNSS 3 and 4. Raw data and GPPS data is intersected and resulting post processed data is filtered by quality. Navigated and interpolated positions are erased and only data with a horizontal and vertical quality of better than 0.055 m is used for further determinations. Such quality selected data is edited with Point ID, UTC time, 3D

position, horizontal position, vertical position as well as 2D and 3D quality and transferred into ASCII format.

TRIMBLE antennae data is interpolated to a data frequency of 2 Hz. ASCII data is transferred and visualized by Northern Instruments NI DIADEM software as time series for quality management. Each position is checked again. Not plausible data as well as not reasonable peaks are manually erased. Final time series is saved as ASCII files for further use.

4.5.2 Determination of fore and aft perpendicular position from single position values

Fore (FP) and aft perpendicular (AP) positions are fixed within the ship's coordinate system. Distances within the ship's coordinate systems are stated in the stability booklet and mariners are used to determine squat and draft for FP and AP position. To determine FP and AP positions, the intersection of all data from each single GNSS antennae positions is necessary.

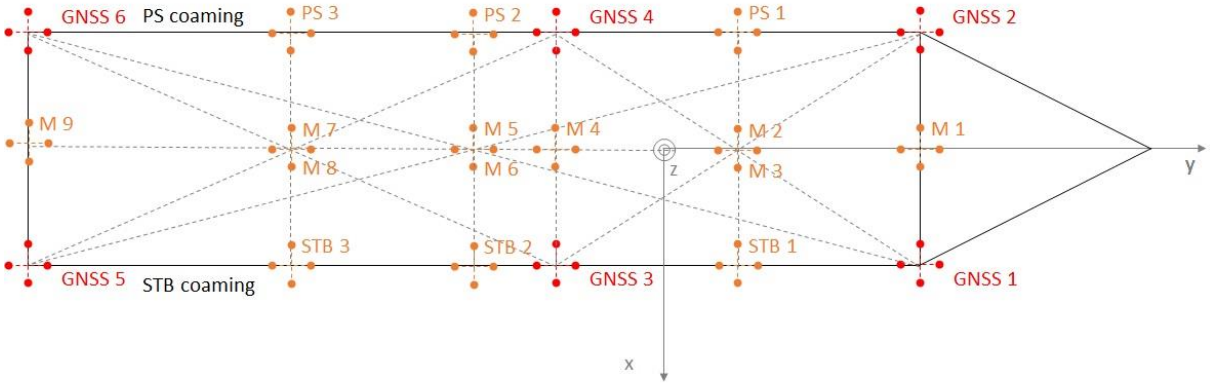

Figure 4.13: Virtual points on coaming reference plane

One approach projects all positions onto one plane layer referenced to the main deck coaming. The horizontal positions of the antennae within the ship's coordinate system as well as the vertical distances between GNSS sensors and coaming are known from the preparatory measurements and the sensors allocation measurements during the campaigns. The vertical distances from coaming to sensor positions are subtracted from the sensor positions, so that the sensors are projected onto the a virtual plane layer.

In a first step, heel at bow, stern and amidships are determined by the angles between the two opposite positions on the lateral axis. The horizontal position of the single point positions are iteratively corrected by the heel results. Then, heel corrected reference plane points are determined.

In a second step, the resulting single point positions on the reference plane are intersected with the opposite single point positions. The intersection knots on the longitudinal centerline are treated as additional virtual points on the reference layer. Figure 4.13 shows the principle of the position intersection and identifies the virtual points on the centerline (M1-M9). The absolute position and position quality of each virtual point is determined from the six heel corrected single point positions.

To determine trim, heading, absolute positions and position qualities of FP and AP, the 9 virtual points are combined to 36 virtual point-pairs. Trim, heading, FP and AP are determined for each virtual point pair. The results are averaged, weighted by the distance between pairs and the point's position qualities.

Another approach determines trim and heading directly between each pair of the single point positions at PS and STB. The results are averaged by weighted distance and position quality and also projected as additional virtual points on the coaming reference layer. Figure 4.13 displays the virtual points on Portside and Starboard. Between two opposite positions, the results are again averaged to gain results for the virtual centerline.

Finally, the differences between the two approached are determined and the initial positions are adjusted by the differences. The two approaches are reiterated until stable results for trim, heading and FP and AP positions are reached. In general, four iteration steps are necessary to gain stable results. The iteration between the two approaches makes it possible to respect heel, torsion and hogging, even if not all six single point positions have sufficient data amounts or sufficient data qualities. The averaged final absolute position and quality for FP and AP became basis for all further determinations.

The application of the two-approach iteration is possible with a data set of minimum three single point positions with a minimum of one data set on PS and one data set on STB. Each further data available increases the positions quality and the result accuracy. If less than three single point data sets were available, no FP and AP positions can be determined and in consequence, no further determination is possible.

4.6 Performance of field-based investigations

Five shipping companies, which run suitable design vessels on a regular basis along the Elbe River passage, have been informed about the planned measurement program in 2013. An intense dialogue was started to inform the companies about the research motivation, the expected outcome and the expected work on board their vessels. The shipping companies provided extensive support and helped to allocate adequate design vessels with respect to Table 4.1.

Between 2013 and 2016 more than 21 measurement campaigns were performed successfully on design vessels between 294 m and 400 m length on the Lower Elbe section between Elbe km 620 and Elbe km 755. A team[8] of more than 10 scientists and student research assistants planned, prepared and performed the field-based measurements. The design vessel research team stayed on board the vessel from Port of Hamburg to the next European port at outbound vessels. At inbound vessels, the team entered the ship at the previous European port and traveled on board to the Port of Hamburg.

Table 4.8 shows the performed measurement campaigns ordered by ship class. For data privacy protection, ship names are not listed. Campaign Class_ID is further used to identify data originating from the campaign.

[8] Investigations were performed by the Institute of River and Coastal Engineering of Hamburg University of Technology (Germany) in cooperation with Consulting Engineers von Lieberman GmbH (Germany) and German Federal Waterway Engineering and Research Institute – Hamburg Office (BAW-DH)

Table 4.8: Measurement campaigns performed between 2013 and 2016

Year	Class	#	Class_ID	In / Out	Dep. / Dest.	LOA	Beam	FWD	C_B
2014	C294	7	C294_1_OUT	Outbound	NLRTM	293.94	32.25	12.00	0.678
2015		17	C294_2_OUT	Outbound	DEBRV	294.16	32.20	12.75	0.666
2015		19	C294_3_IN	Inbound	DEBRV	294.07	32.25	12.00	0.670
2013	C335	3	C335_1_OUT	Outbound	NLRTM	335.07	42.80	13.00	0.653
2014		4	C335_2_OUT	Inbound	NLRTM	335.07	42.80	13.20	0.664
2014		5	C335_3_IN	Outbound	BEANT	335.07	42.80	12.75	0.652
2014	C347	8	C347_1_OUT	Outbound	DEBRV	347.00	45.20	12.10	0.667
2014		12	C347_2_IN	Inbound	FRLEH	347.45	45.20	13.10	0.684
2015		13	C347_3_IN	Inbound	FRLEH	347.00	45.20	12.90	0.677
2013	C366	1	C366_1_OUT	Outbound	DEBRV	365.50	51.20	11.50	0.663
2013		2	C366_2_OUT	Outbound	DEBRV	365.50	51.20	11.75	0.666
2014		6	C366_3_IN	Inbound	GBSOU	365.50	51.20	12.20	0.672
2014	C396	9	C396_1_OUT	Outbound	DEBRV	396.00	53.60	11.70	0.672
2014		10	C396_2_OUT	Outbound	DEBRV	396.00	53.60	11.55	0.669
2014		11	C396_3_IN	Inbound	GBSOU	396.00	53.60	12.30	0.679
2015	C400	14	C400_1_IN	Inbound	NLRTM	399.67	58.60	10.40	0.592
2015		15	C400_2_OUT	Outbound	BEZEE	399.67	58.60	11.60	0.606
2015		16	C400_3_OUT	Outbound	BEZEE	399.67	58.60	12.00	0.609
2016		21	C400_4_IN	Inbound	NLRTM	399.67	58.60	12.10	0.613
2015	Bulk	18	BULK_1_IN	Inbound	NONAR	299.92	50.00	13.30	0.816
2016		20	BULK_2_IN	Inbound	NLRTM	327.00	55.00	14.20	0.837

4.6.1 Preparatory measurements on design vessels

A research team visited an identically constructed vessel of each vessel class during berthing time at Hamburg Port several weeks prior the first measurement campaign with equivalent vessels of such class. With support of the local shipping companies, the measurement team entered the berthed vessel and asked the master for permission to copy the General Arrangement plan (GA) and the stability booklet.

During the visit of the vessel, all sensor carrying constructions, like steel clamps and antennae poles were installed to test their fitting on the vessel. Using distance meters, the device carriers were allocated with horizontal and vertical positions within the ship's coordinate system. Several control-points on the moored vessel were leveled with a tachymeter from the quay wall.

The preparatory visit and measurements makes it possible to compare the measurements with the GA. The pre-installation of the carrier systems ensure suitable device allocations and guarantee that the carrier systems would work on the equivalent vessels of that class as well. The research team established a device installation plan based on the preparatory measurement results. On each vessel, identical to such vessel, the measuring devices were located in the exact same way and at the exact same location within the ship's coordinate system. That procedure guarantees the repeatability of the sensor installation. Furthermore, it fastens up the installation process on the following vessels.

After the preparatory measurements, pictures of the vessels and the device locations were taken. All interesting specifications of that vessel class concerning device installation were documented and the carrier devices uninstalled. Figure 4.14 shows the application of a tachymeter and distance meter to allocate a control-point near GNNS 2 position at the vessel's bow.

Figure 4.14: Preparatory measurements with tachymeter and distance meter

4.6.2 Execution of measurement campaigns

Campaign performance on inbound design vessel

Inbound vessels are accompanied from Hamburg Port to the next European Port and inbound vessels vice versa. The design vessel measurement team, consisting of four scientists, enters the berthed design vessel minimum 12 hours before departure with all measurement devices and carrier systems as well as installation, maintenance and safety equipment.

First of all, the measurements team informs the master about the installation and measurement procedures and confirms on board safety regulations. In alignment with the shipping companies, master and chief are instructed to refrain from applying ballast or changing ballast water conditions during Elbe passage. The team copies the GA and the stability booklet and performs a test run on VDR data download. If VDR download is successful and all vessel specification regarding the installation of the carrier devices are reviewed, the carrier devices are installed at the intended locations. The horizontal and vertical position of the carrier devices is metered ones more with distance meters and folding rule. The functionality of all sensors as well as the battery status is checked and the sensors are synchronized to Coordinated Universal Time (UTC).

One team member leaves the ship before unberthing and meters draft at the fore and aft perpendicular and amidships landside on the draft meters. Metered data is transmitted to the team

on board via walky-talky. Three team members stay on board, connected with hand-held radio. With periodic switches, one member is assigned to the bridge, one is assigned to constantly monitor the sensors and one is off duty for a certain amount of time for recreation. The team members are connected via hand-held radio.

Campaign performance on outbound design vessel

On outbound vessels, all sensors are switched on into logging mode 1 hour prior unberthing. The radar gauges are switched out around 1 hour after unberthing. On inbound vessels, GNSS sensors and video cameras are switched on 1 hour prior entering the Elbe passage. The radar gauges are switched on around 1 hour before berthing.

During berthing and unberthing, the mooring and tug situation is monitored. Especially the moment of the unmoored vessel without tug impact is explicitly documented. During Elbe passage, all sensors, carriers and their positions are frequently checked once an hour. All situations like encounters, overtakers and pilot changes are documented. The measurement team had contact to the team on the research vessel via hand-held radio as well as via mobile phones.

After berthing at Hamburg Port or after leaving Elbe passage at buoy E11, all sensors are switched of and unmounted from the carrier devices. The data from internal data loggers is downloaded and stored on a PC. A copy of the data is stored redundantly on a portable USB drive. Afterwards, all carrier devices are uninstalled. All sensors, devices and equipment are packed. The measurement team leaves the vessel after berthing and after customs and immigration control. All sensors, carriers and equipment are transported to TUHH for maintenance and storage.

Campaign performance on inbound research vessel

The research vessel is stationed in Cuxhaven Port. Prior the first measurement campaign with that research vessel, the vessel is metered with distance meters and tachymeters from the quay wall. The measurements are compared to the General Arrangement plan and the sensor carrier positions are allocated. A team of three scientists plus the vessel's crew with one master and one bosun performs the measurement campaigns on board the research vessel. The scientists enter the research vessel one day before the campaign with all sensors and carrier devices as well as all installation, maintenance and safety equipment.

The carrier devices for the GLONASS antennae are installed at the bow and at the stern. The antennae are mounted on the carrier poles and connected to the data cables. Horizontal and vertical positions of the antennae are metered and documented.

The DVL is installed on a carrier pole and connected to the DVL data cable. The DVL is lowered down through a duct in the bow of the vessel. At a depth of 1.5 m, the pole is fixed and the vertical position of the DVL is metered and documented. The position of the duct is fixed within the ship's coordinate system and documented in advance. The CTD-probe is mounted to the cantilever arm and connected to the data cable. The cantilever arm is lowered down into the water and fixed in a depth of 1.5 m at an already known horizontal position. Vertical position of the CTD probe is documented.

Two research PCs are set up in the vessel cabin and connected with the data cables via RS232 intersections. CTD-probe, DVL and PCs are connected to the on-board power supply. A self-constructed uninterrupted power supply (UPS) unit buffers the on-board supply to uninterrupted supply. Transformers supply the sensors with the correct voltage. AIS system is set up in the cabin

and the GPS and the VHF antenna are installed on the cabin roof. All sensors are switched on and tested. CTD and DVL settings are checked and corrected if necessary. After positive checkup, all sensors are switched off. The GLONASS antennae and the PCs are uninstalled and the prepared vessel is locked.

For measurement campaigns with inbound vessels, measurement team and crew board the research vessel again 4 hours before the estimated time of arrival of the design vessel at the entrance of the Elbe waterway at Buoy E1. GLONASS antennae and PCs are installed and the distance between water level and antennae heights are metered and documented. All sensors are switched on and all sensors settings are checked again. The sensors are synchronized to UTC and the vessel is prepared for departure. 2 hours before the estimated time of arrival of the design vessel at buoy E11, the research vessel sails from Cuxhaven Port and takes course to buoy E11. Water police and pilots are informed via VHF about the measuring campaign.

After arrival at buoy E11, the research vessel waits for the arrival of the design vessel. All sensors are set into logging mode. The measurement teams on design and research vessel are in constant contact at that point of time. The distance between both vessels is monitored and communicated constantly. At a distance of three miles between the vessels, the research vessel enters the radar line of the fairway and sails ahead the design vessel with inbound direction and maximum speed. Distance between both vessels is reduced down to one mile. Distance is held constant between Brunsbuettel Port and Hamburg Port. Functionality and logging status are checked and documented on a regular basis every 30 minutes.

With arrival at Hamburg Port, seaside perpendiculars of the design vessel are metered from the research vessel. Draft is documented and communicated with the team of the design vessel. After berthing of the design vessel, the research vessel sails to Finkenwerder Port, where all data is downloaded from the logging devices. Data is stored on a mobile PC and additionally on an external, portable USB drive. All sensors are switched off, demounted and all carrier devices are uninstalled. All systems are carried back to TUHH for maintenance and storage.

Campaign performance on outbound research vessel

For measurement campaigns on outbound vessels, the research vessel's crew transfers the vessel from Cuxhaven to Finkenwerder Port several days before the campaign. The measurement team enters the vessel at Finkenwerder 4 hours prior design vessel's departure. The team installs and checks all sensor systems in the same way as abovementioned.

1 hour before the design vessel departure, all sensors are switched on and set into logging mode. The research vessel departs and sails to the berthing point of the design vessel. At the berthing point, the perpendiculars of the design vessel are read out, documented and communicated with the design vessel crew.

After unberthing, research vessel sails ahead the design vessel. Distance is increased to one mile and held constant between Hamburg and Brunsbuettel Port. Afterwards, research vessel sails on maximum speed and increases the distance up to 3 miles. The research vessel accompanies the design vessel to buoy E11. At that point, the research vessel goes out of the fairway. Sensors are stopped and data is downloaded to PC and external USB drive. The research vessel returns to Cuxhaven Port, where all sensors and carrier systems are demounted and transported to TUHH for maintenance and storage.

5 Data processing and parameter determination

5.1 Channel factors

5.1.1 Density

Direct measurements of water density are only possible by analyzing water samples. Nevertheless, in-situ measurements can be applied using the indirect potential density method. That method determines potential density by analyzing the three basic factors pressure, temperature and salinity. MILLERO & POISSON (1981) state, that potential density matches in-situ density with high precision, especially in shallow water depths at low pressure.

During the field investigations, such basic factors are directly measured in-situ applying the CTD-probe. The CTD-probe data is supplemented and validated by additional data from fixed CTD-gauging stations that German Federal Waterways and Shipping Administration (WSV) and Hamburg Port Authority (HPA) run.

Salinity is calculated by using conductivity with the approach of CHEN-TUNG & MILLERO (1977). CTD data is post-processed, verified and validated so that timelines for temperature, depth and salinity could be extracted. Potential density is determined via UNESCO equation of state formula for all measurements campaigns. Potential density is calculated using a polynomial fit, which is based on work of MILLERO & POISSON (1981) and defined in equation 5.1.

Figure 5.1 presents potential density over all measurement campaigns and shows, that there is freshwater between the Port of Hamburg at Elbe-km 620 and Elbe-km 680. From Elbe-km 680 to the mouth of the Elbe River at Elbe-km 750 potential density increases almost linearly to maximum density values between 1015 and 1030 kg/m³ which equal seawater density. A maximum range of 20 kg/m³ can be observed around Elbe-km 630. Range is caused by influences of wind, temperature, tidal currents as well as upstream afflux situation.

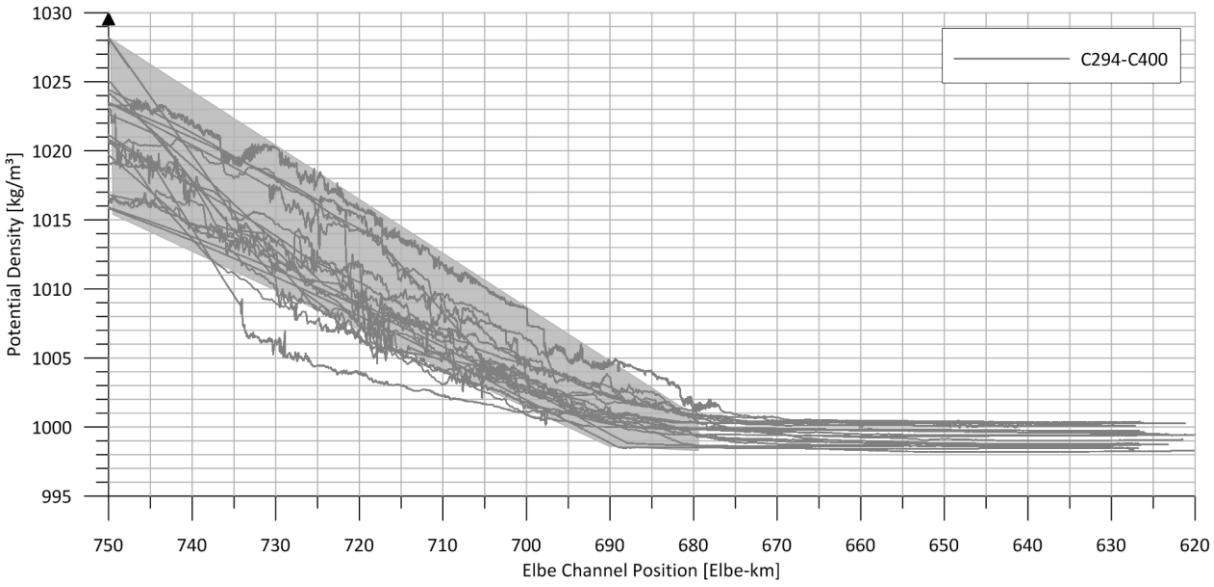

Figure 5.1: Potential density along Elbe passage for all campaigns

$$\rho = \rho_0 + AS + BS^{1.5} + CS^2 \quad (5.1)$$

with

$$\rho_0 = 999.842594 + 6.793952 * 10^{-2}T - 0.0959290 * 10^{-3}T^2 + 1.001685 * 10^{-4}T^3 - 1.120083 * 10^{-6}T^4 + 6.536332 * 10^{-9}T^5$$

$$A = 8.24493 * 10^{-1} - 4.0899 * 10^{-3}T + 7.6438 * 10^{-5}T^2 - 8.2467 * 10^{-7}T^3 + 5.3875 * 10^{-9}T^4$$

$$B = 5.72466 * 10^{-3} + 1.0227 * 10^{-4}T - 1.6546 * 10^{-6}T^2$$

$$C = 4.8314 * 10^{-4}$$

5.1.2 Water level

WSV and HPA provide water level data from 20 gauging station along the Lower Elbe waterway (Figure 4.2) for each measurement campaign. Such data is post processed and short-time fluctuations due to waves as well as sinkage due to vessel passages are corrected. Water level between gauging stations is spatiotemporally interpolated using a spline interpolation. Final data is transferred from gauging zero (PN) into values of normal height null (NHN). Vessel position is projected on the spline and a continuous time series for water level at the position of the design vessel is determined for each measurements campaign. Figure 5.2 and Figure 5.3 show water levels for inbound and outbound campaigns.

WSA and HPA also provide navigational soundings for each measurement campaign. The actual data set is transferred into a Digital Terrain Model (DTM) and referenced on NHN according to Table 4.3. The vessel's plane area is projected onto the topography with a rectangle of the vessel's length times twice the vessel's width. Channel bed height is spatially averaged over the rectangular area and a continuous time series for channel bed height at each vessel position is determined. In combination with the water level time series, a continuous water depth time series is determined.

Figure 5.2 shows water depths for inbound campaigns. With one exception, all inbound water levels range between 0 and +2 mNHN. Inbound vessels enter the Elbe passage with the tidal wave and use it to overcome the shallow water section. They also use the additional propagation speed of the tidal current. The vessels run at wave propagation speed so that water level timeline at vessel´s position forms an almost constant line for inbound vessels. They arrive at the port of Hamburg around the time of high water level.

Outbound vessels use two different approaches to leave the port of Hamburg. Some vessels leave the port of Hamburg at that time, which allows them, to meet high water levels within the middle section of the Elbe passage. That approach guaranties sufficient under keel clearances during the shallow section. During the shallow water section passage, the water levels range between 0 and 2 mNHN as well. A few outbound vessels leave the Port of Hamburg at high water level and overcome the shallowest section at Elbe-km 680 with water levels still over 0 mNHN (Figure 5.3).

All vessels use tidal elevation to overcome the shallowest section. At Elbe-km 680 it can be observed, that all vessels, inbound and outbound, have always water levels over 0 mNHN, which means that they use the tidal range to increase their under keel clearance.

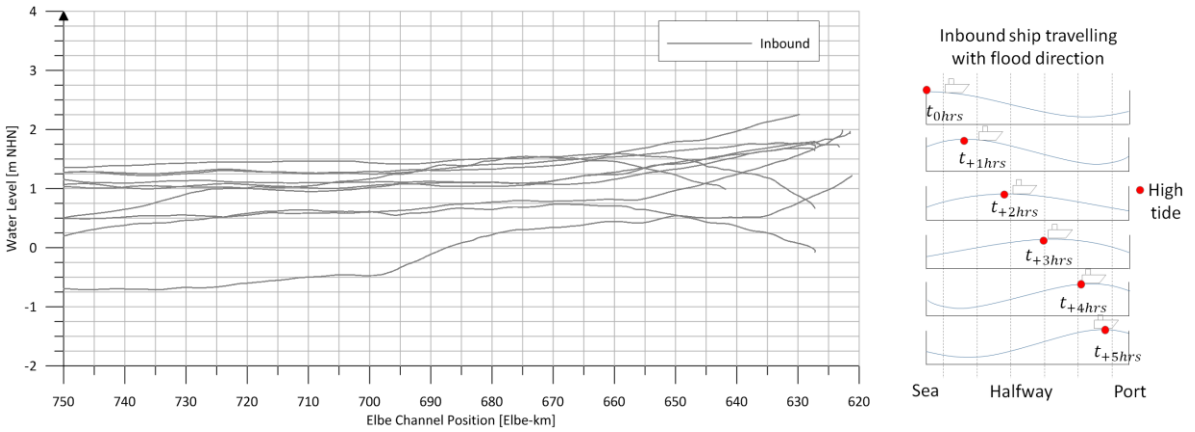

Figure 5.2: Water level along Elbe passage for inbound vessel, travelling with flood wave crest

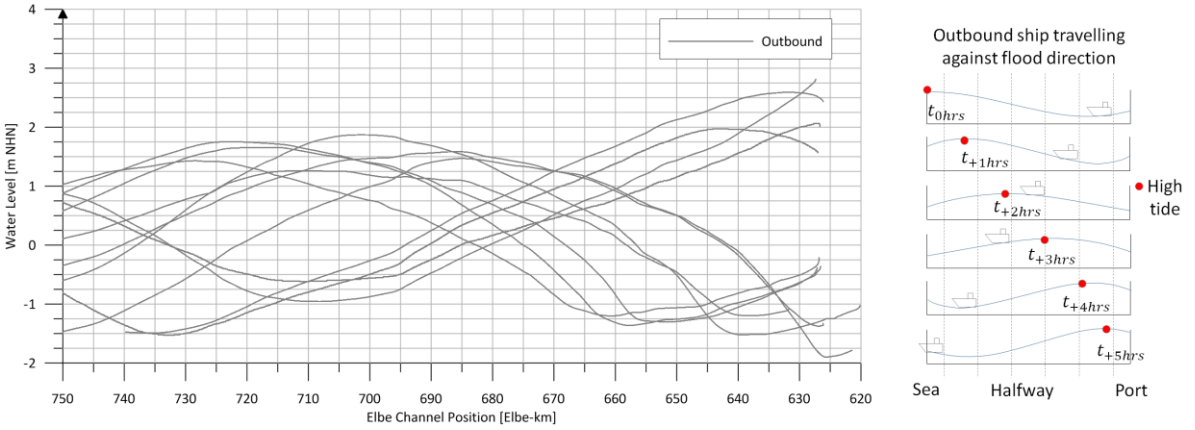

Figure 5.3: Water level along Elbe passage for outbound vessels, meeting flood wave crest halfway

5.1.3 Waterway cross-sections and channel types

From the abovementioned DTM, waterway cross-sections along the vessel track are generated. Cross-section profiles are determined along the vessel track with distances of 50 m. The cross-section profiles are intersected with the water level time series for each campaign. Water-tangent cross-sections are calculated with maximum effective widths of 11.27 times vessel beam. Figure 5.4 shows the wetted cross-sections along the Elbe passage for inbound and outbound campaigns.

The wetted cross-section of a C294 vessel is exemplarily marked in green, the wetted cross-section of C400 vessel is marked in red. That indication stresses out, that the biggest vessels of course lead to the biggest wetted cross-section areas due to their major width.

According to section 2.1.1, the waterway cross-sections should be categorized into unrestricted (U), restricted (R) and canal (C) types of waterway. U is characterized by an extensive channel width. R is characterized with a trench and a channel width less than effective width. C is characterized by a very small channel width and steep banks without trenches. All criteria are weak criteria without definite numbers and vary due to the dependence on the effective widths between the vessel classes.

To categorize Elbe channel cross-sections, the characterization is pragmatically based on channel bottom width and trench height existence. If channel bottom widths exceeds 350 m, the cross-

section is categorized as U. If the channel bottom width is less than 350 m and trench height to water depth ratio is around 0.5, cross-section category is R. And if channel bottom width is way below 350 m without a trench, category is C. With such criteria, Elbe waterway is divided into eight sections (Figure 5.4). Table 5.1 defines the channel types along the Elbe passage.

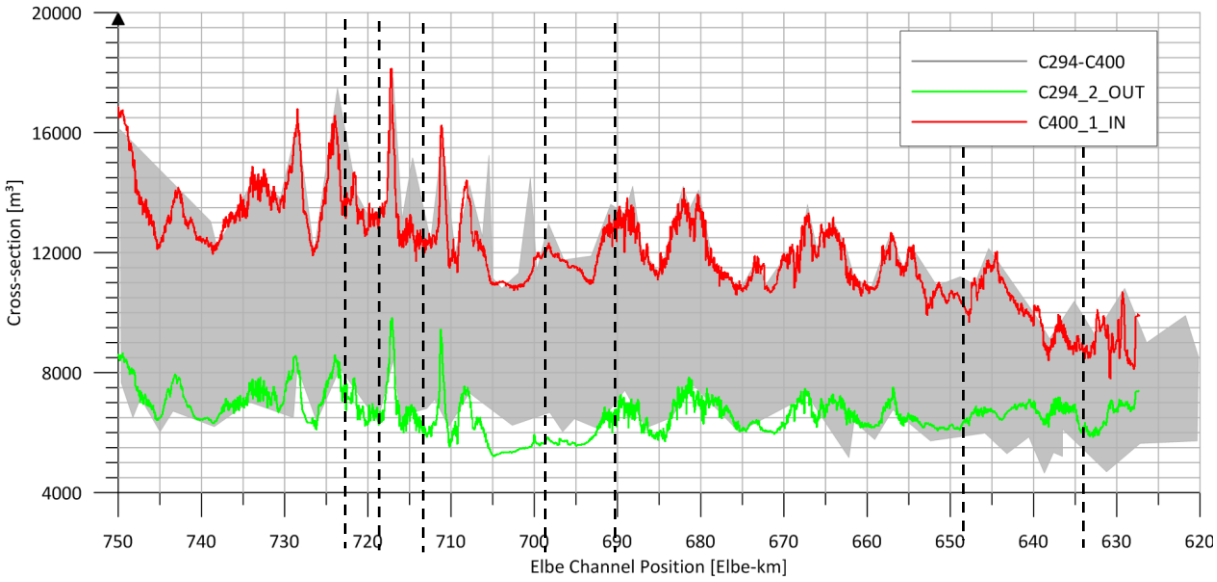

Figure 5.4: Wetted cross-sections along the Elbe River for all vessels

Table 5.1: Sections of channel types

Section	Elbe-km	Elbe-km	Channel type
1	620	633	C – Canal
2	634	647	R – Restricted Channel
3	648	690	U – Unrestricted Channel
4	691	698	C – Canal
5	699	713	U – Unrestricted Channel
6	714	719	C – Canal
7	720	723	R – Restricted Channel
8	724	752	U – Unrestricted Channel

5.2 Hydrostatic ship factors

5.2.1 Ship´s draft at rest

The seaside mounted radar gauges meter the distances between sensor position within the ship's coordinate system and water level. Within 2 hours around berthing and unberthing, the gauges were activated. They logged continuously data with 1 Hz frequency. The positions of the gauges are known from the preparatory measurements and the tachymeter measurements of the sensor positions. The distances between sensor positions and keel are determined from the GA plan. With knowledge of the ship's heel and torsions at bow and stern, the sensor position is projected on the ship's centerline

and the draft values are calculated. Gauge data is visualized with NI DIADEM and MS Excel. Data is filtered with a running average over 21 values to average out short-term waves and disturbing oscillations of the water surface. Subtracting the resulting distance between sensor and water level from the sensor distance to the keel, the actual draft at the sensor position is calculated for each time step. The moment of the unmoored ship at-rest without tug impact after unberthing or before berthing is documented by the measurement team and the video cameras. For that short moment, the gauge data is analyzed and averaged over a time slot of 20 seconds.

The resulting values are corrected by heel and hogging and projected onto the centerline. Final draft at-rest values are determined at FP and AP positions. The values are the basis for absolute squat determination and therefore redundantly compared with the draft meter measurements taken and photo documented by the accompanying ship's measurement team. Table 5.2 shows the draft values from radar gauges (RG) at FP and AP as well as the draft values from the draft meters (DM) at FP, AP and amidships perpendiculars (MP).

Table 5.2: Draft at FP and AP based on RG in comparison with redundant draft meter values

Class	**Ship_ID**	**In / Out**	**RG FP**	**RG AP**	**DM FP**	**DM MP**	**DM AP**
[-]	**[Class_#]**	**[-]**	**[m]**	**[m]**	**[m]**	**[m]**	**[m]**
C294	C294_1_OUT	Outbound	11.92	11.98	12.00	11.80	12.00
	C294_2_OUT	Outbound	11.16	12.76	11.25	11.60	12.75
	C294_3_IN	Inbound	10.92	11.94	10.95	11.40	12.00
C335	C335_1_OUT	Outbound	12.72	12.92	12.90	12.65	13.00
	C335_2_OUT	Inbound	13.16	13.20	13.20	13.05	13.20
	C335_3_IN	Outbound	12.63	12.72	12.70	12.65	12.75
C347	C347_1_OUT	Outbound	12.08	12.04	12.10	11.90	12.05
	C347_2_IN	Inbound	13.09	12.84	13.10	12.55	12.90
	C347_3_IN	Inbound	12.72	12.83	12.80	12.70	12.90
C366	C366_1_OUT	Outbound	11.23	11.51	11.20	10.80	11.50
	C366_2_OUT	Outbound	11.60	11.74	11.55	11.20	11.75
	C366_3_IN	Inbound	12.11	12.20	12.10	11.70	12.30
C396	C396_1_OUT	Outbound	11.68	11.74	11.70	11.20	11.70
	C396_2_OUT	Outbound	11.46	11.49	11.45	11.25	11.55
	C396_3_IN	Inbound	12.10	12.30	12.15	11.95	12.30
C400	C400_1_IN	Inbound	9.61	10.37	9.60	9.50	10.40
	C400_2_OUT	Outbound	11.10	11.52	11.00	11.10	11.60
	C400_3_OUT	Outbound	11.34	12.01	11.40	11.60	12.00
	C400_4_IN	Inbound	12.15	12.11	12.10	11.90	12.10
Bulk	BULK_1_IN	Inbound	13.36	13.23	13.30	13.30	13.30
	BULK_2_IN	Inbound	14.14	14.06	14.20	14.10	14.10

5.2.2 Hogging, trim and heel at rest

The basic assumption for theoretical trim and heel determination is an even keel without torsion and bending (hogging or sagging). As mentioned above, sensor data shows, that design vessel's hull is always influenced by torsion.

Figure 5.5 shows draft meter values at fore and aft perpendicular as well as amidships.

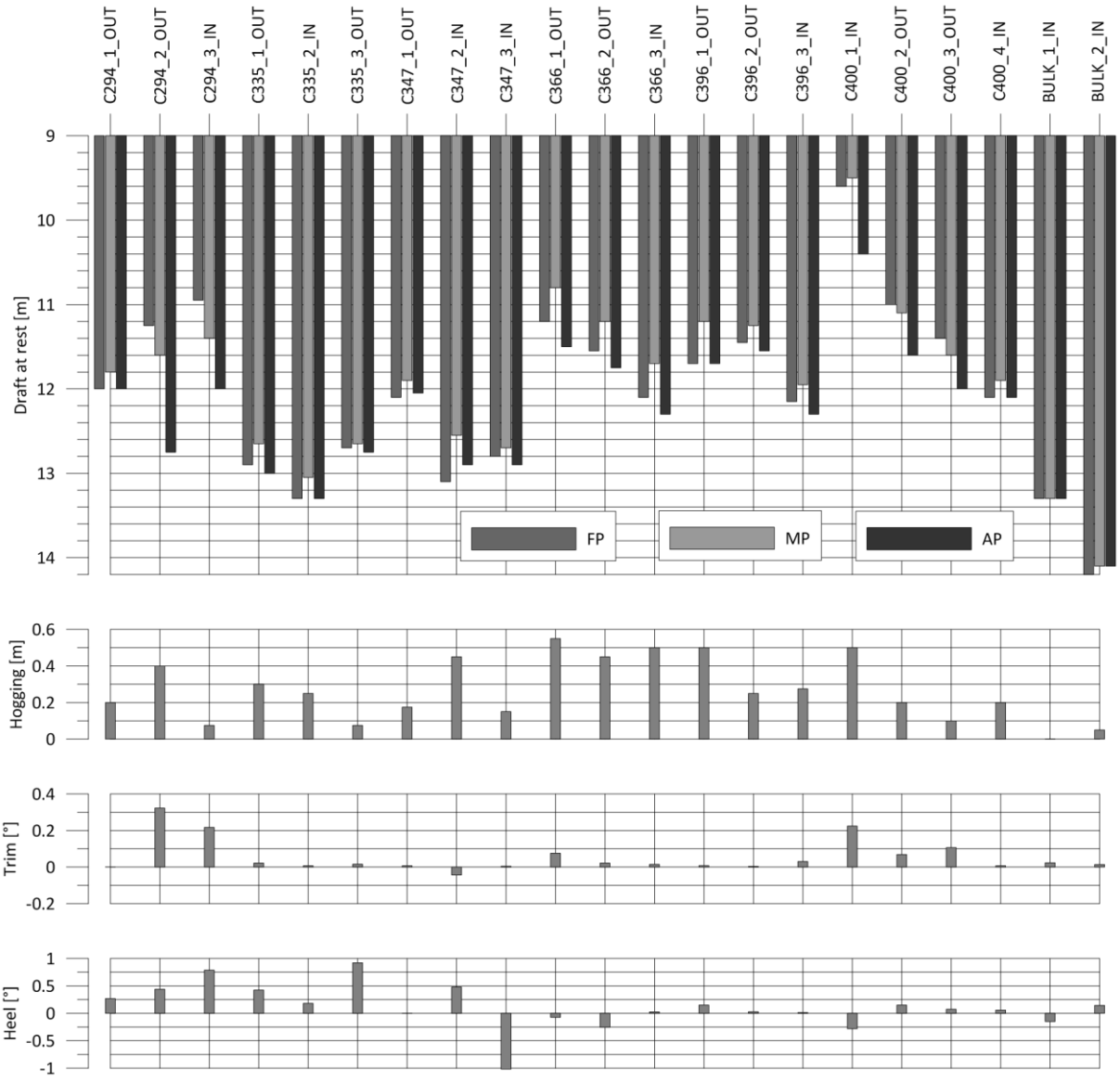

Figure 5.5: Draft, hogging, trim and heel at rest

Usually, the FP and AP draft values exceed the draft values amidships, e.g. C400_1, where draft amidships is 0.2 m lower than at FP and AP. That bending effect, in upward direction is called hogging, in downward direction it is called sagging. Hogging originates if buoyancy amidships exceeds the weight at FP and AP due to loading conditions or waves. The opposite is sagging, when the weight amidships is higher than the buoyancy amidships.

In every measurement campaign, the vessels are hogged with values between 0.03 m at C335_3 and 0.55 m at C366_1. In 6.2, trim, heel and hogging are considered within the projection of the single point positions onto the coaming reference plane.

Hogging is determined as the distance between the average of FP and AP draft readings and the draft reading amidships. Redundantly it is calculated as the vertical distance between single point positions average at bow and at stern and the average single point position at the bridge wing. If both calculations match, hogging is included within all further determinations. Figure 5.5 shows draft at rest of the design vessels at FP and AP positions and amidships. For each design vessel, it shows also static hogging as well as trim and heel as a basis for all further determinations.

With exception of BULK_1_IN, every design vessel is hogged with values between a few centimeters (e.g. C294_3_IN, C335_3_OUT and BULK_2_IN) up to more than 5 decimeters (e.g. C366_1_OUT). In general, ship categories from C366 to C396 list the highest hogging values.

Nearly all design vessels are loaded to an almost even keel balance but still with trim tendency towards stern (bow up). Only exception is C347_2_IN that is trimed towards bow (bow down). C294_1_OUT, C294_3_IN and C400_1_IN show significant trim at rest with values above 0.2°.

12 design ships are evenly loaded on Starboard and Portside with static heel values below +/- 0.25°. 9 design ships show significant static heel values up to +/- 1°. Especially C335_3_OUT and C347_3_IN are unevenly loaded and display heel values of +0.923° (Starboard up) and -1.017° (Portside up).

Combined influence of hogging, trim and heel is analyzed and discussed in detail in section 6.2.

5.2.3 Change of draft and change of trim caused by change of density

Inbound and outbound vessels experience a change in density from seawater to freshwater and vice versa. There are two vessel specific factors, that depend on density and determine the value of hydrostatic change. Such factors are Tons per Centimeter Immersion (TPC) as well as the Moment to Change Trim (MTC).

The influence of density change on TPC leads to a certain change in immersion over the complete hull. Change in MTC leads to a changed hydrostatic trim and changes the immersion of bow and stern in opposite directions. Figure 5.6 shows the influence of density on TPC and MTC for inbound and outbound vessels.

Under the assumption of an even keel vessel, TPC and therefore ship's displacement depends directly on water density, which means, that changes in density lead to changes in displacement of the ship.

Change in displacement is directly proportional to the change in density. With knowledge of the displacement of the ship and the corresponding density at one point of time as well as the knowledge of the density at another point of time, change in displacement is determined by:

$$\nabla_{t2} = \nabla_{t1} \frac{\rho_{t2}}{\rho_{t1}} \qquad 5.2$$

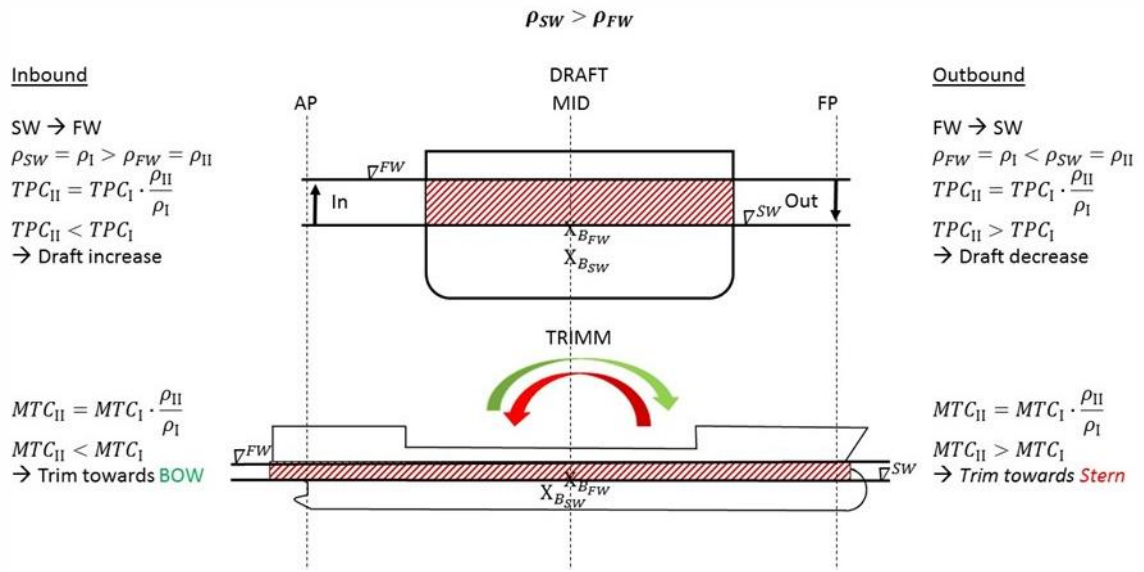

Figure 5.6: Influence of density on TPC and MTC

For inbound vessels, density decreases from seawater to freshwater, which leads to an increase in displacement, thus the ship immerses and draft increases. Outbound vessels discover an increase in density from freshwater to seawater. Displacement decreases and therefore draft decreases as well.

To determine the change in draft due to change in density, a determination approach based on Stability Booklet values is invented. The Stability Booklet states mould volume values in dependence from mean draft values in seawater. With such values, a linear regression model is set up for each investigated vessel. Based on the averaged mean draft at rest, 11 stability booklet values of mould volume are read out. That is done for different drafts in steps of 0.05 m within a range of values of 0.5 m around draft at-rest. Resulting values are interpolated linearly and furthermore, a trend curve is determined. The regression equation of such trend is determined as well.

Using equation 5.2, the displacement of the investigated vessel is determined at each point of time in dependence of the determined density from the CTD sensor. Using the regression equation, displacement values influenced by density are transferred into draft values. With that process it becomes possible, to determine the change in mean draft in dependence of the change in density for each time step of a measurement campaign (Figure 5.7).

Figure 6.18 affirms the dependence of change in draft of change in density. Similarly to density, all vessels experience almost no change in draft between Elbe-km 620 and 680. Density increases from Elbe-km 680 to 750. With increasing density, the draft decreases by values between -0.15 and -0.28 m. Maximum range of changed draft values is around Elbe-km 730 with 0.15 m +/- 0.09 m.

Due to the specific form of the ship's hull as well as the individual weight and load distribution, changes in density lead to changes in the position of the Longitudinal Center of Buoyancy (LCB) and furthermore to changes of the position of the Longitudinal Center of Gravity (LCG).

Such dislocation leads to changes of MTC, which causes an inclination around the lateral axis of the ship in hydrostatic state. The trim of the ship changes and therefore basic draft at FP and AP change. For inbound vessels, MTC decreases from seawater to freshwater. As a result, ship trims towards bow. For outbound vessels, MTC decreases with the decrease in density and the ship trims towards stern.

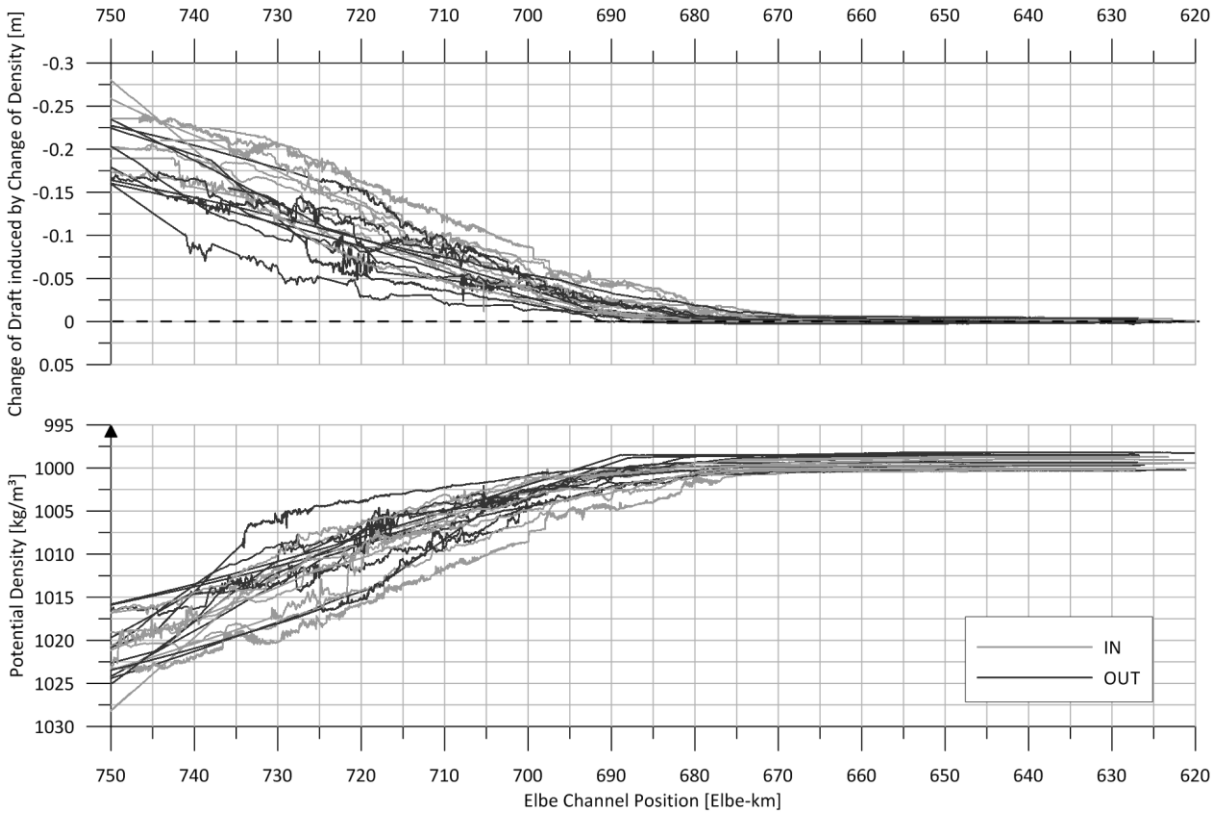

Figure 5.7: Change of draft due to change of density for all classes

To calculate the absolute amount of change in trim and to allocate the relative amount of draft change at FP and AP, the following approach is set up:

Equation 5.3 is used to calculate the change of trim. Under the assumption of an even keel, MCT and LCB values within a 0.5 m draft range around draft at rest are read out of the Stability Booklet in dependence from mould volume. The values are then interpolated linearly and the regression equation is determined.

For the vessel at rest, LCG is determined from trim at rest using equation 5.3. Assuming a constant LCG value for the first step of iteration, MCT and LCB are determined from the regression equations in dependence from displacement. With equation 5.3 the absolute change in draft is determined iteratively for each time step

$$\Delta T = \frac{\nabla(LCB - LCG)}{MCT}$$
$$\leftrightarrow LCG = \frac{\Delta T * \mathrm{MTC}}{\nabla} \qquad 5.3$$

To distribute the absolute trim change value onto relative draft changes at FP and AP, the position of the longitudinal center of flotation (LCF) is determined for each time step as well. LCF is read out of the Stability Booklet and a regression model in dependence of the displacement is built in the same way as explained above for MCT and LCB. With knowledge of the displacement change due to density, the change of draft due to change of trim is determined for FP and AP position at each time step.

Figure 5.8 displays the absolute change of draft due to change of trim induced by density at FP and AP perpendiculars. Maximum change of draft at each perpendicular is always less than 0.1 m. Figure 5.8 affirms the hypothesis, that inbound ships trim towards bow and outbound vessels trim towards stern. Amount of draft change at FP is generally similar to draft change at AP. Amount of change at FP in relation to change at AP is insignificantly higher with a maximum difference between FP and AP of 0.025 m in absolute value.

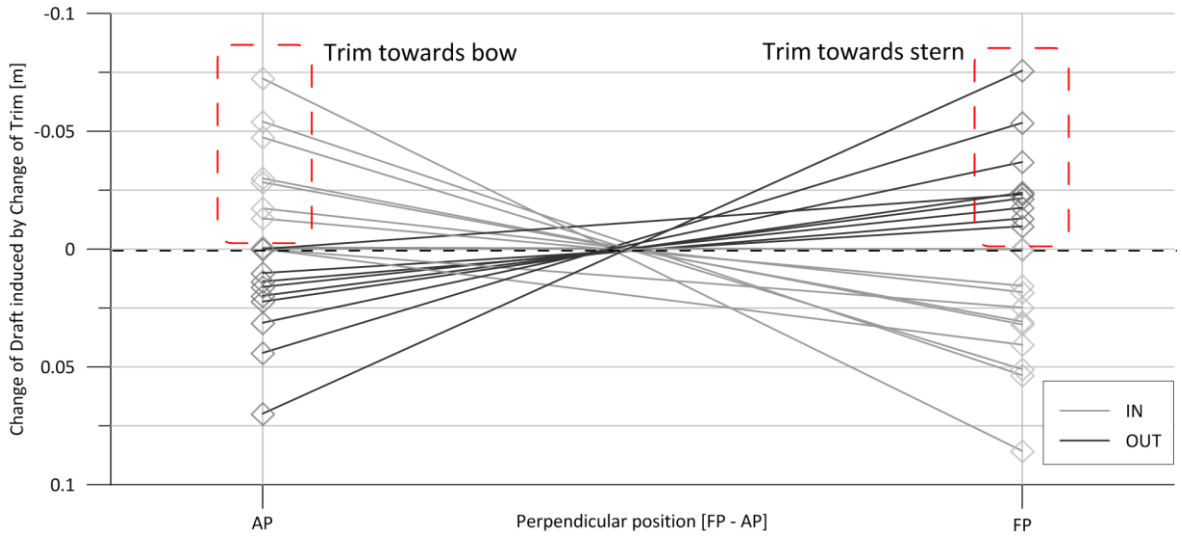

Figure 5.8: Change of draft due to change of trim for all classes

5.3 Dynamic ship factors

5.3.1 Heading and course over ground

Heading (HDT) is that direction, the bow of the vessel points at. It is a static component at each point of time. It differs from the dynamic component course over ground. Heading shows the forward-looking extension of the longitudinal centerline of the vessel. Course displays the extension of the interpolation between two already passed positions.

Heading is calculated at each time step for each single position pair as well as for every virtual point pair. The weighted average from both approaches is determined based on the FP and AP positions. Peaks and not plausible data are eliminated. The resulting values are filtered and smoothed by a median 10 filter as well as a floating average over 21 values.

Figure 5.9 shows the final HDT results for inbound and outbound measurement campaigns along the Elbe passage between channel entrance at buoy E11 at Elbe-km 755 and berthing points at Hamburg Port at Elbe-km 620. Next to HDT determination from the single point positions, also HDT data from the VDR is used to validate and to compliment HDT determination, if necessary. Main heading is between 70° and 170° north for inbound vessels and shifted by 180° for outbound vessels to values between 250° and 350° north.

Course over ground differs from heading by its dependence on the dynamic component. Based on the abovementioned approaches, FP and AP positions are calculated from all single point positions between two time steps. Course over ground is determined from the vessel's track between two following values of FP and AP horizontal positions. Data is visualized with NI DIADEM and compared with COG data from VDR. Peaks and not plausible data are eliminated and values are filtered by median 10 and moving average over 21 values.

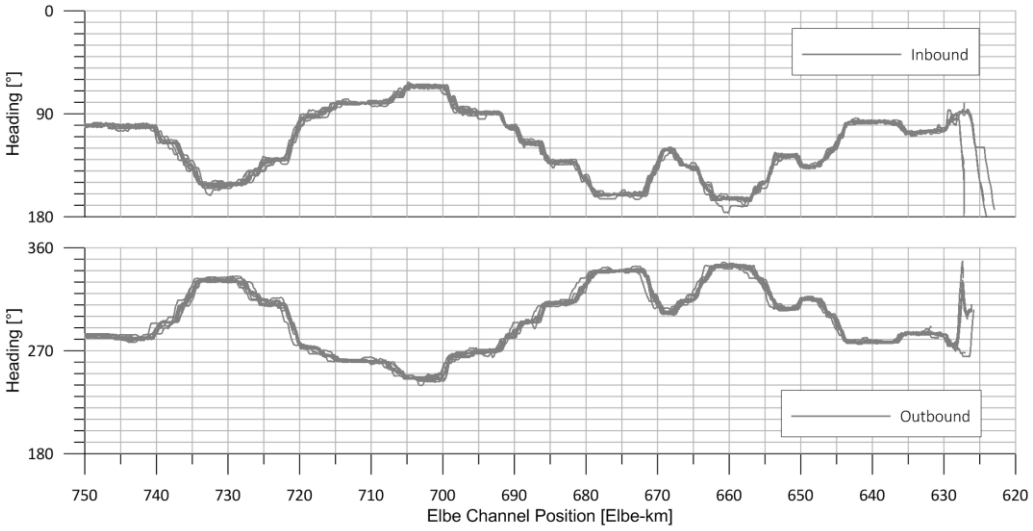

Figure 5.9: Design vessel heading

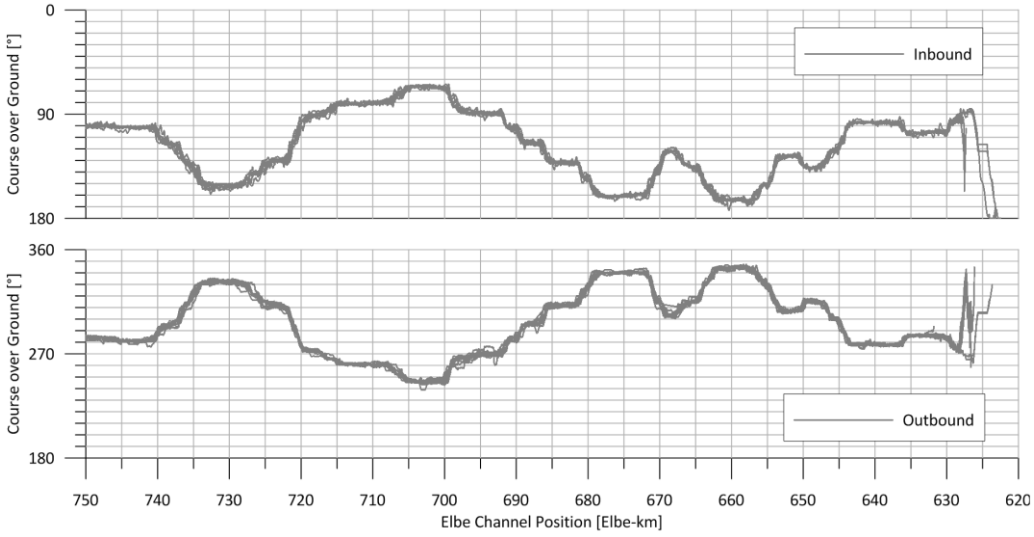

Figure 5.10: Course over ground at FP

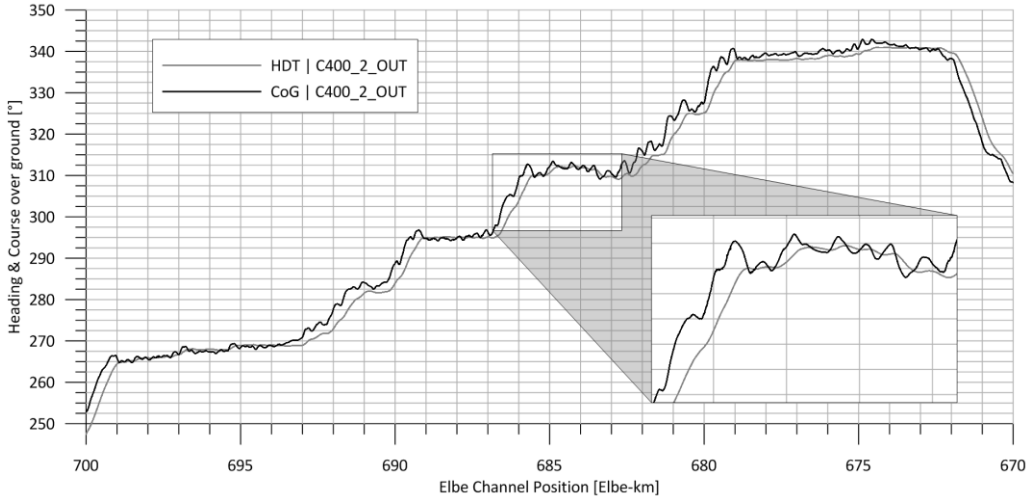

Figure 5.11: Course over ground at FP and AP position for C400_2 outbound vessels

Figure 5.10 shows course over ground at FP position for all vessels. Differences between HDT and COG are due to turning maneuvers and drift due to currents and wind. Figure 5.11 shows the difference between heading (marked in grey) and course over ground (marked in black) at the example of a C400 outbound vessel. Main course direction is aligned to HDT values. Differences in COG and HDT are due to turning maneuvers, course corrections and impact of current.

5.3.2 Speed through water

Speed through water is the sum of water velocity and vessel speed over ground. Speed over ground is calculated from the horizontal values of FP and AP positions between to time steps. The travelled distanced as well as travelled time between the time steps is calculated. The ratio between travelled distance and time travelled is speed over ground (SOG).

Water velocity and velocity directions are determined from the DVL data. DVL heading values are corrected by heading values, which are determined from GNSS sensors on board of the research vessel. Preset speed of sound values of the DVL probe are corrected by speed of sound calculations based on salinity, temperature and pressure values from CTD probe. Speed of sound calculations are conducted using the approach of CHEN-TUNG & MILLERO (1977). Based on that post processed values, velocity and direction are determined from DVL data.

Finally, velocity values are projected from the research vessel position onto the design vessel's position under the assumption of stable current states between the research vessel and the design vessel location. Water speed and speed over ground are intersected with respect to velocity direction and course over ground. Resulting sum is speed through water (STW) of the design vessel. STW data is displayed in NI DIADEN, peaks and not plausible data are erased. The final data is averaged by median 10 and floating average 21 filter.

Figure 5.12 displays speed through water. The range is marked in light grey with highest values around 10 m/s from an outbound vessel of class C335 (marked in red). Lowest values are obtained from an inbound vessel of class C347 (marked in green). In general, STW ranges between 6-10 m/s from mouth of the Elbe River to Elbe-km 700. From Elbe-km 700 towards the Port of Hamburg, the STW decreases steadily. Three peaks with very low STW values become obvious at Elbe-km 725, 695 and 655. At these three points, the pilots for the specific areas enter or leave the vessel. Thus, vessel reduces speed to facilitate the transfer between the pilot transfer boat and the design vessel.

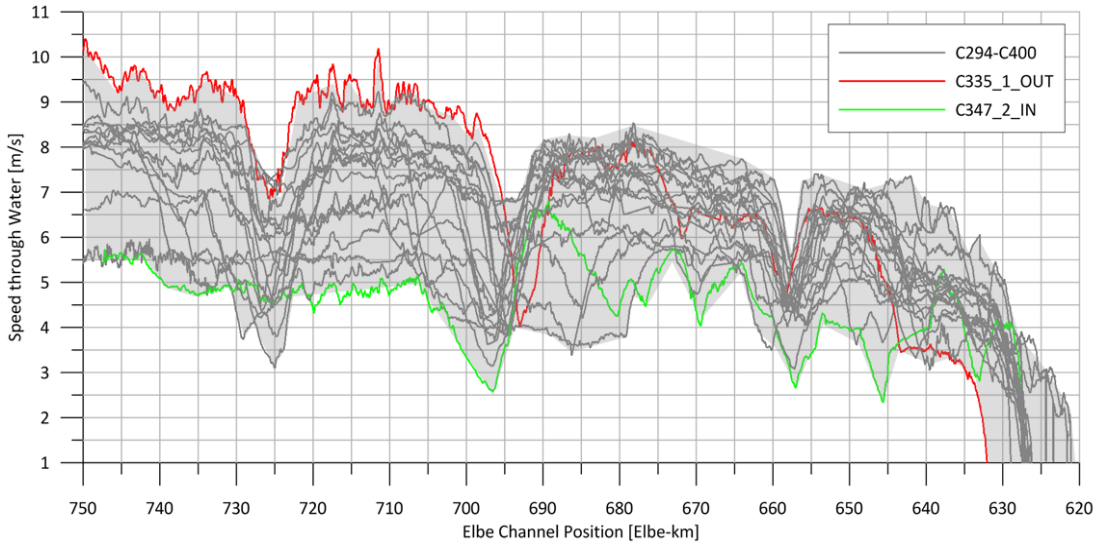

Figure 5.12: Speed through water of all vessels

5.3.3 Heel and dynamic roll

At rest, heel is the inclination around the longitudinal axis. Heel depends mainly from the hydrostatic forces e.g. loading etc. When travelling, turning maneuvers, waves and wind cause additional medium-periodic oscillations around the longitudinal ship axis, called roll. Roll is determined in line with heel from opposite single point positions and displayed according to algebraic conventions of Figure 4.1. Based on position qualities and distances, the main roll angle is determined for each time step. To average the roll angles, the basis assumption is a plane deck area and a ship's hull without torsion. Based on that assumption, it is possible to determine main heel angle, although the hull, and thus heel is generally influenced by torsion. Table 5.3 shows main averaged heel angle, heel angle at bow and stern as well as maximum roll angle for all accompanied design vessels.

Table 5.3: Basic heel angles and torsions at bow and stern

Class	Ship_ID	In / Out	Heel	Heel Bow	Heel Stern	Max. Roll Amplitude
[-]	[Class_#]	[-]	[°]	[°]	[°]	[°]
C294	C294_1_OUT	Outbound	0.270	0.187	0.317	4.298
	C294_2_OUT	Outbound	0.440	0.542	0.447	5.703
	C294_3_IN	Inbound	0.788	0.807	0.750	4.808
C335	C335_1_OUT	Outbound	0.426	0.459	0.354	3.041
	C335_2_OUT	Inbound	0.183	0.303	0.063	3.167
	C335_3_IN	Outbound	0.923	0.877	0.968	2.780
C347	C347_1_OUT	Outbound	0.001	0.060	-0.058	1.410
	C347_2_IN	Inbound	0.480	0.450	0.513	2.909
	C347_3_IN	Inbound	-1.017	-1.119	-0.914	3.181
C366	C366_1_OUT	Outbound	-0.073	0.043	0.209	0.878
	C366_2_OUT	Outbound	-0.254	0.281	0.219	0.797
	C366_3_IN	Inbound	0.027	0.055	0.005	1.125
C396	C396_1_OUT	Outbound	0.152	0.127	0.177	0.955
	C396_2_OUT	Outbound	0.031	0.115	-0.053	0.992
	C396_3_IN	Inbound	0.015	0.094	-0.064	0.801
C400	C400_1_IN	Inbound	-0.281	-0.924	-0.268	0.783
	C400_2_OUT	Outbound	0.151	0.113	0.189	1.032
	C400_3_OUT	Outbound	0.074	0.057	0.091	1.380
	C400_4_IN	Inbound	0.060	0.050	0.070	0.888
Bulk	BULK_1_IN	Inbound	-0.149	-0.158	-0.140	0.216
	BULK_2_IN	Inbound	0.147	0.148	0.146	0.221

Figure 6.11, Figure 6.12 and Figure 6.13 show roll angle as sum of basic static main heel angle and dynamic roll for ship categories C294, C347 and C396 along the Elbe passage. Table 5.3 and the figures stress out a decreasing amplitude of oscillation around the longitudinal ship axis with

increasing ship sizes. While C294 ships with beams of around 32.20 m have average roll amplitudes of 4.94°, average roll amplitude of C347 ships with 45.20 m beam is 3.00° and only 2.50° at ships of category C396 with 53.60 m in beam. That leads to the conclusion that roll amplitude mainly depends on the ship's beam and decrease with increasing beam.

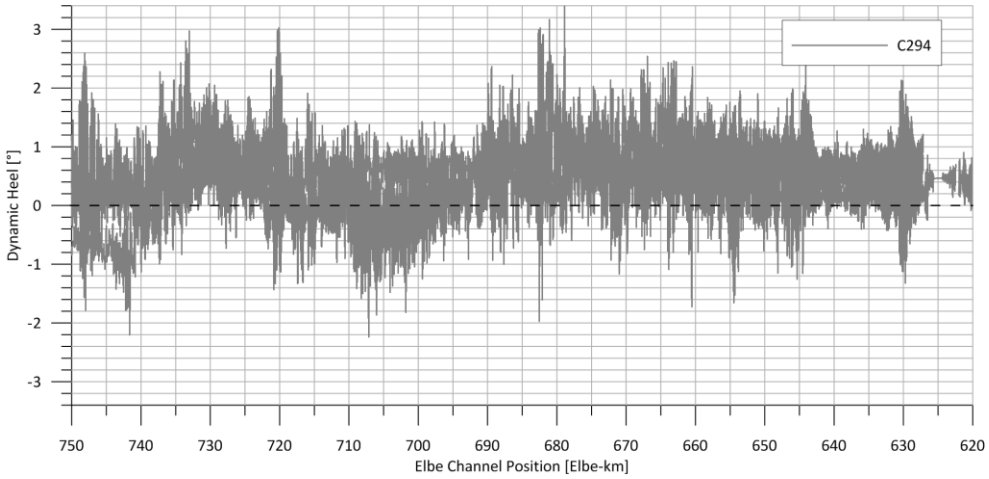

Figure 5.13: Roll angles for vessel class C294

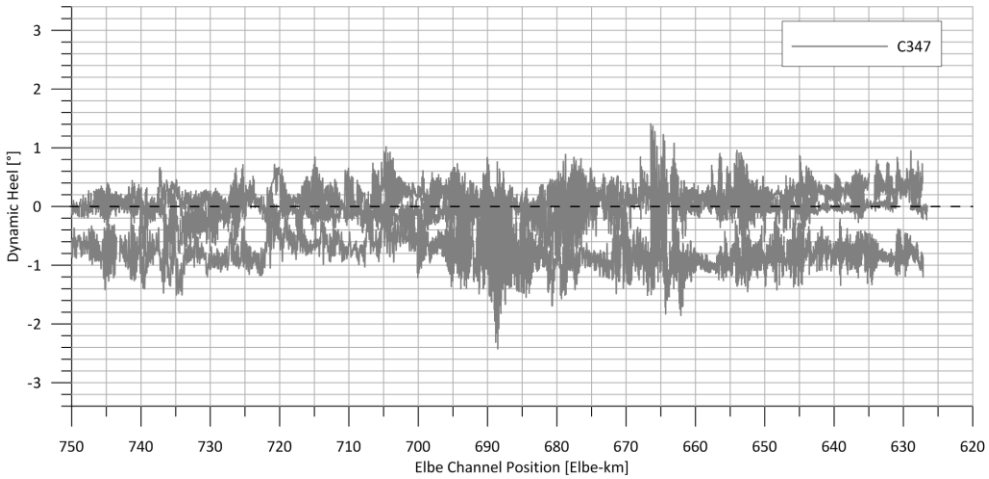

Figure 5.14: Roll angles for vessel class C347

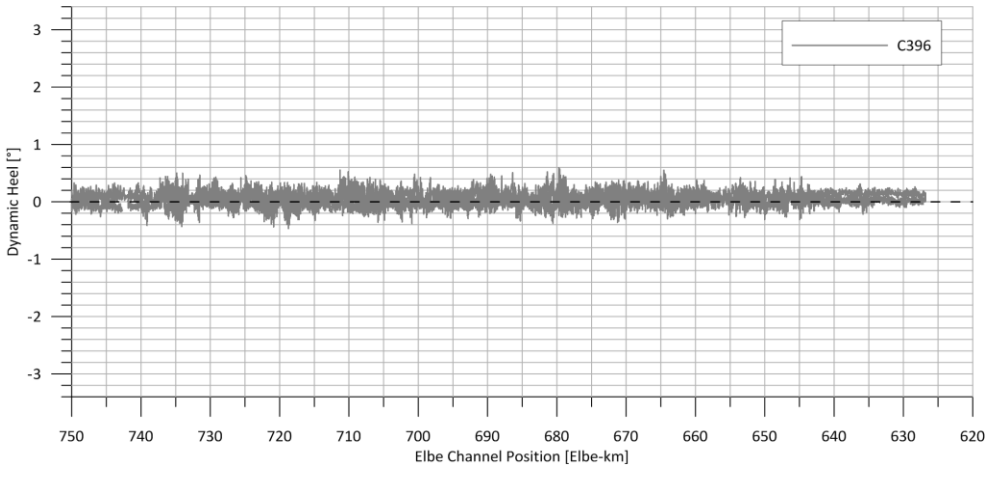

Figure 5.15: Roll angles for vessel class C396

According to section 2.4, heel and roll can lead to off-centric draft increase. With decreasing oscillation amplitudes with increasing ship size and beam values, also additional off-centric draft should decrease. Further analysis on that topic are performed in section 6.2, where the combined influence of hogging, trim and roll is discussed in depth.

5.3.4 Trim and dynamic pitch

Trim is the hydrostatic inclination around the lateral vessel axis. Trim is based on ship's hull and loading situation at rest. Pitch is the dynamic trim underway, influenced by accelerating and decelerating maneuvers. Trim and dynamic pitch are determined for each time step between single point position pairs and virtual point pairs parallel to the longitudinal ship's axis. Based on position quality and distance, main average is determined for the centerline of the vessel. Trim and dynamic pitch are based on the assumption of an even keel without hogging or sagging effects. Basic trim is listed in Table 5.4. Dynamic pitch is displayed exemplarily for C294 and C396 in Figure 5.16 - Figure 5.17. Pitch the sum of basic trim angle and additional inclinations underway.

Table 5.4: Basic trim angle overview

Class	Ship_ID	In / Out	Trim	Trim	Pitch Amplitude
[-]	[Class_#]	[-]	[°]	[m]	[°]
C294	C294_1_OUT	Outbound	0.001	0.004	0.089
	C294_2_OUT	Outbound	0.323	1.597	0.121
	C294_3_IN	Inbound	0.217	1.064	0.253
C335	C335_1_OUT	Outbound	0.022	0.122	0.111
	C335_2_OUT	Inbound	0.007	0.036	0.120
	C335_3_IN	Outbound	0.016	0.090	0.074
C347	C347_1_OUT	Outbound	0.007	-0.039	0.136
	C347_2_IN	Inbound	-0.043	-0.248	0.090
	C347_3_IN	Inbound	0.005	0.105	0.103
C366	C366_1_OUT	Outbound	0.076	0.273	0.099
	C366_2_OUT	Outbound	0.022	0.127	0.114
	C366_3_IN	Inbound	0.015	0.092	0.118
C396	C396_1_OUT	Outbound	0.008	0.053	0.140
	C396_2_OUT	Outbound	0.004	0.024	0.106
	C396_3_IN	Inbound	0.031	0.205	0.075
C400	C400_1_IN	Inbound	0.224	0.762	0.160
	C400_2_OUT	Outbound	0.069	0.461	0.264
	C400_3_OUT	Outbound	0.107	0.715	0.140
	C400_4_IN	Inbound	0.007	-0.044	0.140
Bulk	BULK_1_IN	Inbound	0.024	-0.121	0.138
	BULK_2_IN	Inbound	0.014	-0.080	0.127

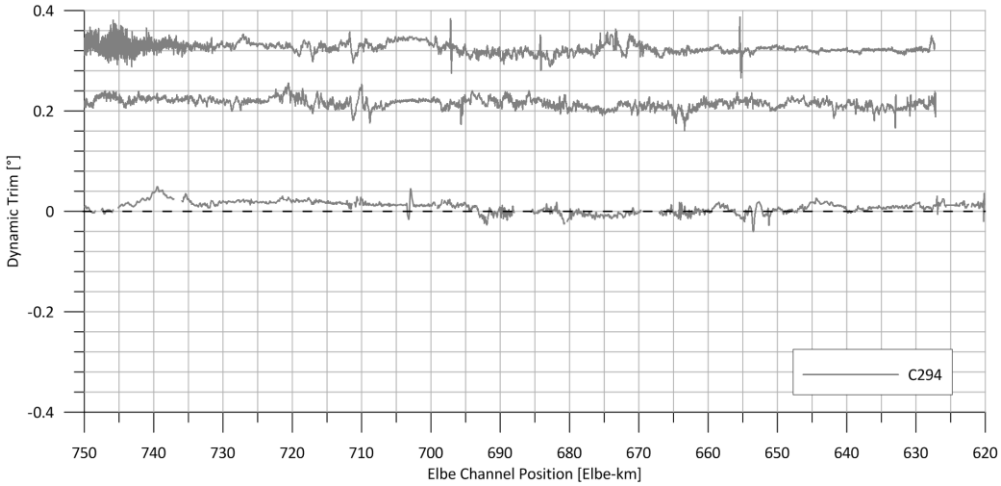

Figure 5.16: Pitch angles for vessel class C294

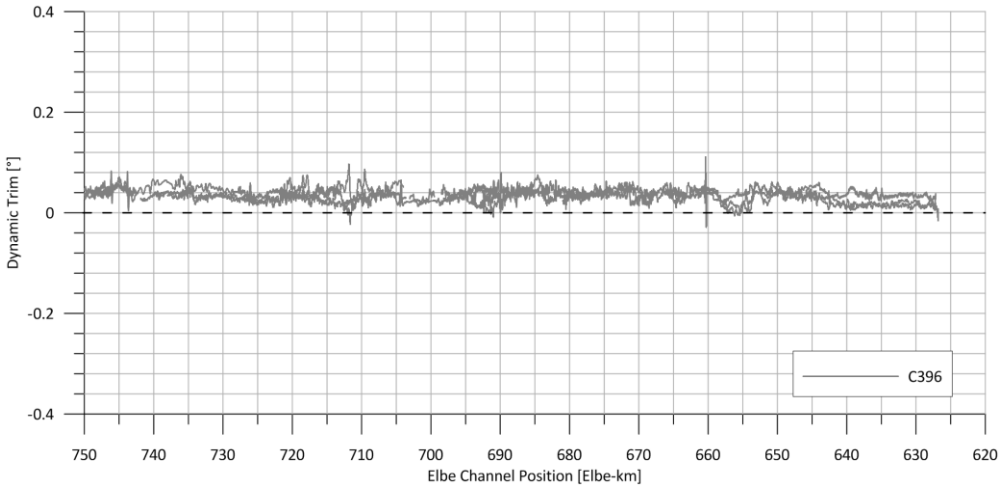

Figure 5.17: Pitch angles for vessel class C396

Table 5.4 and the figures display very similar trim and pitch characteristics among all investigated ship categories. Even with different basic trim values, pitch amplitude is on average between 0.10° at C335 and 0.1.76° at C400. The similar pitch characteristics lead to the conclusion that pitch might be not directly dependent from vessel size. Nevertheless, basis trim and maneuver dynamics influence dynamic draft at the perpendiculars. Especially basic trim determines the maximum dynamic draft in a significant way that is further discussed and analyzed in section 6.2.

5.4 Combined factors

5.4.1 Measured ship squat

Squat is defined in section 2.1.1 as the vertical change in UKC of a travelling vessel at constant water depth. Investigations of BAW showed, that it is possible to measure squat in the field. In that regard, squat is defined as the maximum vertical change of draft (MAUSHAKE & JOSWIG, 2004).

After determination of the static draft at rest, the geodetic heights of all single point positions at each point of time and the geodetic water level height at each point of time, calculation of squat becomes possible. The distance between the single point positions and the water level is calculated within the reference period during design vessel at-rest. For each other time step, the distance

between the single point positions and the water level at the design vessel's position is calculated as well.

The final difference in distance between the distances at rest and the distances underway gives the maximum vertical sinkage of the design vessel. That maximum vertical sinkage is the gross squat (Equation 5.4). Gross squat is still influenced by draft changes due to density. Change of draft due to density is calculated based on density values and draft at rest. During the passage between seawater and freshwater, the design vessel experiences a change of trim due to change of density. Change of trim causes a slide but still measurable change in draft at FP and AP position. Change of draft due to density and change of draft due to change of trim due to density are highlighted in section 6.1. Such values are subtracted from gross squat and the result gives the net squat (Equation 5.5), which is the ship's real squat, measured in the field.

Net squat is calculated for FP and AP position. Figure 5.18 shows the net squat values at the FP position for all container vessel classes from C294 to C400. Figure 5.19 shows the net squat values for AP position for all container vessel classes. Figure 5.20 shows a box-whisker-plot of net squat values.

$$S_{Gross,FP} = (z_{FP\ at\ rest} - z_{WL\ at\ rest}) - (z_{FP} - z_{WL})$$
$$S_{Gross,AP} = (z_{AP\ at\ rest} - z_{WL\ at\ rest}) - (z_{AP} - z_{WL}) \qquad 5.4$$

$$where\ z_{FP/AP} \triangleq Geodetical\ height\ of\ FP\ and\ AP\ position$$
$$and\ z_{WL} \triangleq Geodetical\ height\ of\ water\ level\ at\ vessel\ position$$

$$S_{Net,FP} = Gross\ Squat_{FP} - COD_{FP\ Density} - COD_{FP\ Trim}$$
$$S_{Net,AP} = Gross\ Squat_{AP} - COD_{AP\ Density} - COD_{AP\ Trim} \qquad 5.5$$

$$where\ COD_{FP/AP\ Density} \triangleq Change\ of\ Draft\ due\ to\ change\ of\ density$$
$$and\ COD_{FP/AP\ Trim} \triangleq Change\ of\ Draft\ due\ to\ change\ of\ trim\ due\ to\ density$$

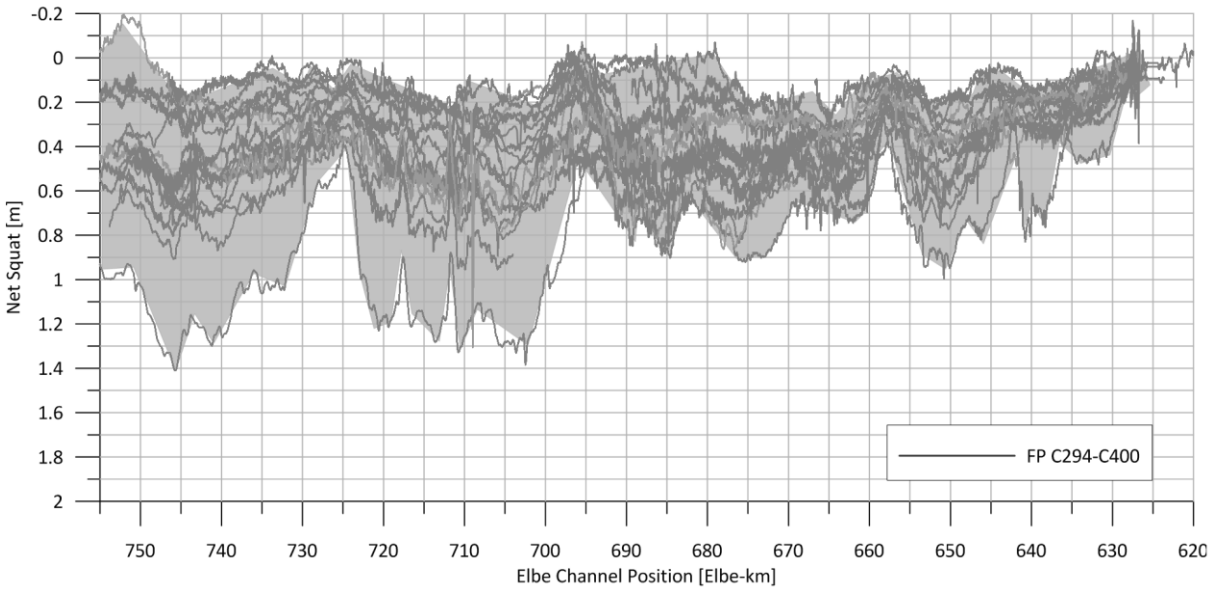

Figure 5.18: Net squat values at FP for vessel classes C294 – C400

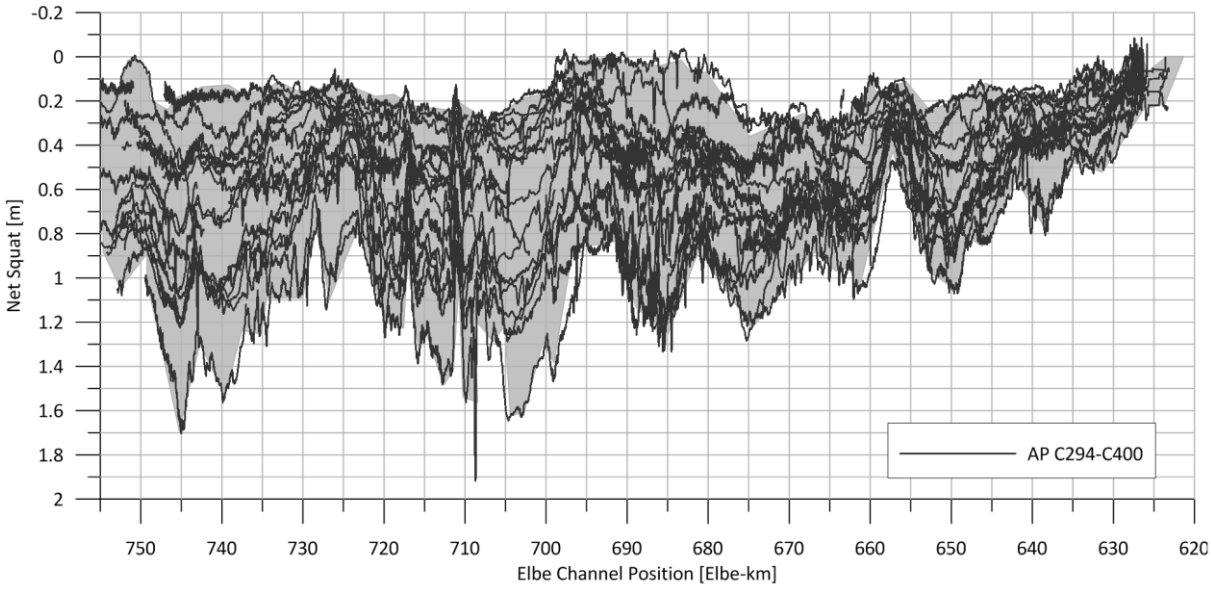

Figure 5.19: Net squat values at AP for vessel classes C294 – C400

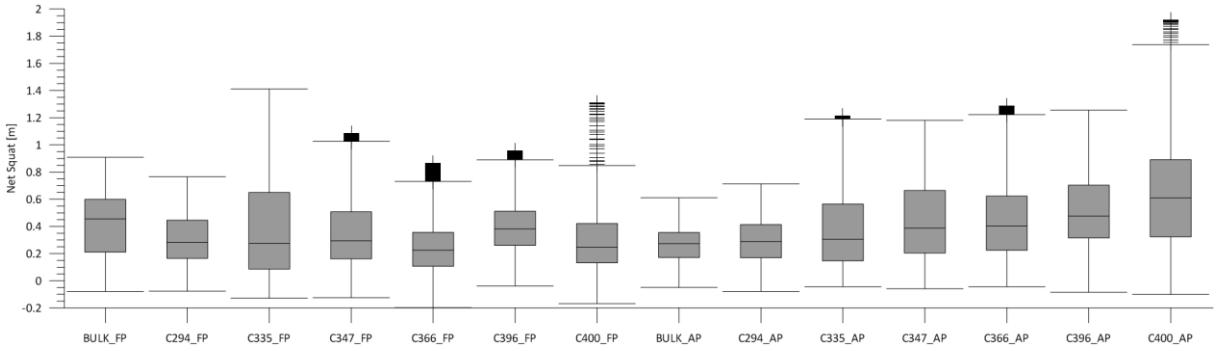

Figure 5.20: Box-whisker-plot for net squat values for all vessel classes

Table 5.5: Box-whisker-values of net squat at FP and AP position for each vessel class

Quartile		C294	C335	C347	C366	C396	C400	BULK
	[-]	[m]	[m]	[m]	[m]	[m]	[m]	[m]
FP	Q1	0.15	0.10	0.15	0.10	0.25	0.1	0.20
	Med.	0.30	0.28	0.33	0.35	0.40	0.25	0.45
	Q3	0.45	0.65	0.50	0.35	0.50	0.45	0.60
	Q4	0.75	1.45	1.00	0.75	0.90	0.85	0.90
AP	Q1	0.20	0.15	0.20	0.25	0.30	0.35	0.20
	Med.	0.30	0.33	0.40	0.43	0.45	0.60	0.30
	Q3	0.45	0.60	0.65	0.60	0.70	0.90	0.35
	Q4	0.70	1.2	1.2	1.25	1.3	1.8	0.6

The box-whisker-plot (Figure 5.20) shows mean net squat values between 0.25 m and 0.45 m at FP position. 3rd quartile values range between 0.35 m and 0.65 m at FP. Maximum values range between 0.75 m and 1.45 m.

For AP position, the box-whisker-plot gives mean net squat values between 0.3 m and 0.6 m. 3rd quartile values range between 0.35 m and 0.9 m and maximum values range from 0.6 m up to 1.8 m.

In general, AP net squat values are higher in contrast to net squat values at FP. Exceptions are C335 and BULK, where ships are trimed towards bow. Bow squat values follow that initial trim direction. While FP net squat values of all classes are in similar ranges, AP net squat values increase significantly with increasing ship sizes.

BULK and C294 have median rear squat values of 0.3 m. Ship categories from C335 to C396 have median rear squat values between 0.33 m and 0.45 m. For C400 median rear squat increase significantly to values of 0.6 m. The significant increase of AP net squat median values can be obtained from Figure 5.20.

5.4.2 Deltasquat from ship-ship interactions

When it comes to ship to ship interactions on the Lower Elbe, there are in general three different scenarios of interaction:

1. The design vessel encounters another vessel head on,
2. the design vessel overtakes another vessel and
3. the design vessel is overtaken by another vessel.

During all ship-ship interactions, the measurement team documented the scenario as well as name and MMSI of the interacting vessel. After a measurement campaign, the interacting vessels are identified by MMSI and information of the encountering vessel is extracted from AIS data, recorded by the AIS sensor onboard the research vessel. Based on AIS position data, the exact moment of encountering is determined and all encounter information like length, beam as well as course and speed over ground is extracted.

Encountering vessel data sets are intersected with design vessel data sets like length, beam and draft as well as course over ground and speed through water. Such intersection makes it possible to determine the points in time, where bow, midship section and stern of the vessels are on the same line rectangular to the design vessel's course. According to the Relative Longitudinal Position (RLP) from section 2.2, that are the points defined as -1 (bow-bow), 0 (midship-midship) and 1 (stern-stern). Along the RLP section, minimum rectangular distance between both ships hulls (distance shoulder to shoulder) is determined. Speed over ground of the encounter is intersected with speed over ground of the design vessel and the total encounter speed is determined.

Squat values at FP and AP positions of the design vessel are displayed along the RLP section for each ship-ship interaction. Figure 5.21 shows the FP and AP squat curves along a ship-ship head on encountering interaction between a C335 vessel with 13 m draft and a Post-panamax vessel with 333 m LOA and 13 m draft. Squat curves on FP and AP display the significant oscillation due to head-on encountering, described in section 2.2. To determine the additional sinkage, caused by the interaction, the level of squat at FP and AP is averaged within 20 seconds outside RLP, which means within 20 seconds before $RLP \triangleq -1$ and within 20 seconds after $RLP \triangleq +1$. Reference squat levels inside RLP are calculated as average between both outside squat levels. Additional squat, called deltasquat is defined and calculated for FP and AP position as the distance between the reference squat level and the actual squat curve. Final deltasquat is the maximum of additional deltasquat values at FP and AP (Figure 5.22).

The measurement team documented 568 datasets of ship-ship interaction over all. 504 of these datasets are formally complete and possible to analyze. Figure 5.23-a shows the cumulative curve of all ship-ship interactions and the associated deltasquat values. The curve expresses that 90% of all

interactions cause additional squat values of less than 0.1 m. Nevertheless, the remaining 10% evoke deltasquat values between 0.11 m and 0.82 m (Figure 5.23- b).

The highest deltasquat value is determined to 0.82 m for a head-on encountering scenario between a C400 vessel and a 369 m long Post-panamax vessel. Those interactions, which result the 18 highest deltasquat values, are listed in Table 5.6. Except for the maximum value, all deltasquat values range between 0.18 and 0.36 m.

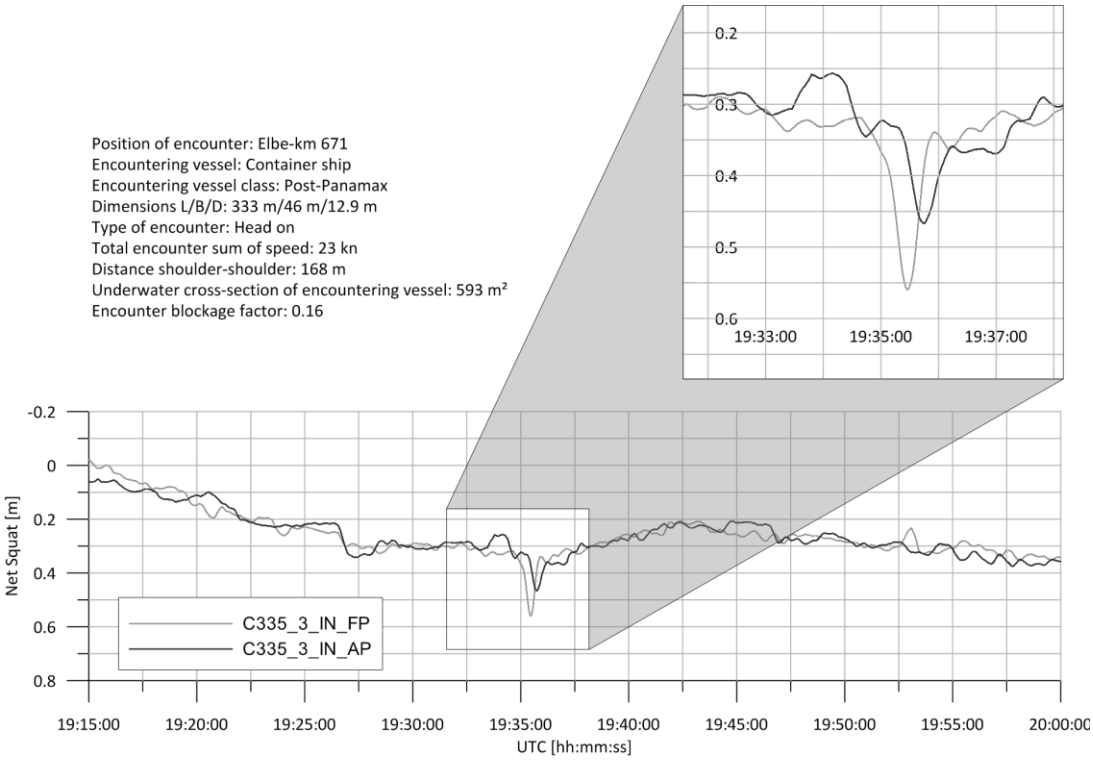

Figure 5.21: Influence of encounter situations on squat

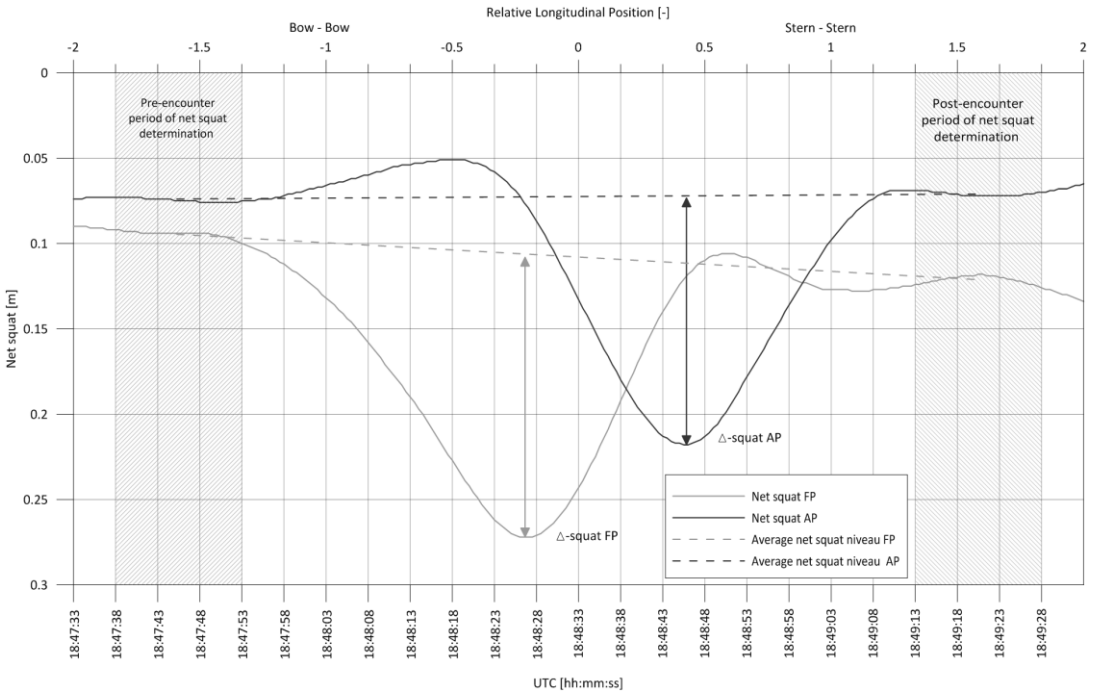

Figure 5.22: Determination of deltasquat values

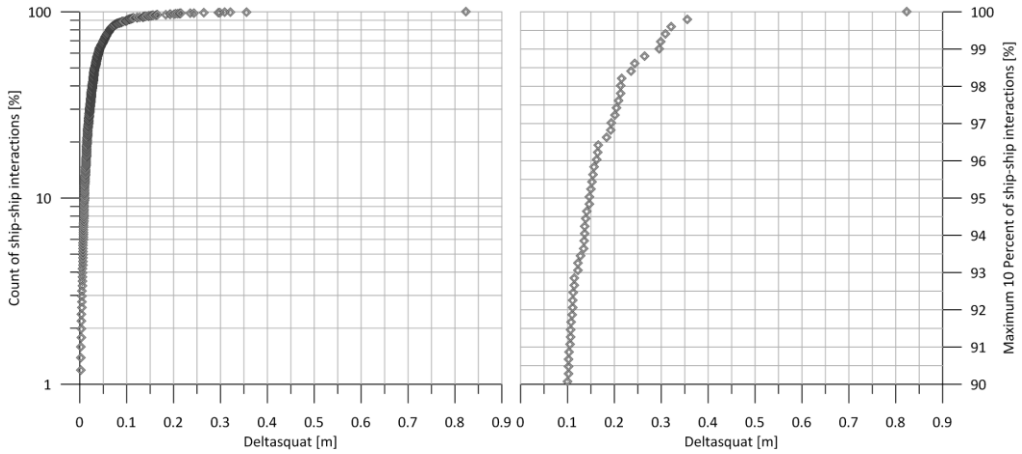

Figure 5.23: Deltasquat values of all ship-ship interactions (a – left) and maximum 10% (b – right)

Table 5.6: Ship-ship interactions causing the 18 highest deltasquat values

Deltasquat	Encounter type	Class	Encounter type	Encounter size	Length	Beam	Draft	Position
[m]	[-]	[-]	[-]	[-]	[m]	[m]	[m]	[Elbe-km]
0.82	head-on	C400	Container Ship	Post-Panamax	369.00	51.00	11.90	708.86
0.36	head-on	C396	Ro-Ro Cargo	Handymax	214.00	32.00	7.30	660.11
0.32	head-on	C400	Container Ship	Panamax	300.00	41.00	12.30	743.09
0.31	head-on	C347	Container Ship	Feeder	178.00	26.00	9.10	646.48
0.30	head-on	C400	Container Ship	PPM	366.00	48.00	11.20	696.35
0.30	head-on	C294	Container Ship	PPM	366.00	48.00	13.20	655.10
0.26	head-on	C400	Container Ship	PPM	336.00	46.00	12.50	684.66
0.24	head-on	C400	Container Ship	Panamax	299.00	48.00	9.60	729.61
0.24	overtaking	BULK	General Cargo	Handysize	200.00	28.00	7.90	741.07
0.22	head-on	C294	Container Ship	Panamax	275.00	40.00	10.20	696.94
0.21	head-on	C400	Container Ship	PPM	368.00	51.00	10.20	687.06
0.21	head-on	C335	Container Ship	PPM	333.00	46.00	12.90	671.63
0.21	head-on	C396	Container Ship	Panamax	294.00	32.00	10.40	745.85
0.20	head-on	C396	Container Ship	PPM	333.00	48.00	11.50	743.48
0.20	head-on	C396	Container Ship	Panamax	294.00	32.00	12.80	690.12
0.19	head-on	C400	Container Ship	Panamax	275.00	40.00	11.50	682.94
0.19	head-on	C335	Container Ship	PPM	335.00	46.00	12.10	630.52
0.18	head-on	C396	Ro-Ro Cargo	Handymax	214.00	32.00	8.30	704.56

5.4.3 Dynamic draft

Dynamic draft is the actual value of keel immersion at each location and point of time of the design vessel. Dynamic draft is based on draft at rest plus dynamic sinkage due to squat, pitch, change of

draft due to density and change of draft due to change of trim caused by density. Using equation 5.4, dynamic draft is draft at rest plus gross squat. All values are determined for FP and AP positions on the centerline of the design vessel. Dynamic roll is not an element of dynamic draft within that definition. Dynamic draft is determined using equation 5.6. Figure 5.24 shows dynamic draft values for vessel classes C294-C400 at FP position. Figure 5.25 shows additionally the dynamic draft values at the aft perpendicular position.

$$d_{Dyn,FP} = d_{at\ rest,FP} + S_{Gross,FP}$$

$$d_{Dyn,FP} = d_{at\ rest,FP} + S_{Net,FP} + COD_{FP\ Density} + COD_{FP\ Trim}$$

$$d_{Dyn,AP} = d_{at\ rest,AP} + S_{Gross,AP} \qquad 5.6$$

$$d_{Dyn,AP} = d_{at\ rest,AP} + S_{Net,AP} + COD_{AP\ Density} + COD_{AP\ Trim}$$

Mean dynamic draft values at the fore perpendicular range mainly between 11 m and 14 m with minimum values at 9.5 m and maximum values around 14.5 m. Range of mean dynamic draft values at the rear section is between 12 m and 14 m with minimum values around 11m and maximum values around 14.5 m (Table 5.7). Maximum difference is at C400 with 1.5 m difference in draft between FP and AP.

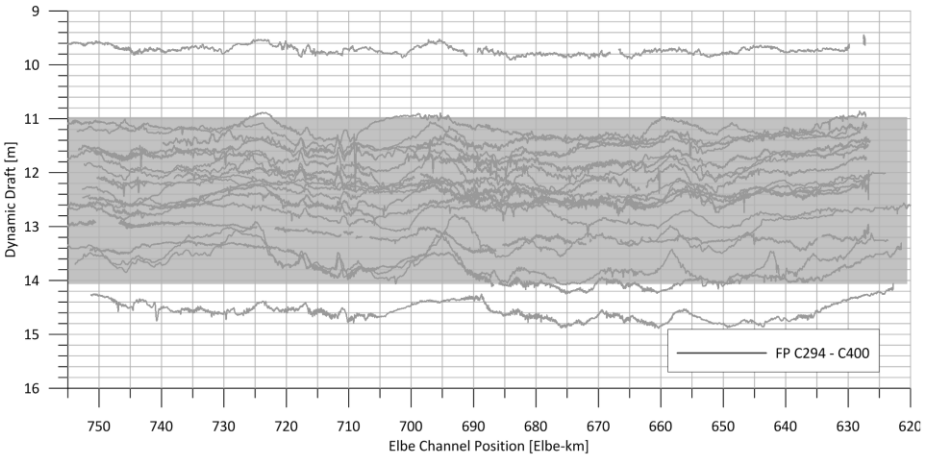

Figure 5.24: Dynamic draft values at FP for container vessel classes C294 to C400

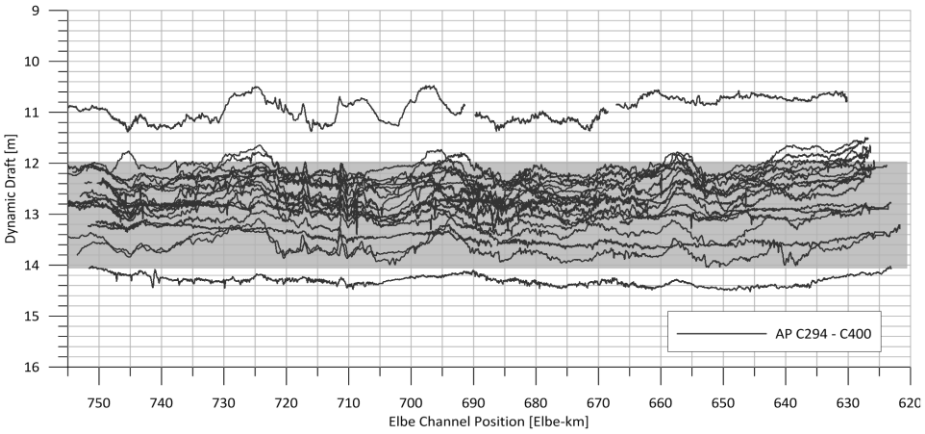

Figure 5.25: Dynamic draft values at AP for all vessel classes C294 to C400

Table 5.7: Minimum and maximum dynamic draft values at FP and AP position for each vessel class.

	C294	C335	C347	C366	C396	C400	BULK
[-]	[m]	[m]	[m]	[m]	[m]	[m]	[m]
Min.	11.0	12.5	12.0	11.0	11.8	9.5	13.2
Max	13.8	13.8	13.0	12.6	13.0	13.2	14.4
Δ FP-AP	**1.0**	**0.2**	**0.2**	**0.8**	**0.4**	**1.5**	**0.4**

5.4.4 Under keel clearance

Under keel clearance is the distance between the ship's keel and the bottom of the waterway. UKC is calculated by the dynamic draft amidships subtracted from the water depth. Dynamic draft amidships is the averaged value from dynamic draft at FP and AP positions (equation 5.7). The underlying assumption to average dynamic draft amidships is an even keel between FP and AP without bending, which means, that hogging is not considered within the calculation. The water depth is averaged over the vessel's plane area.

The UKC is determined at each point of time. Figure 5.26 shows the UKC for all inbound and outbound vessels along the Elbe passage.

$$UKC = h - \frac{1}{2}\left(d_{Dyn,FP} + d_{Dyn,AP}\right) \qquad 5.7$$

Minimum under keel clearance for all vessels range between 2.0 m and 3.0 m. Most shallow sections are around Elbe-km 740, 705 and 650. At Elbe-km 705, UKC values are 2.1 m for BULK (marked in green) and C335 (marked in red), 2.5 m for C294 and 3.0 m for C366 and C400. At the shallow section around Elbe-km 650, UKC values are 2.0 for C347 (marked in blue), 2.1 for BULK and 2.6 m for C396.

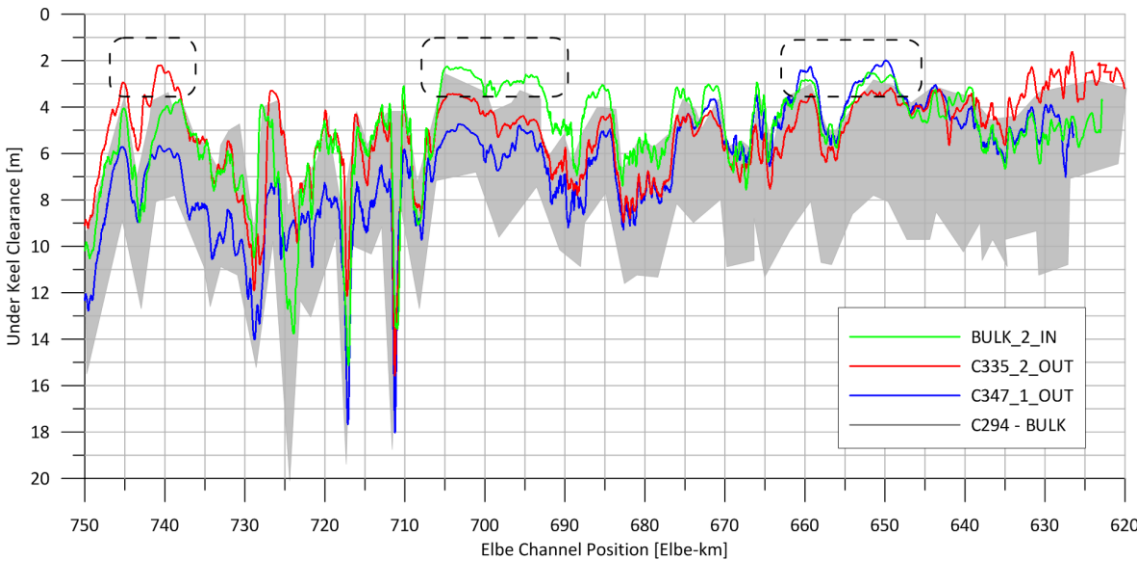

Figure 5.26: Under keel clearance for all vessels

6 Results

This section combines the influences of all factors presented in section 5. It analyses and quantifies the aggregated effects on dynamic draft. Furthermore, it examines and assesses single steps of the generally accepted dynamic draft determination approaches. The results presented form the basis of recommendations to optimize the dynamic draft determination for extraordinary large ships.

6.1 Influence of density on draft and trim

6.1.1 Effects of density on main draft

Section 5.1.1 shows the characteristics of density at the Lower Elbe passage. Section 5.2.3 discusses how changes in density influence main draft and hydrostatic trim. In order to calculate dynamic draft, influence of change in density on draft and influence of change in density on trim need to be expressed in absolute values.

Figure 6.1 displays the absolute changes in draft due to density in relation to absolute changes in density. Following the theoretical derivations of section 5.2.3, the change in main draft is proportional to the change in density. The field measurements confirm the theoretical assumptions with the results displayed in Figure 6.1. All container vessels (squared marks) experience a change in draft of 0.01 m per 1 kg/m³ change in density. Bulk carriers (circle marks) experience a slightly higher change in draft per 1 kg/m³ change in density.

For inbound and outbound container vessels, the maximum draft increase due to density between seawater and freshwater is around 0.25 m. For bulk vessels, the value is slightly higher with a maximum of around 0.28 m. In combination with the density distribution along the Elbe passage (section 5.1.1), the spatial dependence of the influence of density becomes obvious. Between Elbe-km 750-730, seawater draft of inbound vessels increases by 0.05 m, between Elbe-km 711-730 it increases by 0.10 m, between Elbe-km 690-710 by 0.20 m and the final value of 0.25 m can be applied onto seawater draft at Elbe-km < 690. For outbound vessels, the freshwater draft decreases by the same values within the abovementioned sections.

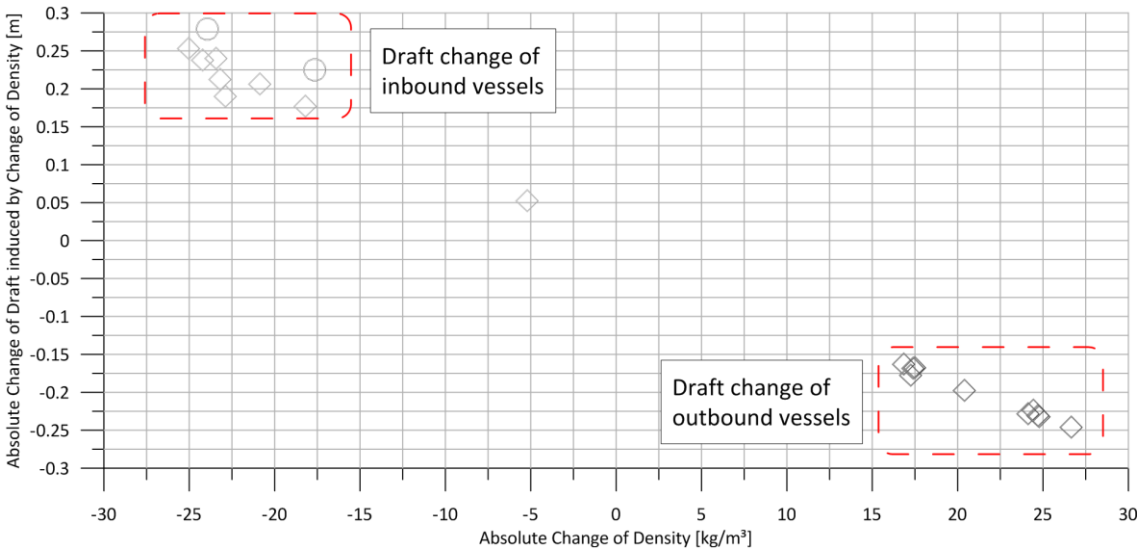

Figure 6.1: Absolute change of draft due to change of density for inbound and outbound vessels

6.1.2 Effects of density on trim

Figure 6.2 displays absolute values of draft change due to change of trim influenced by change of density. The results show the range of values in dependence of each vessel class with maximum values below 0.10 m for C294 and C335, values below 0.06 m for BULK and C347 and finally values below 0.04 m for C366, C396 and C400.

Influence of density on change of draft due to change of trim was unknown so far with respect to channel design. Nevertheless, the results show, that there is indeed a measurable but not significant influence on FP and AP. With respect of the trim direction and the spatial distribution of density, inbound vessels discover averagely an additional trim of around 0.05 m or less at the bow in the area at Elbe-km < 690. Draft at stern decreases by the same value in that reach. Outbound vessels discover the same quantity of the effect, but in the opposite direction. They discover a decrease in draft at FP, while draft at AP increases by the same value. With increasing ship size, the effect diminishes with an average of 0.04 m at C347, 0.03 m at C396 and finally 0.02 m at C400.

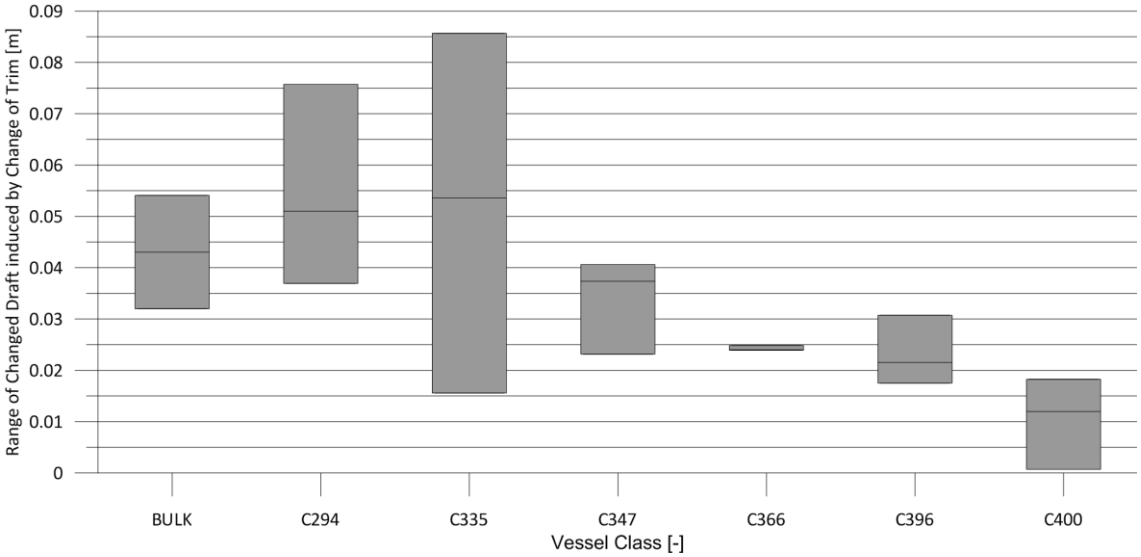

Figure 6.2: Range of changed draft due to change of density for inbound and outbound vessels

6.2 Influence of hogging, trim and roll on dynamic draft

Traditionally, the maximum static draft is calculated or read out at AP or FP position. Maximum dynamic roll is then estimated for MP position, assuming a rectangular underwater body of the vessel. The draft due to roll at MP is added to the static draft at AP or MP (section 2).

The data presented in sections 5.2 shows, that latest ship sizes discover hogging effects, that are still not used for draft determination. Furthermore, keel radius is still neglected within off-centric draft determination. Finally, off-centric draft is still determined at MP position, while the area of maximum cross-sections extends over a wide range around MP.

All named effects are presented and assessed in the following sections. Adapted determination methods are derived from the presented results and final recommendations towards an optimized dynamic draft determination process are prepared.

6.2.1 Consideration of keel radius

According to the BARRAS & DERRET approach in equation 2.37, e.g. a static draft at AP position of 12.75 m in combination with a maximum heel and roll amplitude of 3.2° would lead for C294_2_OUT to an off-centric draft of 13.10 m plus squat effects etc.

Thus, neglecting the keel radius leads to an overestimation of off-centric draft. On the other hand, equation 3.2 leads to slightly underestimated off-centric draft values. The correct application of the keel radius therefore is a focal point within off-centric draft determination.

Figure 6.3 displays the influence of the keel radius on the location of the additional draft value. Table 6.1 lists the keel radius for each investigated vessel class. The values are determined from the General Arrangement plans and Stability Booklets.

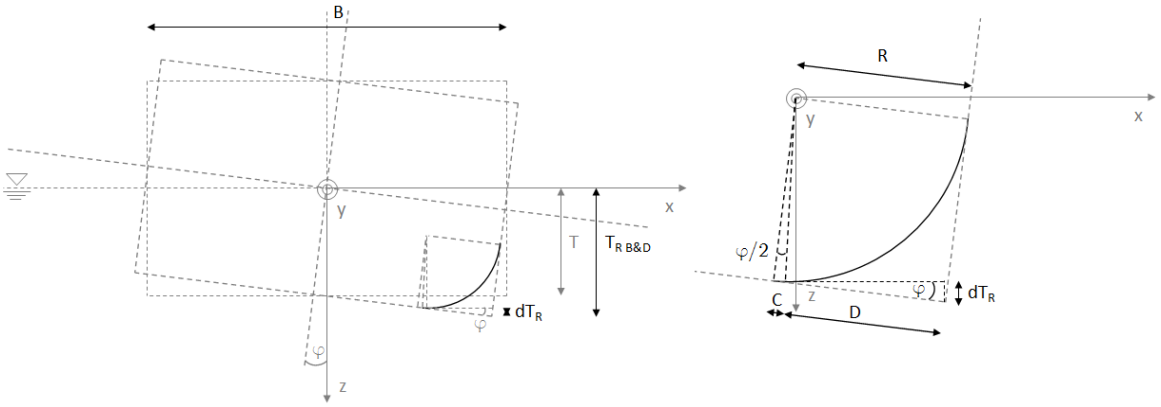

Figure 6.3: Influence of keel radius on draft change due to heel and roll

Table 6.1: Keel radii of all investigated vessel classes

	C294	C335	C347	C366	C396	C400	BULK
[-]	[m]	[m]	[m]	[m]	[m]	[m]	[m]
Min.	4.3	4.5	4.7	5.0	5.3	5.6	2.5

On the basis of Figure 6.3 and the BARRAS & DERRET approach with

$$\mathrm{T}_R = \frac{B}{2} * \sin\varphi + T * \cos\varphi$$

The diminishing influence of the keel radius with the diminishing value of dTR, which is shown in Figure 6.3 can be calculated with the heel and roll angle by:

$$d\mathrm{T}_R = D * \sin\varphi$$

$$with\ D = R - C$$

$$and\ C = R * \tan\varphi$$

$$dT_R = \left[R\left(1 - \tan\frac{\varphi}{2}\right)\right]\sin\varphi \qquad 6.1$$

Finally, the subtraction of dTR leads to a determination approach that delivers an off-centric draft value due to heel and roll under the consideration of the vessel`s beam and keel radius:

$$T_R = \frac{B}{2} * \sin\varphi + T * \cos\varphi - \sin\varphi\left[R(1 - \tan\frac{\varphi}{2})\right] \qquad 6.2$$

6.2.2 Location of off-centric draft

BARRAS & DERRET (2012) determines off-centric draft amidships based on the assumption, that the cross-section with the maximum underwater beam at keel level is allocated exactly there. However, General Arrangement plans show that the cross-section with maximum beam is not only allocated at MP position. It rather extends over several bays around MP along the longitudinal axis.

Figure 6.4 shows the deck plan for the 2nd deck of a C396 vessel. FP, MP and AP positions are market with grey dotted lines. Furthermore, the figure displays the keel level of the vessel in black. That view stresses out, that for C396 vessels, the maximum beam at keel level is not only at MP position. It is rather an area of cross-sections with maximum beam that extends from bay 34 to bay 58 over a range of 6 holds at a length of 99.50 m.

The cross-section with maximum beam towards FP is market with MF. It has a distance of 43.55 m from MP. The distance between the cross-section with maximum beam towards AP, market as MA, has even a distance of 55.95 m from MP. Table 6.2 lists the MF and MA positions for all investigated vessel classes.

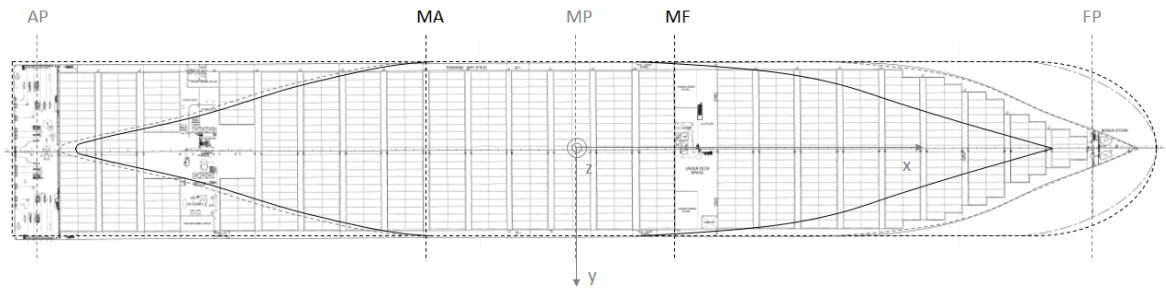

Figure 6.4: Extension of cross-sections with maximum beam at keel level

The determination of off-centric draft at MP position is valid as long the vessel moves on an exact even keel. If trimming and pitching moments lead to an inclination around the lateral axis of the vessel, off-centric draft location is relocated to the utmost bay of the maximum cross-section. In case of trim towards stern (bow up) the off-centric draft position is at MA. Opposite case of trim towards bow (stern up), relocates off-centric draft position to MF.

Table 6.2: Maximum cross-section extensions all investigated vessel classes.

	C294	C335	C347	C366	C396	C400	BULK
[-]	[m]	[m]	[m]	[m]	[m]	[m]	[m]
Bay MF	4F	27	33	30	34	37	-
Bay MA	6A	51	55	55	58	59	-
Number of holds	6	7	6	6	6	6	-
Distance MP - MF	41.86	51.20	35.20	41.70	43.55	33.20	140
Distance MP - MA	-43.47	-42.30	-49.65	-55.95	-55.95	-54.75	161
Distance MF - MA	85.33	93.5	84.85	97.65	99.50	87.95	301
LPP	281.60	319.00	331	349.5	378.40	383	318

6.2.3 Effects of hogging on off-centric draft value

Hogging value is the expression, that the sum of vertical forces is different between the section amidships and the sections around perpendiculars. Hogging means that keel bends around the lateral axis with lower draft values at MP than at FP and AP positions. Figure 6.5 shows that local phenomenon. Sagging expresses the opposite with higher draft values at MP than at FP and AP perpendiculars.

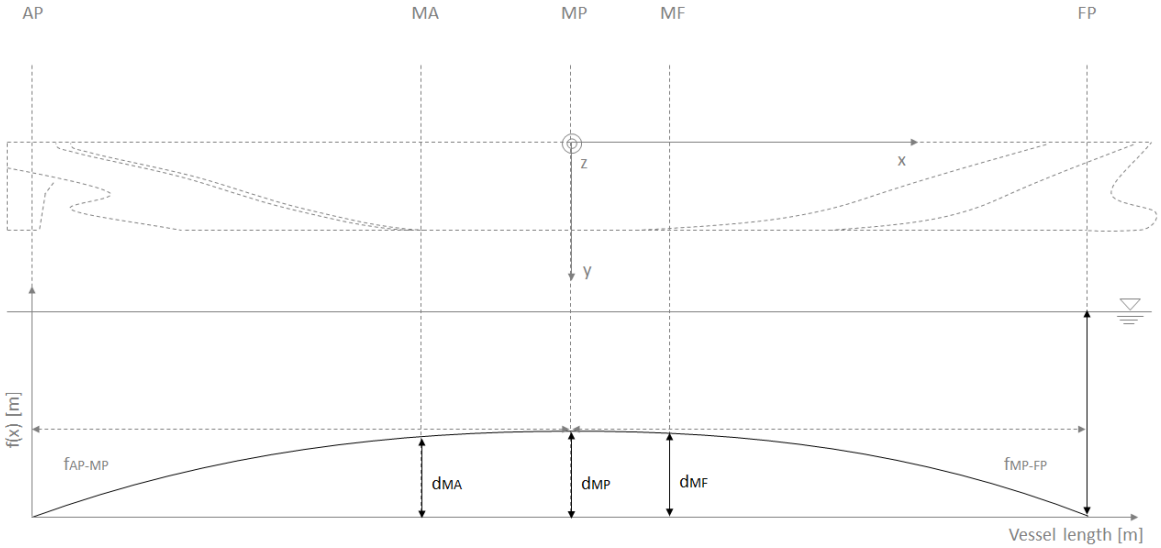

Figure 6.5: Determination of hogging parabola

Calculation basis for off-centric draft determination is usually the assumption of an even keel without any hogging and sagging amidships. That overall assumption is no longer valid as expressed in section 5.2.1, where it is shown, that nearly none of the investigated vessels travelled on even keel. Table 6.3 lists the draft meter at FP, MP and AP positions as well as the hogging values for all investigated vessels. Hogging value is the difference between draft at MP and the average draft from drafts at AP and FP.

That in mind it becomes obvious that off-centric draft determination at any position of the keel needs to include hogging values in order to determine correct absolute values of draft increase. In case of draft determination at MP position, the subtraction of hogging value at MP position, d_{MP}, from relative off-centric draft generates the correct absolute value for off-centric draft (Figure 6.5).

To calculate hogging values for MF and MA, in extension to section 6.2.2, the deformation of the keel is assumed as a parabola between FP and AP (TUPPER, 2013). The parabola results from the hogging value at MP and LPP, the distance between FP and AP. With knowledge of the parabola and the distances FP-MP and MP-AP, the hogging values at MF (d_{MF}) as well as at MA (d_{MA}) can be determined.

Table 6.3: Hogging values of all investigated vessel classes

Class	Ship_ID	#	In / Out	DM FP	DM MP	DM AP	Hogging
[-]	[Class_#]	[-]	[-]	[m]	[m]	[m]	[m]
C294	C294_1_OUT	1	Outbound	12	11.8	12	0.2
	C294_2_OUT	2	Outbound	11.25	11.6	12.75	0.4
	C294_3_IN	3	Inbound	10.95	11.4	12	0.08
C335	C335_1_OUT	4	Outbound	12.9	12.65	13	0.3
	C335_2_IN	5	Inbound	13.2	13.05	13.2	0.15
	C335_3_OUT	6	Outbound	12.7	12.65	12.75	0.08
C347	C347_1_OUT	7	Outbound	12.1	11.9	12.05	0.18
	C347_2_IN	8	Inbound	13.1	12.55	12.9	0.45
	C347_3_IN	9	Inbound	12.8	12.7	12.9	0.15
C366	C366_1_OUT	10	Outbound	11.2	10.8	11.5	0.55
	C366_2_OUT	11	Outbound	11.55	11.2	11.75	0.45
	C366_3_IN	12	Inbound	12.1	11.7	12.2	0.45
C396	C396_1_OUT	13	Outbound	11.7	11.2	11.7	0.5
	C396_2_OUT	14	Outbound	11.45	11.25	11.55	0.25
	C396_3_IN	15	Inbound	12.15	11.95	12.3	0.28
C400	C400_1_IN	16	Inbound	9.6	9.5	10.4	0.5
	C400_2_OUT	17	Outbound	11	11.1	11.6	0.2
	C400_3_OUT	18	Outbound	11.4	11.6	12	0.1
	C400_4_IN	19	Inbound	12.1	11.9	12.1	0.2
Bulk	BULK_1_IN	20	Inbound	13.3	13.3	13.3	0
	BULK_2_IN	21	Inbound	14.2	14.1	14.1	0.05

6.2.4 Method design to pre-assess off-centric draft conditions

Traditionally, the crew transmits draft values at FP and AP position to the maritime administrations and port facilities. Based on such values, the administrations determine maximum draft allowance for FP and AP position.

With the results of the previous sections it becomes obvious, that only by the draft marks information and the knowledge of the ship dimensions, there is a lot more draft information determinable up front.

At the point in time, when loading is completed and before cast-off, the crew of the vessel read the draft marks at FP, MP and AP position. The comparison of draft marks values and radar gauge data shows the high accuracy of such crews' reading values. From these accurate values, trim and hogging

can be determined already before cast-off. With the assumption of almost static trim and static hogging conditions during the Lower-Elbe passage, real draft at FP and AP as well as hogging corrected draft at MF, MP and MA position can now be determined already.

That knowledge, in combination with inclination measurements on board, leads to direct assessment of off-centric draft due to the heel and roll at MF, MP and MA position. Furthermore, with the newly developed approaches of sections 6.2.2 and 6.2.3, it is possible to pre-determine the position of maximum draft due to trim in advance. In addition, threshold value of heel and roll angle, which leads to significant off-centric draft can be identified in advance as well.

Aiming to optimize maximum draft determination, a mathematical model was set up to identify a way to pre-determine whether the influence of off-centric draft has to be considered or not in dependence from initial trim and initial hogging. The calculations were performed in MATLAB for a C400 vessel with a static draft of 12 m. Within that model, initial trim is varied within a range of 0-2.5 m in steps of 0.05 m. Hogging is varied within a range of 0-0.5 m in steps of 0.05 m and finally heel is varied within 0-4.5° in steps of 0.10°.

Figure 6.6 shows the resulting model, which displays the effective threshold area between trim, hogging and heel.

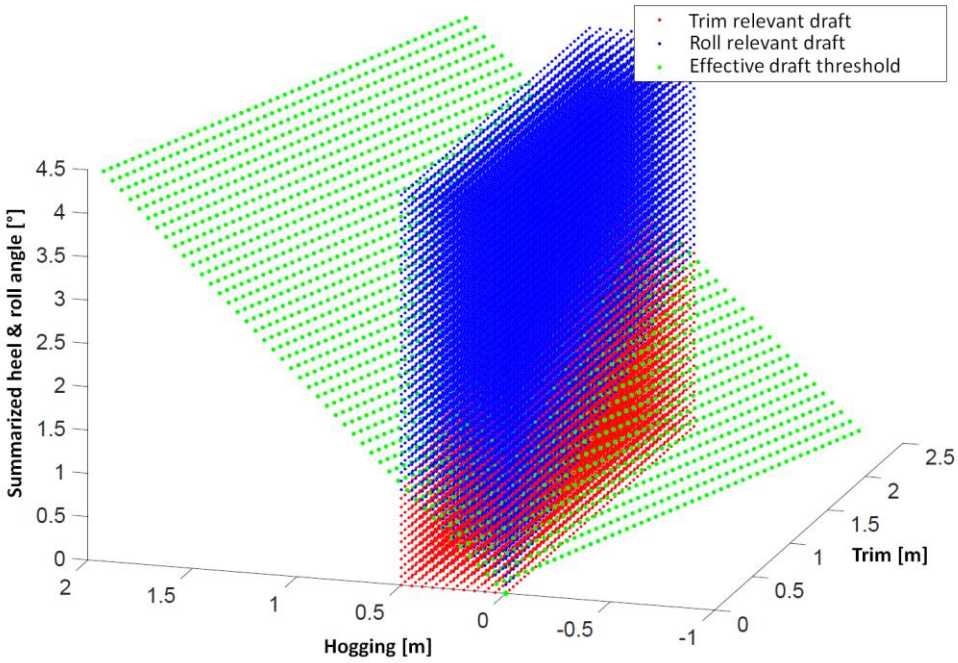

Figure 6.6: 3D-Diagram of interaction between initial trim, hogging and heel angle[9]

With knowledge of initial trim and hogging, the model facilitates, to read out the threshold of the heel angle, which would lead to a significant increase of off-centric draft for a C400 vessel. With knowledge of that threshold, dynamic draft determination could identify in advance, either if off-centric draft has to be considered for a vessels' passage or if not.

The first results express the necessity of further investigations on the interaction of vessels' hull, initial draft at FP and AP as well as initial hogging and dynamic heel angle. It can be assumed already,

[9] KOCH, A., 2016: Entwurf eines Verfahrens zur Berechnung der Tiefgangsänderung von Großcontainerschiffen auf der Schifffahrtsstraße Elbe, Master Thesis (German) unpublished.

that with the utilization of the additional draft mark reading at MP position, the draft determination could be significantly improved by the use of the developed model.

6.3 Analysis of the influence of speed and water depth on ship squat

6.3.1 Influence of speed through water on net squat

Theoretical derivations as well as empirical findings attach significant importance to speed through water as the main driver for net squat. Figure 6.7 shows speed through water of selected measurement campaigns in comparison to the associated net squat values. The gradients of net squat curves of all vessel classes correlate with the gradients of the speed through water curves.

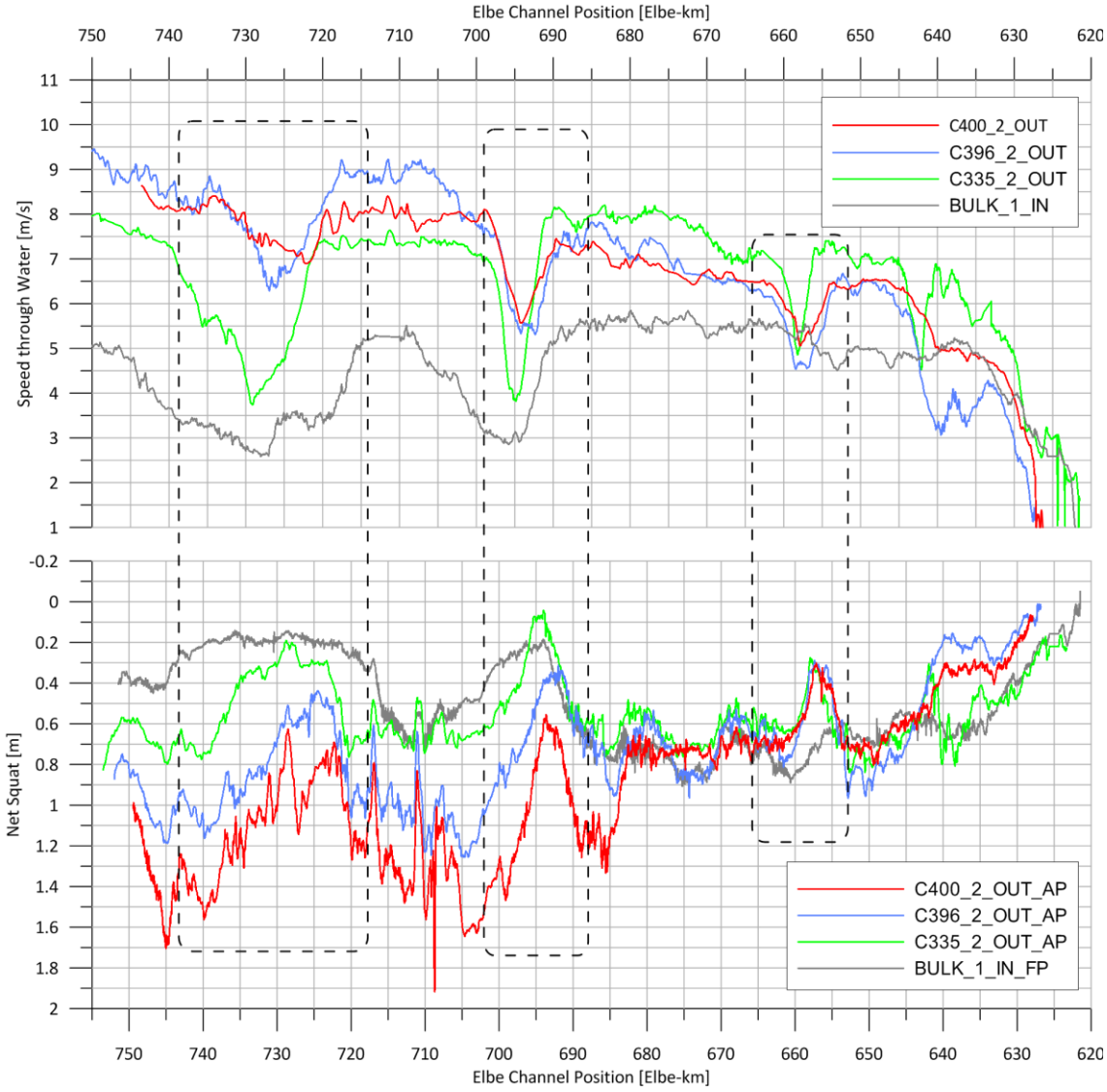

Figure 6.7: Speed through water and net squat

Influence of speed on squat becomes obvious within several Elbe sections, e.g. between Elbe-km 715-735, where vessels slow down due to the passage of Cuxhaven Port. Within that section, also squat declines in line with speed through water. Two other examples are within the section of Elbe-km 685-700, where the vessels pass the entrance of the Kiel-Canal and slow down for the reception of the Elbe Pilots. Between Elbe-km 650-650 the vessels slow down as well to receive the Hamburg

Port Pilots. Net squat declines in both sections in line with the decrease in speed, which confirms speed through has main influence on net squat.

Figure 6.8 presents the correlation between speed through water and net squat for vessels of class C396 and C400. The figures show, that with increasing speed also squat increases. Thus, it is confirmed, that speed through water and net squat have a strong correlation. Regression analysis[10] states, that a quadratic regression curve expresses the best fit to describe such correlation.

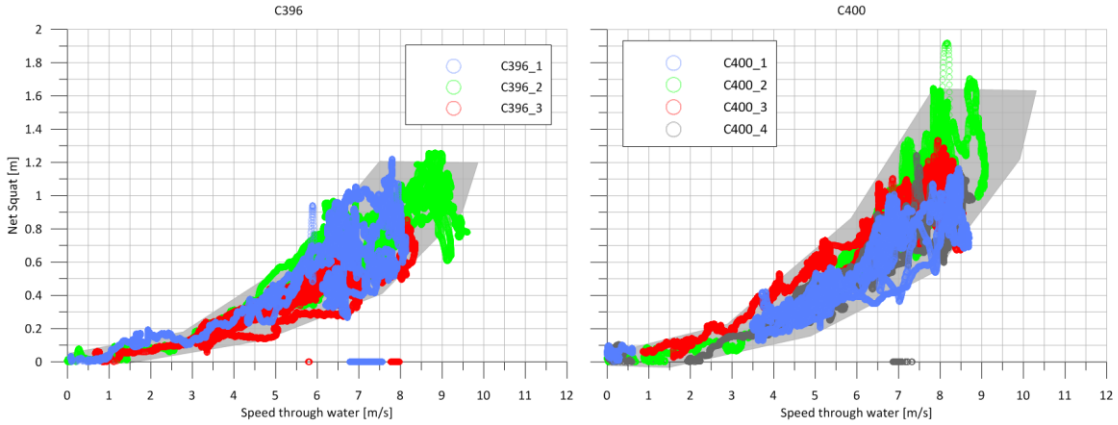

Figure 6.8: Correlation of speed through water and net squat for C396 and C400

6.3.2 Influence of water depth on net squat

Section 2.1.1 states, that next to speed, water depth is also a main squat governing factor. When the water depth is high, squat values should be low and vice versa. Figure 6.9 shows net squat in comparison to water depth.

In several sections, declination of net squat curves correlate with the inclination of water depths. For example at Elbe-km 711 as well as at Elbe-km 718 and 728, the figure shows an abrupt rise in water depth due to high water depth section within the channel bottom. Squat values react by an abrupt decrease in net squat. Such reaction can also be identified between Elbe-km 740-745, where water depth increases slowly and squat curve gradients of vessel classes C335, C396 and C400 react by a slow decrease of net squat values.

Figure 6.9 shows as well, that the correlation between water depth and squat is not as strong as between speed and squat. E.g. the decrease in water depth between Elbe-km 740-745 has no influence on net squat of the Bulk class due to low speed through water of the bulker in that section.

The try to display a strong correlation between water depth and net squat values like in Figure 6.8 for speed and squat did not work out. The correlation becomes obvious only in the direct comparison of a net squat curve and the corresponding water depth curve, displayed over the Elbe passage. Therefore, correlation between water depth and squat is only a weak correlation.

[10] BOCKELMANN, A., 2015: Anwendbarkeit der multiplen Regression zur Analyse gewässerspezifischer Parameter auf die dynamische Tiefertauchung von Fahrzeugen der C335 Klasse, Master Thesis (German)

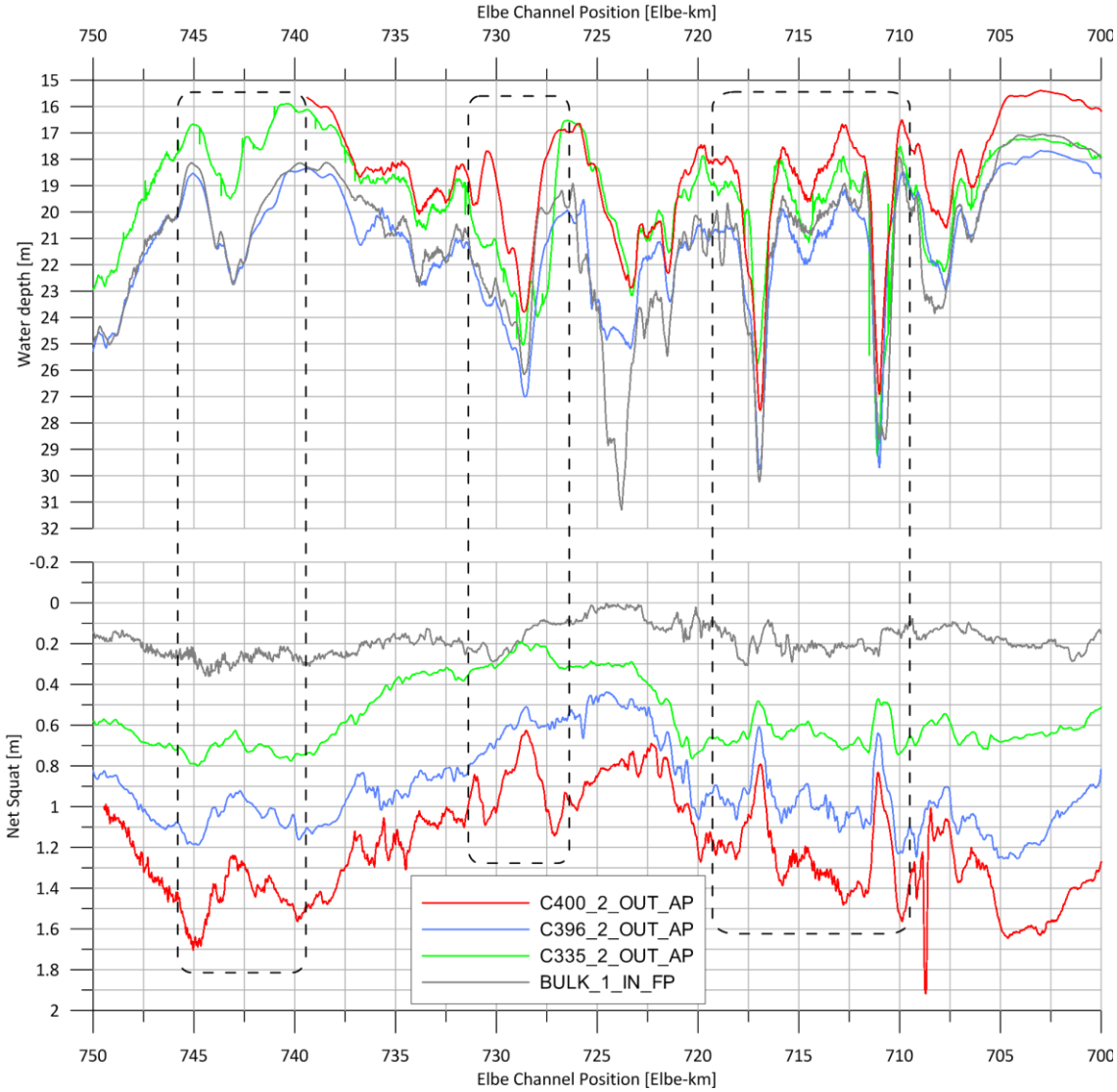

Figure 6.9: Water depth and net squat

6.3.3 Correlation of TUCK parameter on net squat

TUCK based his theoretical approach on a dimensionless parameter, which combines speed through water and water depth by the use of the depth Froude number $F_{nh}\,(-)$. Figure 6.10 shows the correlation between the Tuck parameter and net squat values with the result of a very strong correlation between both values. It is possible to describe net squat values as a function of the Tuck parameter. The strong correlation is valid for all vessel classes.

Vessels can be clustered into groups with different gradients of correlation. C294 and C335 form one cluster (marked in blue), C347, C366 and C396 vessels form another cluster (marked in green) and finally C400 forms a third cluster (marked in red) within Figure 6.10. The clusters have different gradients within the correlation of Tuck parameter and net squat. With increasing vessel sizes, also the gradient between Tuck parameter and net squat increases.

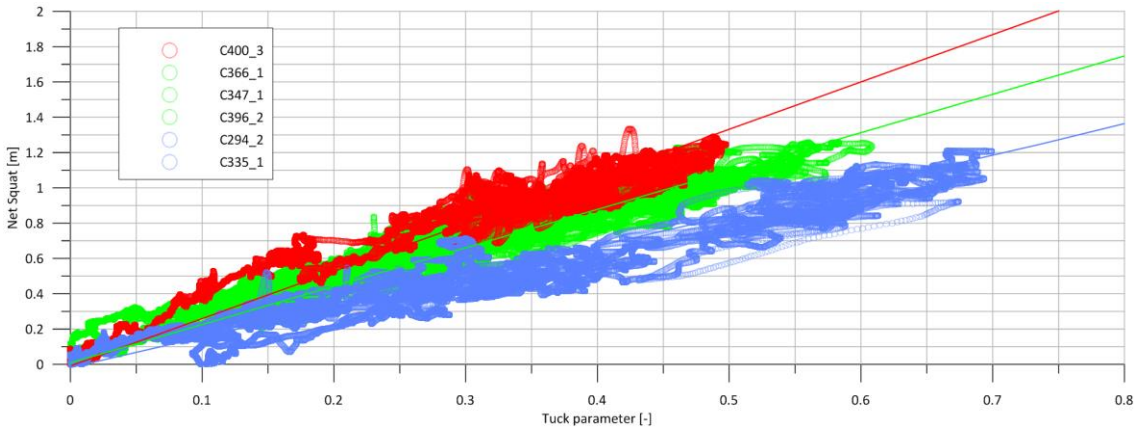

Figure 6.10: Scatter plot of TUCK parameter and net squat

6.4 Assessment of generally accepted squat estimation approaches

Permission to enter the Lower Elbe Passage needs a reliable squat estimation approach. To determine, which approach gives the closest results to the net squat values from the field investigations, recommended squat estimation approaches are performed with data from the field investigation.

BAW investigations proofed, that ICORELS estimation approach is valid for the use on the Lower Elbe. Thus, ICORELS approach is used for real data squat estimation. The calculations are performed with the two generally accepted pre-factors of 2.0 and 2.4. Next to ICORELS, PIANC (2014) recommends BARRAS approach to determined squat. Therefore, latest BARRAS III approach is used for squat calculations as well. Calculations are also based on data from the field investigations. BAW investigation came to the conclusion, that squat estimation approach of SCHMIECHEN is generally applicable to roughly estimate ship squat. Therefore, also SCHMIECHEN approach is performed with field investigation data.

Basic data for all calculations in this section are:

- Maximum fresh water draft from section 5.2.1
- Static block coefficient based on draft of section 5.2.1
- Location depending water depth of section 5.1.2
- Location depending speed through water from section 5.3.2
- Static gravitational acceleration of 9.81 m/s²

ICORELS calculation approach is already mentioned above. It is defined as:

$$S_{IC\,n.n} = Ic(x)\,\frac{C_B * B * T_{FW\,max}}{L_{PP}}\,\frac{F_{nh}^2}{\sqrt{1 - F_{nh}^2}}$$

$$with\ Ic_{(x)} = 2.0\ for\ S_{IC\,2.0}$$

$$and\ with\ Ic_{(x)} = 2.4\ for\ S_{IC\,2.4}$$

$$F_{nh} = \frac{v(x_S)}{\sqrt{g * h(x_S, t)}}$$

$$x = Lower\ Elbe\ Passage\ position$$
$$x_S = Ship's position$$
$$v(x_S) = Speed\ through\ water\ at\ ship's\ position$$
$$h(x_S, t) = Time\ depending\ water\ depth\ at\ ship's position$$

PIANC (2014) recommends the latest version of BARRAS, the BARRAS III approach, which is:

$$S_{B\ III} = \frac{C_S * v_{kts}^2}{\left(\frac{100}{K}\right)} \qquad 6.3$$

$$with\ K = 5.74 * S^{0.76}$$
$$S = \frac{A_S}{A_c}$$
$$A_S = 0.98 * T_{FW\ max} * B$$
$$A_C\ according\ to\ section\ 2.1.1\ and\ 5.1.3$$

SCHMIECHEN approach is defined as:

$$S_S = \frac{1}{3} T_{FW\ max} * F_{nh}^3 \qquad 6.4$$

For each approach, the theoretical net squat, based on data from the field investigations, is determined and compared to the directly determined net squat from the measurements within the field. Such calculations are performed for all 21 measurements campaign. As examples for all results, Figure 6.11 and Figure 6.12 show the resulting squat estimations in direct comparison to net measured squat values for campaign C366_3_IN and campaign C400_1_IN.

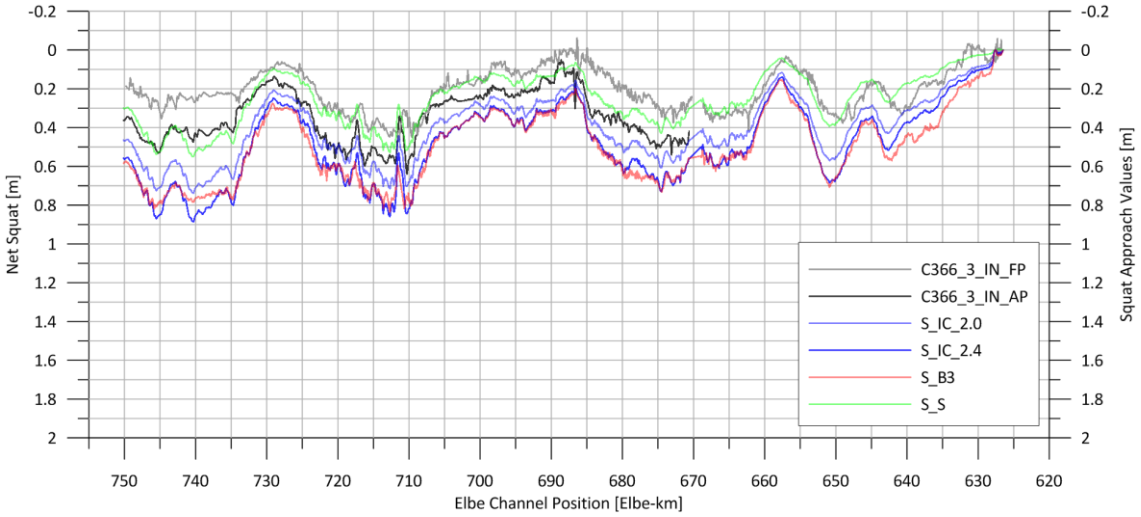

Figure 6.11: Net squat and squat approach estimation values for measurement run C366_3_IN

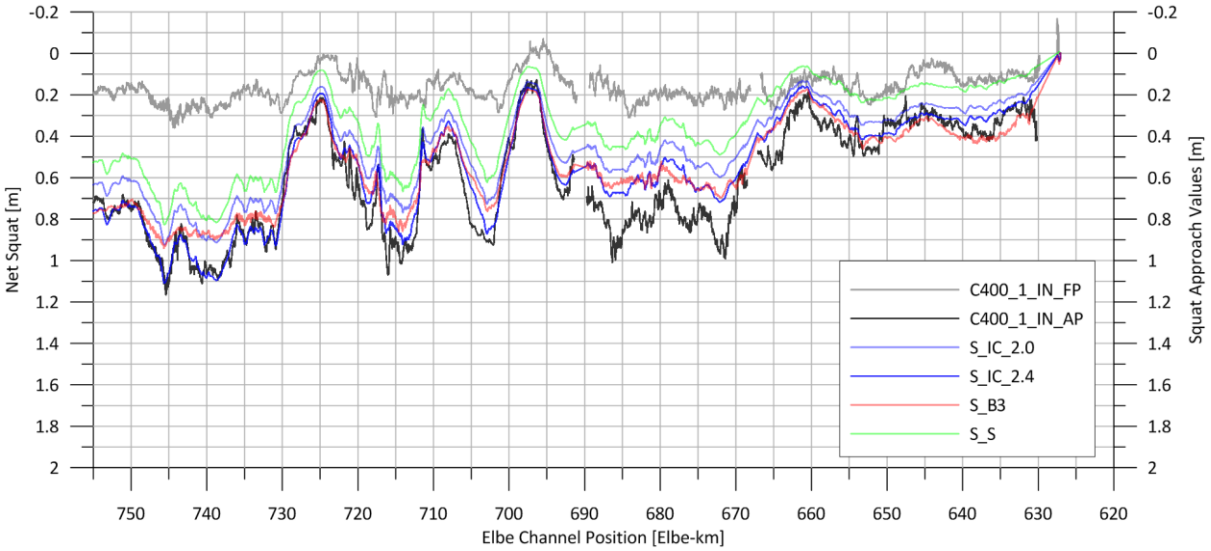

Figure 6.12: Net squat and squat approach estimation values for measurement run C400_1_IN

In both cases, squat estimation approaches are able to determine a squat curve, which is similar to the measured net squat values at AP position. However, in case C366_3_IN, squat estimations determine higher squat values than measured. In case of run C400_1_IN, squat approaches determine values, which are much lower than the measured net squat values from the field. Such squat determinations are performed for all measurement campaigns and the results are compared to the measured net squat values.

Moreover, Figure 8.3 - Figure 8.9 show the overall comparison of the measured net squat values to the results of the following squat estimation approaches, where

S_IC_2	= ICORELS approach with pre-factor 2.0 is marked in light blue
S_IC_2.4	= ICORELS approach with pre-factor of 2.4 is marked in dark blue
S_BIII	= BARRAS III approach is marked in red
S_S	= SCHMIECHEN approach is marked in green

Each figure displays one measurement campaign. The diagonal line shows the ideal fit, the dotted lines show deviations of 0.2 m as a visualization of the threshold of acceptance. All values over the diagonal line overestimate the real net squat, all values beneath the diagonal line underestimate the real net squat. To apply the approaches pragmatically, the area between the dotted lines displays the area of approach validity. Figure 6.13 - Figure 6.19 show the selection of best fitting estimations.

In Figure 8.3, SCHMIECHEN approach (S_S) underestimates net squat values for both BULK measurement campaigns. For BULK_1_IN, ICORELS approach with pre-factor 2.4 (S_IC_2.4) is within the area of acceptance. For BULK_2_IN, ICORELS with pre-factor 2.0 (S_IC_2) (Figure 6.13) as well as BARRAS (S_BIII) generate the best fitting values.

Figure 8.4 displays the results for container vessel class C294. All squat approaches overestimate the net squat of that vessel class. For campaign C294_1_OUT and C294_2_OUT, S_S and S_IC_2 overestimate net squat but give results that are predominantly within the area of acceptance. For C294_3_IN all approaches overestimate. S_S and S_IC_2 (Figure 6.14) determine also the smallest deviations. S_IC_2.4 and S_BIII are not acceptable for vessel class C294.

For vessel class C335, S_S and S_IC_2 are predominantly within the area of acceptance (Figure 8.5). For net squat values up to 0.8 m, SCHMIECHEN gives the best fit for all campaign of that class (Figure 6.15), followed by S_IC_2 with slightly overestimating results. For net squat values over 0.8 m, all approaches overestimate real net squat values. S_IC_2.4 as well as S_BIII generally overestimate net squat for this class.

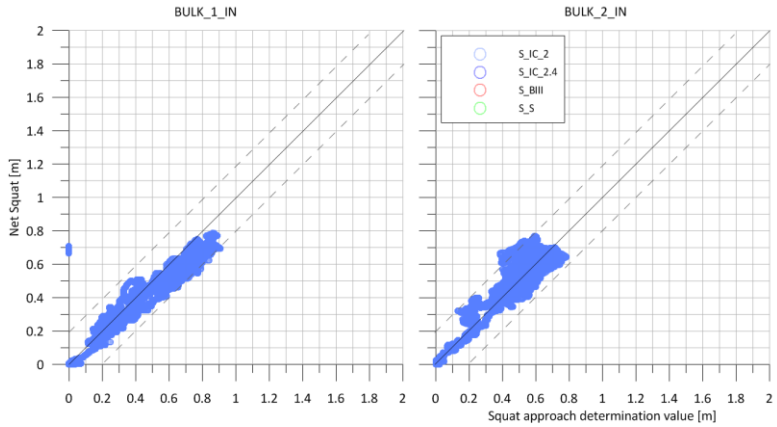

Figure 6.13: Net squat and selected squat estimation comparison for BULK

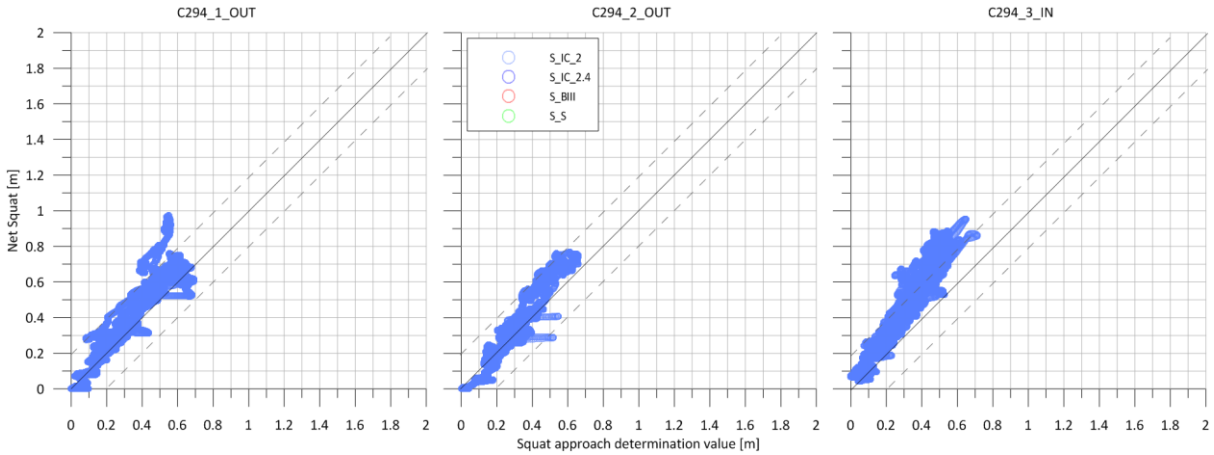

Figure 6.14: Net squat and selected squat estimation comparison for C294

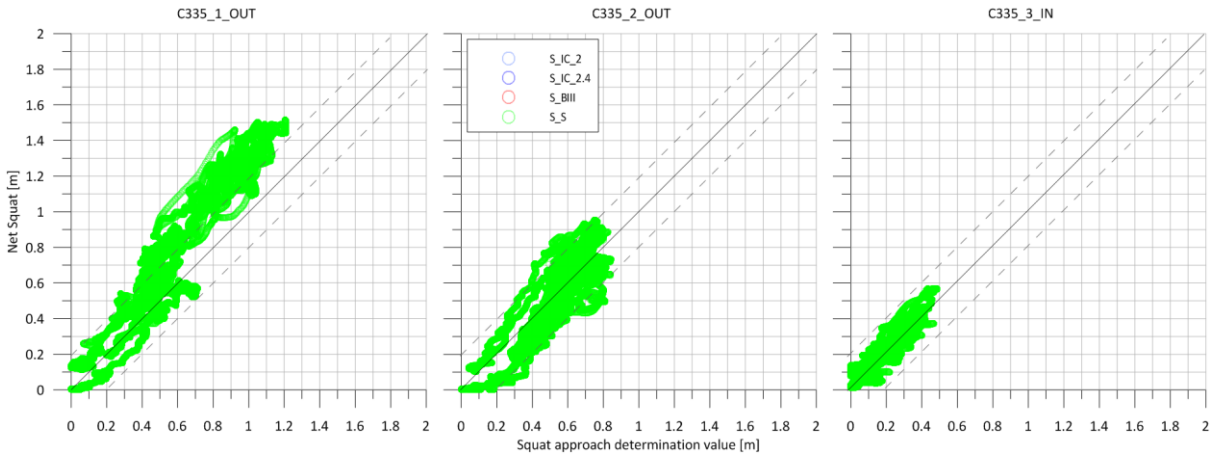

Figure 6.15: Net squat and selected squat estimation comparison for C335

For vessel class C347 all estimation approaches seem to be generally applicable (Figure 8.6). For campaign C347_1_OUT, S_IC_2 gives the best fit (Figure 6.16). S_IC_2.4 and S_BIII overestimate net squat values and S_S underestimates. S_S gives the best fit for campaign C347_2_IN with very low squat values. For C347_3_IN, S_IC_2 gives the best fit and S_S is within the area of acceptance. Results of S_IC_2.4 and S_BIII overestimate squat values and are not acceptable.

Figure 8.7 shows squat estimation results for vessel class C366. For campaign C366_1_OUT and C366_2_OUT, S_IC_2 provides the best fit (Figure 6.17). S_S underestimates net squat and S_IC_2.4 and S_BIII overestimate real squat values. For the third campaign C366_3_IN, S_S and S_IC_2 estimate acceptable values. S_BII and S_IC_2.4 overestimate.

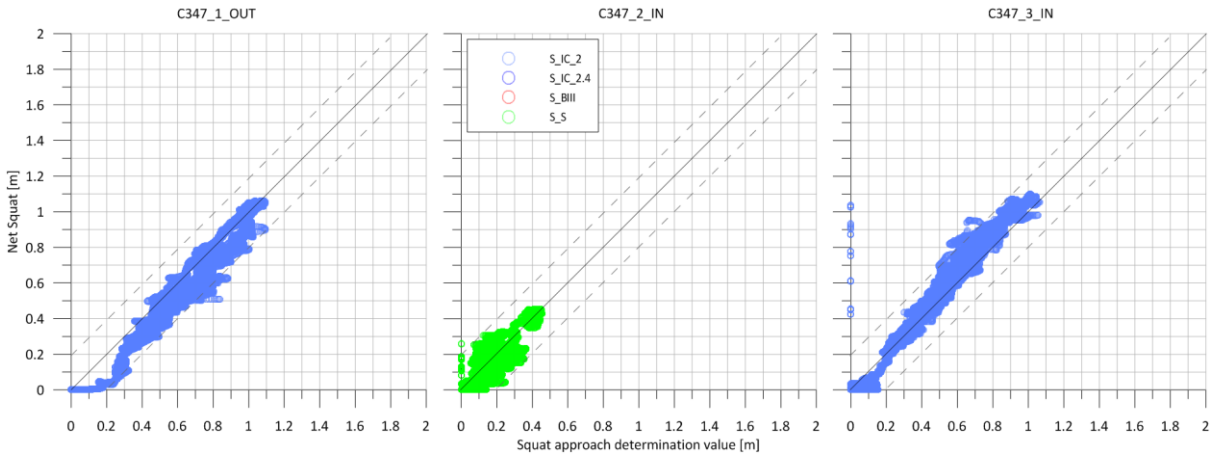

Figure 6.16: Net squat and selected squat estimation comparison for C347

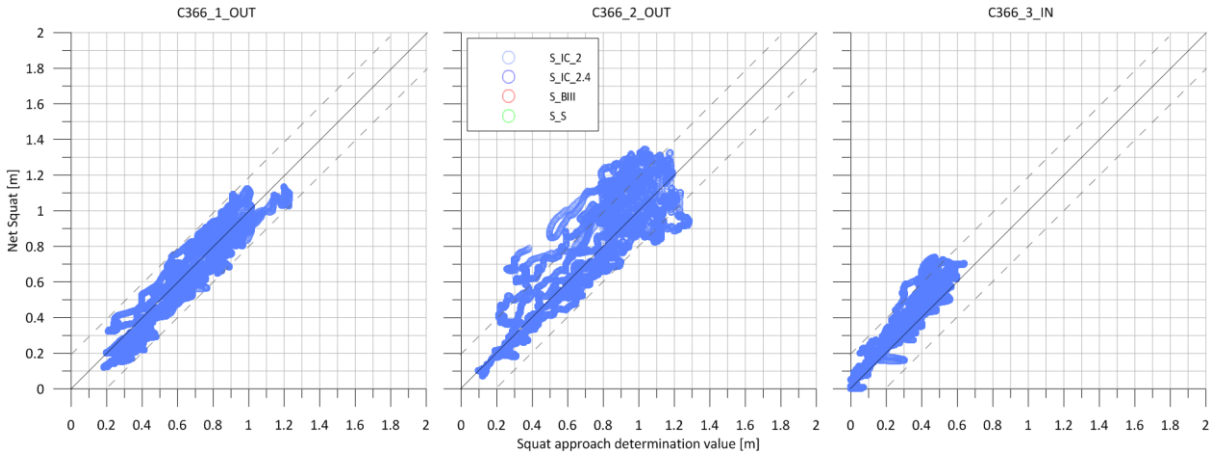

Figure 6.17: Net squat and selected squat estimation comparison for C366

For all campaigns of vessel class C396 (Figure 8.8), S_IC_2 provides most accurate estimations (Figure 6.18). S_S underestimates and S_IC_2.4 and S_BIII overestimate real squat values. All approaches provide predominantly acceptable results.

S_IC_2.4 provides best fitting values for the first two campaigns of vessel class C400 (Figure 6.19). For campaign C400_3_OUT as well as C400_4_IN, S_BIII provides the best fit. For this vessel class, the former acceptable estimations of S_S and S_IC_2 now provide generally underestimating squat values, which are predominantly even not within the acceptable range (Figure 8.9).

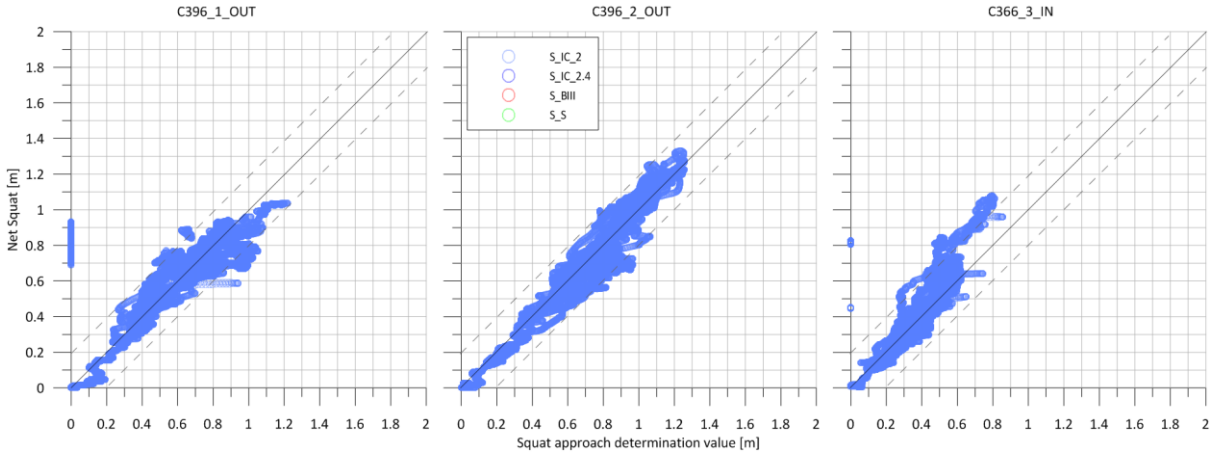

Figure 6.18: Net squat and selected squat estimation comparison for C396

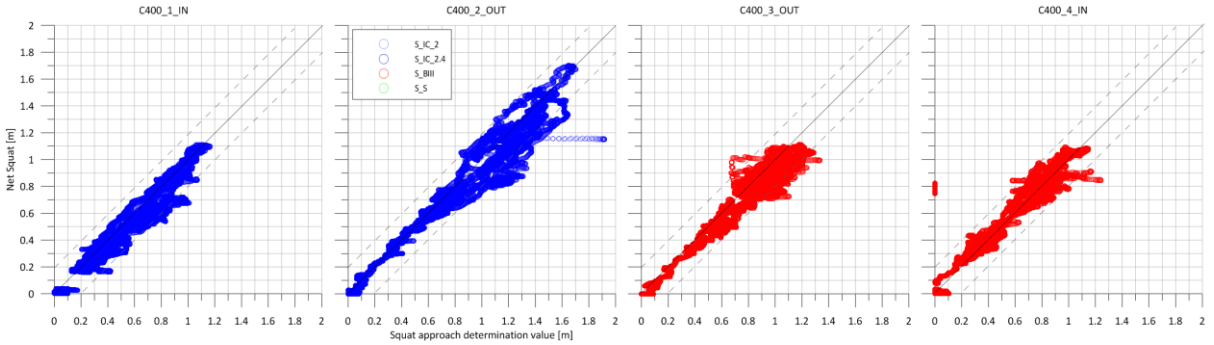

Figure 6.19: Net squat and selected squat estimation comparison for C400

Table 6.4 summarizes the results of the direct comparison between estimation approaches and measured net squat values. That compressed result states, that:

- S_S underestimates vessel classes BULK and all vessel classes bigger than C347
- S_IC_2 can be applied to vessel sizes up to C396 with the exception of class C335
- S_IC_2.4 as well as S_BIII can be applied for BULK and vessel class C400.

Table 6.4: Matrix of approaches with acceptable (A-green), underestimating (U-red) and overestimating (O-yellow) squat estimations in relation to vessel class

	BULK	**C294**	**C335**	**C347**	**C366**	**C396**	**C400**
S_S	U	A	A	A	U	U	U
S_IC_2	A	A	O	A	A	A	U
S_IC_2.4	A	O	O	O	O	O	A
S_BIII	A	O	O	O	O	O	A

6.5 Quantitation of the influence of ship - ship interactions on sinkage

ELOOT (2011) states that those ship-ship interactions, where UKC percentage of draft exceeds 20%, are of minor relevance (section 2.2). In contrast to that, Figure 6.20 expresses clearly, that such statement is not applicable for the Lower Elbe, where all significant deltasquat values > 0.1 m occur at UKC values, which exceed 20 % of draft.

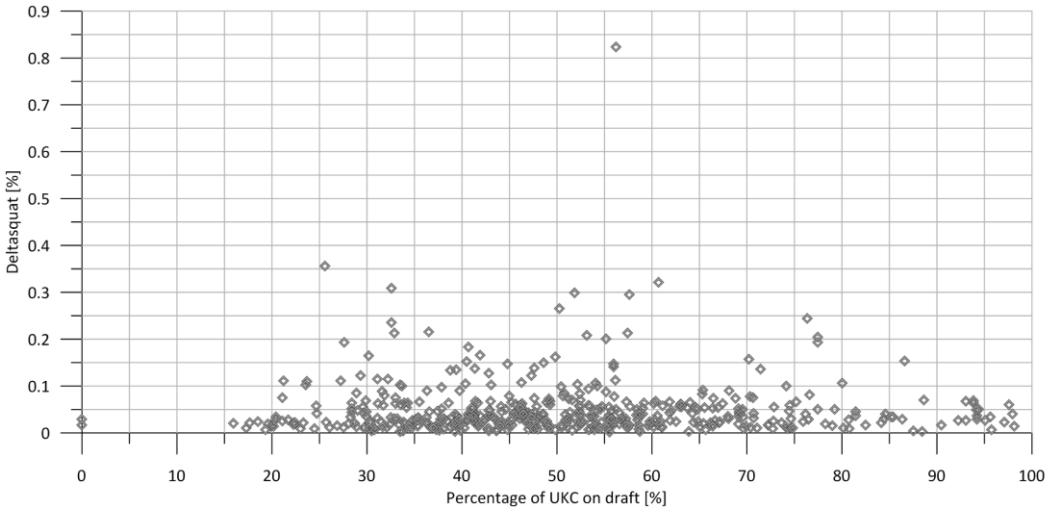

Figure 6.20: Influence of UKC on deltasquat values

According to squat governing factors of section 2.1.1 and theoretical considerations on ship-ship interactions by DAND (1981), it is assumed, that additional specific factors determine the deltasquat value during encountering situations. Such factors are:

- Total accumulated speed of both vessels during the encountering situation,
- distance between the vessels' hulls,
- accumulated underwater cross-sections and
- blockage factor as a ratio of accumulated vessels' cross-sections to river cross-section.

Figure 6.21 and Figure 6.22 display the influences of such factors on deltasquat. In general, the results lead to the interpretation that deltasquat increases when total speed, accumulated underwater as well as encounter blockage factor increase and when ship-ship distance decreases. A strong correlation between each single factor and the final deltasquat value is not observed. Nevertheless, each factor has a certain influence on deltasquat and the combination of all factors determine final deltasquat.

Figure 6.21 and Figure 6.22 show, that significant deltasquat > 0.1 m values occurs, when total speed exceeds 12 kts, shoulder to shoulder distance is less than 260 m, total underwater cross-section exceeds 600 m² and encounter blockage factor is higher than 0.065.

The combination of all influences is shown in Figure 6.23. The figure shows, how the thresholds of each single factor form circumstances, which lead to significant and critical deltasquat values. Displayed are all encountering situations, that lead to deltasquat values > 0.1 m. The radar plot displays the interaction between LOA of the design and the encountering vessel, the total cross-section and the blockage factor as well as total speed and ship-to-ship distance.

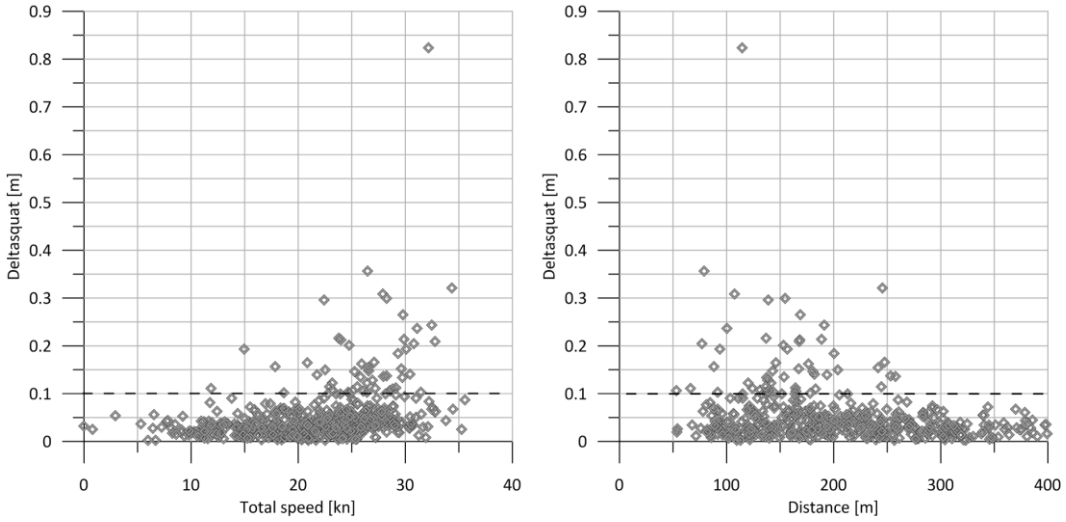

Figure 6.21: Influence of total speed and ship to ship distance on deltasquat

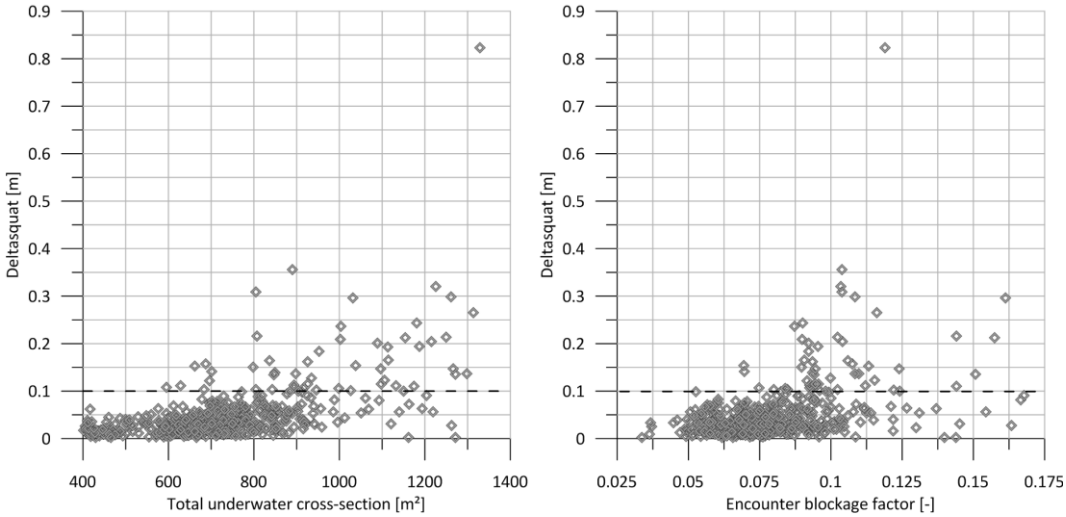

Figure 6.22: Effects of total underwater cross-section and encounter blockage factor on deltasquat

The green polygon contains the area, where all significant factors are below critical thresholds. If no threshold is exceeded, all deltasquat values are below 0.1 m. That green polygon marks the area of not significant ship-ship interactions. If a pre-assessment of an encountering situation lead to the evaluation, that non of the thresholds will be exceeded, there is no need to consider the interaction within the dynamic draft determination.

Oppositely, the figure illustrates, that in case of the maximum deltasquat value of 0.82 m (marked in red) all thresholds are exceeded. Three of four factors, e.g. total speed, underwater cross-section and distance, are even at the outmost limits. Such extreme combination leads to such extreme deltasquat. The figure encourages, to pre-assess encountering situations on the Lower Elbe. If the pre-assessments evaluates a ship-ship interaction to exceed certain thresholds by far, the expected deltasquat value needs either to be considered for dynamic draft determination or the interaction need to be regulated by the designated authorities. E.g. if an interaction with low distance and high vessel speeds of two large size vessels at a narrow waterway positon is assumed, the interaction should be avoided. If the interaction is unavoidable, regulation should be issued to reduce vessels' speeds as much as possible.

The figure illustrates further, that there are e.g. ship-ship interactions (marked in blue), where distance, cross-section and blockage factor are at the outmost limits, but due to the very little total speed, deltasquat is still in the significant range, but not of critical height. In such cases, the pre-assessed deltasquat value needs to be considered for dynamic draft determination.

The comparison between the red and the blue example demonstrates, that also for ship-ship interaction, total speed is the key critical factor for the additional squat.

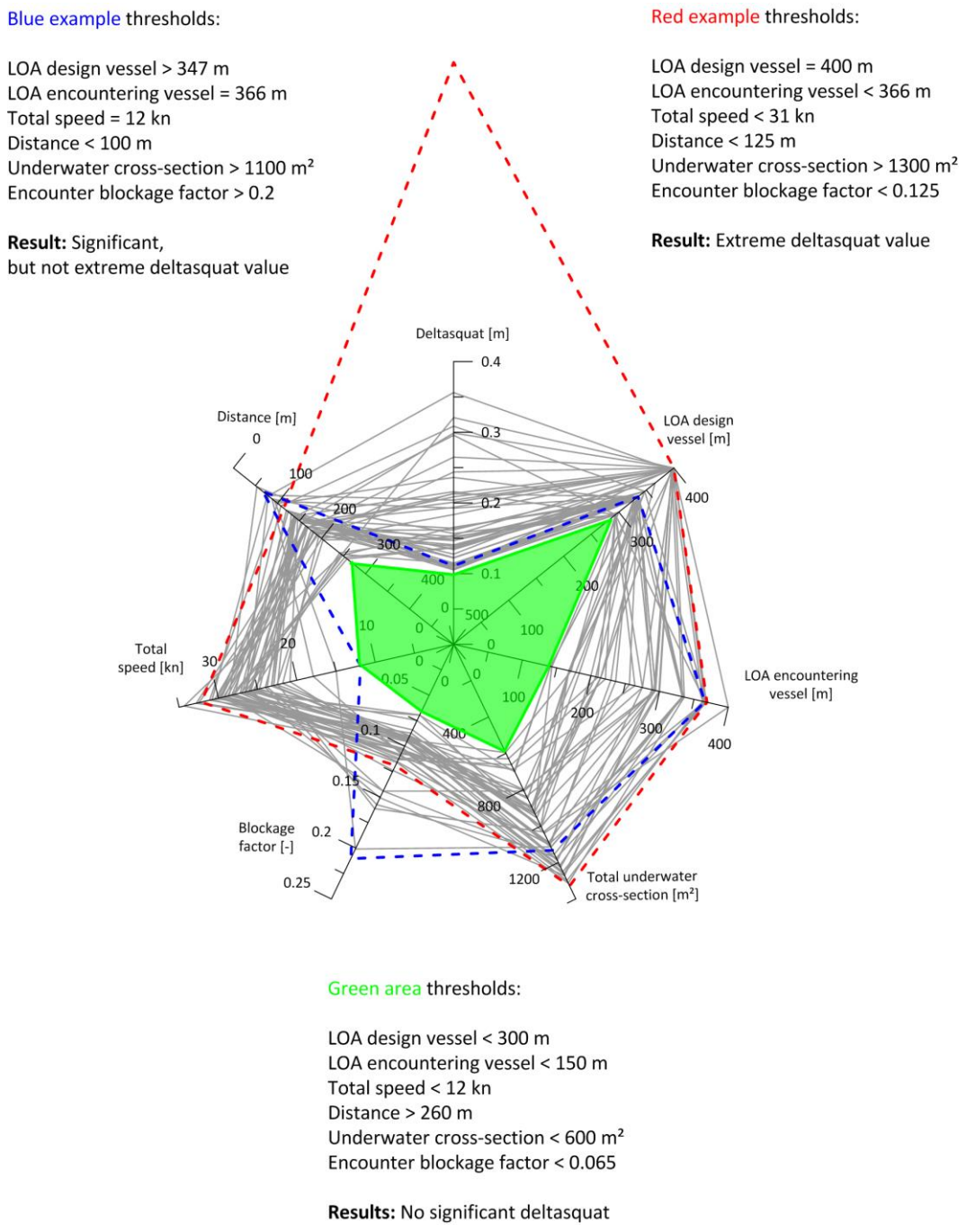

Figure 6.23: Factor thresholds at critical deltasquat

7 Conclusion and recommendations based on the results

Vessels in confined waters discover draft-increasing effects like squat. This dissertation at hand demonstrates, that latest vessel generations with capacities of 20000 TEU and lengths of 400 m experience immensely higher maximum squat values than former generations of smaller vessel size and less capacity. Measured net squat values at C400 vessels of up to 1.6-1.8 m as well as position of occurrence at AP position have been completely unknown net squat dimensions and characteristics so far. Such results confirm the obligation to analyze the dynamic draft behaviour of extraordinary large vessels in confined waters fundamentally based on measurements within the nature. Moreover, to assess, if commonly used dynamic draft determination approaches and channel design methods are still applicable for latest vessel generations.

This work presents the wide variety of net squat estimations approaches and discovers, that commonly used approaches like ICORELS and BARRAS found upon hydrodynamic theory and empirical findings in model basin tests (PIANC, 1997). There have been only a few investigations of net squat measurements in the field to verify and validate such theoretical and empirical approaches. Furthermore, the latest squat measurements on the Lower Elbe waterway have been performed in 2003 (MAUSHAKE & JOSWIG, 2004). Despite significant results, even such investigations on 7500 TEU vessels have lost their meaning with respect to vessel sizes of frequently travelling vessel on the Lower Elbe nowadays with capacities up to 20000 TEU and unit lengths of 366, 396 and even 400 m.

The generally recognized codes of practice for channel design use abovementioned net squat approaches to determine dynamic draft for channel design (PIANC, 2014). The same code of practice is still in use for dynamic draft determination and channel design at the Lower Elbe waterway. That circumstance led to the necessity of measurements in the field to gather net squat data of actual vessel sizes and to analyze and assess dynamic draft determination methods for the Lower Elbe.

The dissertation at hand performed extensive field investigations on the Lower Elbe waterway between 2013 and 2016. 21 measuring campaigns have been performed successfully on 1 bulk and 6 container vessel classes with lengths ranging from 294 m, 335 m, 345 m and 366 m up to lengths of 396 m and 400 m. On such vessels, all dynamic draft parameters have been monitored. The raw data was gathered by the broad use of GNSS receivers, cameras, radar gauges as well as the application of a Data Velocity Log and a CTD-probe. Measured data was complemented with data from Voyage Data Recorders and draft meter readings.

The work discussed the measurement set up of the measuring devices, presented preparatory measures as well as a performance description of the campaigns. Furthermore, the dissertation explained the process of complex data handling and GPPS post processing procedures to determine each single parameter that is necessary to calculate net squat.

The final results show a considerable increase of maximum net squat at AP position with increasing vessel size, ranging from 0.70 m at C294 vessels over 1.25 m at C366 vessels up to 1.8 m at C400 vessels. Generally, the maximum squat occurs at AP position, which is contrarily to most theoretical approaches that determine squat at bow as the significant value. The results confirm that initial trim has a crucial influence on the final position of maximum net squat occurrence. In contrast to the assumption for dynamic draft determination, that vessels generally travel on even keel, the data from the field investigations shows, that most of the vessels actually travel with initial static trim.

Squat results show the very strong correlation of net squat values with vessel speed through water, which reassures speed as the main driving factor for ship squat. The dissertation performed a comparison of four generally accepted net squat determination approaches. ICORELS with pre-factors 2.0 and 2.4 is compared to the approaches of BARRAS III and SCHMIECHEN.

The comparison discovers, that for vessel sizes up to 347 m all approaches determine safe net squat values. For such vessel classes, the speed through water is the overall significant component for squat determination. Nevertheless, all approaches overestimate net squat for such vessel classes. Though that leads to net squat values with internal safety margin, the results are not acceptable in terms of economical draft maximization. For vessels with lengths of 366 and 399 m, the safety margins within the determinations decrease and ICORELS with a pre factor of 2.0 determines accurate net squat values. For vessel classes of 400 m the applicability of ICORELS with a pre factor of 2.4 and of BARRAS III progresses.

Next to speed as the main driving component, also the ratio between underwater cross-section of the vessel and wetted cross-section of the waterway becomes a significant component. Therefore, the dissertation recommends to use BARRAS III approach for dynamic draft and channel design determination for the latest vessel generations. It should be noticed, that for such vessel dimensions, the determination approaches do not provide systemic safety margins anymore. Furthermore, the results show, that with tendency towards further increasing vessel capacities beyond 20000 TEU, the influence of the cross-section ratio between vessel and waterway on net squat values should become a focal point of further investigations.

The dissertation determines further draft increasing influences like the influence of density on dynamic draft and static trim. The determination shows a general increase of draft of 0.25 m for container vessels and a slightly higher increase for Bulkers along the Lower Elbe. Such results confirm the necessity to consider density for dynamic draft determination as well as for channel design.

The results show, that a change of density evokes a change of static trim during the Lower Elbe passage. Inbound vessels discover an increase of trim towards bow and outbound vessels discover an increase of trim towards stern. Generally, the relative trim changing values can be applied with 0.05 m for dynamic draft determination but are not of significance for channel design.

Off-centric draft due to heel or rolling motions around the longitudinal axis of a vessel increases dynamic draft. Generally accepted codes of practice determine such off-centric draft in a very pragmatic way and assume a rectangular underwater ship’s body and a ship on even keel. Such assumptions are acceptable for vessels with maximum widths of around 30 m and less. But for actual vessels with beams up to 60 m and keel radii of around 5 m, that assumptions lead to unjustifiable overestimations of off-centric draft.

Furthermore, the position of maximum off-centric draft is generally assumed to be at MP position. However, latest vessel generations do not have a point of widest beam anymore, they rather have an area of maximum beam around MP position. E.g. for a C396 vessel, such area has a reach of almost 100 m around MP between FP and AP.

In addition, hogging effects have never been considered in the determination of off-centric draft, because of the assumption of an even keel. Therefore, the dissertation developed a new concept to determine off-centric draft increase due to roll. That concept finally considers the diminishing effects of the keel radius, determines the position of off-centric draft occurrence and considers initial trim

and initial hogging. The concept is based on mandatory draft meter readings at FP, MP and AP position, which are recommended to become standard basis of administrative draft regulation.

In addition to that, the dissertation examined ship-to-ship interactions during the Lower Elbe passage, based on a comprehensive analysis of AIS data. The results show, that 90 of all interaction do not have any significant influence on dynamic draft. However, the final 10% show a very critical influence on net squat of the interacting vessels with additional deltasquat values mainly between 0.1 and 0.4 m. Therefore, the dissertation determined threshold values, which, if exceeded, lead to such significant deltasquat values.

The results show that deltasquat is of negligible influence as long ship-ship distance is > 260 m, total speed < 12 kn, underwater cross-section < 600 m² and blockage factor > 0.065. If one threshold is assumed to be exceeded significantly, the consideration of ship-ship interactions becomes necessary for channel design. The results of this dissertation permit the consideration of additional dynamic draft due to ship-to-ship interactions within dynamic draft determination.

In general, there are existing systemic safety margins within the net squat determination procedure, which are still not used for draft maximization. Firstly, there are abovementioned systemic safety margins at net squat determination for vessel classes up to C347. Secondly, there are safety margins within the off-centric draft determination due to the assumption of a rectangular underwater cross-section by neglecting the keel radius. Furthermore, hogging has been neglected completely so far. Finally, the assumption of an even keel provides systemic safety margins within off-centric draft determination.

Conclusively, this dissertation provides an extensive database, which was established by the combined application of advanced and state of the art data acquisition methods. The examination of the database enriches the knowledge about the dynamic draft behaviour profoundly and enables the performance of a foresight assessment of expected dynamic draft values of extraordinary large vessels on the Lower Elbe waterway.

The work provides a procedure to pre-determine initial trim and hogging based on draft meter readings. With these values, off-centric draft due to dynamic roll can now be estimated in advance. Another procedure to determine the allocation and the characteristics of off-centric draft is presented.

Influences of density can now be considered more accurately and net squat values can be determined by the application of the BARRAS III approach more precisely. This dissertation even facilitates the pre-assessment and regulation of additional squat due to ship-to-ship interactions at encountering and overtaking maneuvers.

The extensive analysis of the measured data leads to an advanced understanding of hydrostatic and hydrodynamic draft influencing processes. Such knowledge enables the future draft determination and channel design to utilize formerly unknown safety margins within several determination steps.

Thus the dissertation optimizes the draft determination procedure economically in terms optimized draft utilization as well as in terms of increased safety for ships and life by an optimized draft determination design.

Finally, this section provides, based on the results of this dissertation, 10 recommendations for administrative dynamic draft determination and regulation of extraordinary large vessels on the Lower Elbe waterway.

Recommendation on draft increase as well as on change of trim due to change of density:

1. With respect to section 3.2, as channel design factor for draft increase due to density, ΔT_D, a value of max. 0.25 m should be added on seawater draft for inbound container vessels. For bulk carriers, the value should be max. 0.28 m.
2. The design should respect the spatial dependence of the influence of density. Between Elbe-km 750-730, seawater draft of inbound vessels increases by 0.05 m, between Elbe-km 711-730 it increases by 0.10 m, between Elbe-km 690-710 by 0.20 m and the final value of 0.25 m can be applied onto seawater draft at Elbe-km < 690. For outbound vessels, the freshwater draft decreases by the same values within the abovementioned sections.
3. Influence of density on change of draft due to change of trim was unknown so far with respect to channel design. Nevertheless, the results show, that there is indeed a measurable but not significant influence on FP and AP. For inbound vessels in the area at Elbe-km < 690, a value of 0.05 m should be added to draft at bow. Draft at stern should be decreased by the same value in that reach. For outbound vessels in the reach of Elbe-km > 690, draft at FP should be decreased by 0.05 m and increased at AP by the same value.

Recommendation on the influence of dynamic roll with respect to keel radius, maximum cross-section as well as initial hogging and trim:

4. The analysis of dynamic roll in section 6.3.3 shows the decreasing tendency to roll at the latest vessel generations due to increased ship sizes and beams. Beyond that tendency, channel design should respect the decreasing influence of the keel radius on draft increase due to roll as well. Especially for extraordinary large vessels, draft increase should be determined using the abovementioned newly developed approach in equation 6.2, which includes the influence of keel radius, to calculate the draft increase due to roll.
5. With knowledge of the area of maximum underwater beam at keel level, the determination of draft increase due to roll should no longer be determined amidships only. Furthermore, the complete area of maximum cross-sections should be acknowledged as potential occurrence points of maximum off-centric draft increase due to ship roll in dependence of initial trim and pitching movements. The newly developed concept of MF and MA positions for off-centric draft determination should be integrated in channel design and dynamic draft determination.
6. The assumptions, that vessels always travel on even keel without hogging and that MP is the position of maximum draft due to roll, are not acceptable anymore in the process of channel design. Static trim analysis shows, that most of the vessels experience initial trim as well as initial hogging. Container vessels have a strong tendency to be initially trimed by stern. Furthermore, almost all ships have a strong tendency to show hogging values and especially vessels of class C366 show significant hogging values. In conclusion, the point of maximum draft for channel design is located at MA or MF in dependence of static trim, initial hogging and dynamic roll. The newly developed concept of dynamic draft determination at MF and MA position under the consideration of initial trim and hogging should be integrated in the process of channel design and dynamic draft determination.

Recommendation on ship squat determination:

7. Speed through water is the governing factor to determine ship squat. Second biggest influence comes from water depth as a factor to describe the influence of the channel cross-section itself. The combination of both factors within the TUCK parameter has the strongest correlation to measured net squat values. That leads to the recommendation, that net squat determination approaches should mainly base upon the TUCK parameter. The approaches should then be fitted specifically to the vessel size clusters, for example with different pre-factors. C294 and C335 form one cluster, C347, C366 and C396 form another cluster and finally C400 forms the third cluster.
8. For BULK vessel class, all approaches except SCHMIECHEN are valid to be used for dynamic draft determination. For vessel classes C294, C335 and C347 all squat approaches are qualified for dynamic draft determination. Nevertheless, it should be noticed from the economical perspective that the approaches often overestimate real squat, which means, that there are already systemic safety margins within the use of such approaches.
   With increasing vessel sizes from C366 to C396, the ICORELS approaches are recommended to be used for dynamic draft determination. The ICORELS factor should be 2.0 to generate a safe and economic determination. For the extraordinary large vessels of the C400 class, ICORELS with a pre-factor of 2.4 and alternatively BARRAS III re recommended to be used. With further increasing vessel dimensions, the relative wetted cross-section area between vessel and waterway cross-sections becomes of utmost significance. In that case, BARRAS III approach should be used for dynamic draft and channel design determination. Due to the tendency towards vessel capacities beyond 22000 TEU, the influence of the wetted cross-section area within net-squat determination should become a focal point of further investigations.

Recommendations on ship-ship interactions:

9. The results show that deltasquat is of negligible influence as long ship-ship distance is < 260 m, total speed < 12 kts, underwater cross-section < 600 m² and blockage factor < 0.065. If one threshold is assumed to be exceeded significantly, the consideration of ship-ship interactions becomes necessary for draft determination and channel design.
10. In dependence of the interacting vessel speeds, sizes and drafts as well as the wetted cross-section area at the position of the interaction, the design value for the interaction should meet the range between 0.1 -0.4 m. If an interaction with low distance and high vessel speeds of two large size vessels at a narrow waterway positon is assumed, the interaction should be avoided. If the interaction is unavoidable, the recommendation is to reduce vessels' speeds as much as possible.

8 Need for further research

Influence of wetted cross-section areas within net squat determination

The recommendations of this work state, that the significance of the channel wetted cross-section increases with increasing vessel size. E.g. for C396 and C400, BARRAS III provides the most correct squat estimations. Thus, it is valid to assume, that the direct integration of the wetted cross-section is one reason for such fitting estimations for extraordinary large vessels.

Figure 8.1 displays the main difference between ICORELS and BARRAS III approach. ICORELS sums up ship and channel related factors within the ICORELS factor. Directly channel related factor is only the local water depth. In contrast to that, BARRAS III especially respects the channel depth and channel width within the wetted cross-section area.

To determine the wetted area, channel depth is directly used. But channel width is the assumed by the application of the effective width, which is determined by a multiple of the vessel's beam. The concept of the effective width originates from former model basin tests. With the increasing significance of the wetted cross-section area also the significance of the correct effective width increases to the utmost extend.

Therefore, it is recommended to perform further investigations and model basin test to determine the effective width for actual vessel classes with capacities of 20000 TEU and more.

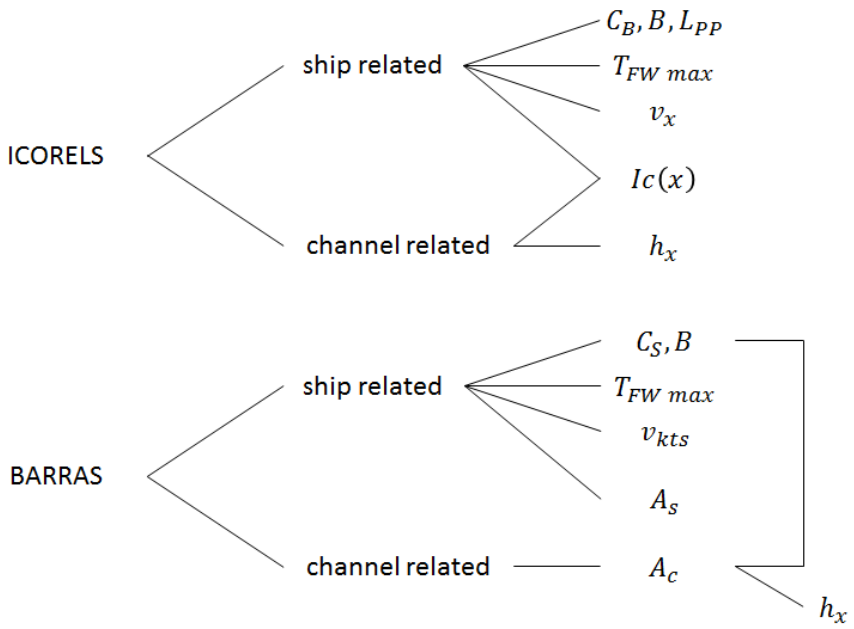

Figure 8.1: Comparison of squat approach components

Nautical bottom approach: Utilization of water depth with increased density

German Federal Waterways and Shipping Administration (WSV) and Hamburg Port Authority (HPA) run soundings on daily basis to determine the vertical horizon of the waterway bottom in the Port of Hamburg and on the Lower Elbe. Both administrations use ship based multibeam echosounders to determine the bottom at each position.

Latest investigations by SCHMEKEL & OHLE identify, that the applied echosounders with a working frequency of 200 kHz define the bottom at that vertical horizon, where the density of detected material exceeds 1050 kg/m³. In contrast to that, a specific sediment echosounder with a working frequency of 24 kHz detects two further horizons, one with a density of 1100 kg/m³ and one with a density of 1200 kg/m³. Between the upper horizon with a density of 1050 kg/m³ and the deeper horizon of 1200 kg/m³ density, there is often a vertical difference of up to 2 m (Figure 8.2).

The question at hand is which horizon fulfills the PIANC criteria for the nautical bottom:

"The nautical depth is the level where physical characteristics of the bottom reach a critical limit beyond which contact with a ship's keel causes either damage or unacceptable effects on controllability and maneuverability." (PIANC, 1997)

Presently, the density threshold, where the physical characteristics exceed acceptable nautical properties, is still unknown. The assumption, that the 1200 kg/m³ horizon is the real nautical bottom, would lead to already existing depth safety margins of up to 2 m.

In consequence, that would lead to another 2 m of usable water depth for dynamic ship draft and UKC. Thus, the "Nautical Bottom Project" by the HPA is of urgent demand to be continued and broadened onto the Lower Elbe waterway.

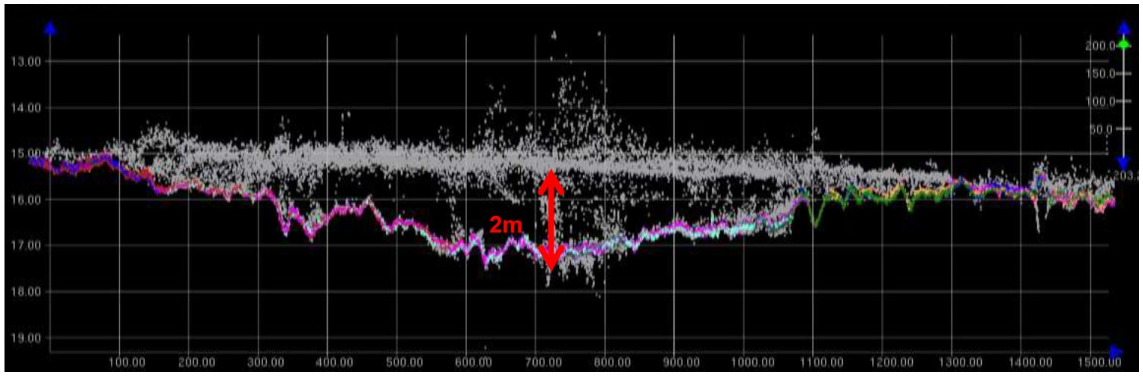

Figure 8.2: Comparison of depth of different density horizons at the Port of Hamburg[11]

Extension of net squat measurements onto other estuaries and port approach channels

This work shows, that measurements in the field facilitate the analysis and the assessment of nearly all hydrostatic and hydrodynamic processes, which determine dynamic draft of extraordinary large ships. The results provide a solid basis to validate and adapt the dynamic draft determination methods. That leads to an increase in safety for ships and life and facilitates to economically optimize present dynamic draft regulations.

Thus, the provided method of squat measurements in the field should be transferred and extended onto other estuaries and port approach channels with extraordinary large vessels. Especially the Weser-River as port approach to Bremerhaven as well as the Ems-River as transfer channel for extraordinary large cruise ships should be focal points of further investigations and real-squat measurements within the nature.

[11] SCHMEKEL, U. & OHLE, N. (2018): Das Projekt „Nautische Tiefe" im Hafen Hamburg; 10. Rostocker Baggergutseminar 12.09.2018; (German) unpublished

References

ANKUDINOV, V., DAGGETT, L., HUVALL, C. & HEWLETT, C., 1996. Squat predictions for manoeuvring applications. In: A. A. Balkeema, ed. *Proceedings MARSIM'96.* Rotterdam: s.n., pp. 467-495.

ANKUDINOV, V. K. & JAKOBSEN, B. K., 1996. Squat Predictions at an Early Stage of Design. *Marine simulation and ship manoeuvrability; proceedings of the International Conference MARSIM'96*.

BARRAS, B. & DERRET, D. R., 2012. *Ship Stability for Masters and Mates.* 7 ed. Oxford: Butterworth-Heinemann.

BARRAS, C. B., 1979. A Unified Approach to Squat Calculations for Ships. *PIANC Bulletin No. 32*, pp. 3-10.

BARRAS, C. B., 1979. Ship Handling Problems in Shallow Water. *Marine Engineers Review*, pp. 17-19.

BARRAS, C. B., 1979. The Phenomena of Ship Squat. *International Shipbuilding Progress*, Band 26, pp. 44-47.

BARRAS, C. B., 1981. Ship Squat - A Reply. *The Naval Architect*, pp. 268-272.

BECK, R. F., NEWMAN, J. N. & TUCK, E. O., 1975. Hydrodynamic forces on ships in dredged channels. *Journal of Ship Research*, Volume 19, pp. 166-171.

BRIGGS, M. J., 2006. *Ship Squat Prediction for Ship/Tow Simulators,* Vicksburg: US Army Corps of Engineers.

BRIGGS, M. J., KOPP, P. J., ANKUDINOV, V. K. & SILVER, A. L., 2013. Comparison of Measured Ship Squat with Numerical and Empirical Methods. *Journal of Ship Research*, Volume 57, pp. 73-85.

CHEN-TUNG, C. & MILLERO, F. J., 1977. Speed of Sound in Seawater at High Pressures. *The Journal of the Acoustical Society of America*, 62(1129).

DAND, I. W., 1981. *Some measurements of interaction between ship models passing on parallel courses.* Feltham, Middlesex : National Maritime Institution.

ELOOT, K. et al., 2011. Squat during ship-to-ship interactions in shallow water. In: R. I. o. N. Architects, Hrsg. *2nd International conference on ship manoeuvring in shallow and confined water : ship to ship interaction.* London: s.n., pp. 117-126.

GOURLAY, T. P., 2010. A brief history of mathematical ship-Squatprediction focussing on the contributions of E.O. Tuck. *Journal of Engineering Mathematics*, Volume 70, pp. 5-16.

GOURLAY, T. P. & TUCK, E. O., 2001. The Maximum Sinkage of a Ship. *Journal of Ship Research*, March, Issue 1, p. 50–58.

GULIEV, U. M., 1971. On Squat Calculations for Vessels Going in Shallow Water and Through Channels. *PIANC Bulletin No. 7*, pp. 17-20.

HOOFT, J. P., 1974. The Behaviour of a Ship in Head Waves at Restricted Water Depth. *International Shipbuilding Progress*, Volume 21, pp. 367-390.

HUUSKA, O., 1976. *On the Evaluation of Underkeel Clearances in Finnish Waterways,* Otaniemi: Helsinki University of Technology.

ICORELS, 1980. Report of Working Group IV. *PIANC Bulletin No. 35, Supplement*.

JACHOWSKI, J., 2008. Assessment of ship squat in shallow water using CFD. *Archives of Civil and Mechanical Engineering*, Volume 8, pp. 27-36.

KOESTERS, F., ULICZKA, K., BÖTTNER, U. & KASTENS, M., 2017. Interaction of Ships and Waterways in Coastal Areas - A Review of Scientific Methods. *BAW Mitteilungen*, Volume 100, p. 147169.

MAUSHAKE, C. & JOSWIG, S., 2004. Messung von Squat, Trimm und Krängung sehr großer Containerschiffe im Rahmen von Grundsatzuntersuchungen auf der Elbe. *Hydrographische Nachrichten*, Band 72.

MICHELL, J. H., 1898. The wave resistance of a ship. *Philisophical Magazine*, pp. 106-123.

MILLERO, F. J. & POISSON, A., 1981. International One-Atmosphere Equation of State of Seawater. *Deep Sea Research Part A, Oceanographic Research Papers*, pp. 625-629.

MILLWARD, A., 1990. A Preliminary Design Method for the Prediction of Squat in Shallow Water. *Marine Technology*, 27(1), pp. 10-19.

MILLWARD, A., 1992. A Comparison of the Theoretical and Empirical Predistion od Squat in Shallow Water. *International Shipbuilding Progress*, Volume 39, pp. 69-78.

MILLWARD, A., 1996. A review of the prediction of squat in shallow water. *The journal of navigation*, 49(1), pp. 77-88.

MOCTAR, O. e., SHIGUNOV, V. & ZORN, T., 2012. Duisburg Test Case: Post-Panamax Container Ship for Benchmarking. *Ship Technology Research*, Band 50, pp. 50-64.

PIANC, 1997. *Approach Channel: A Guide for Design,* Brussels: PIANC Secrétariat Général.

PIANC, 2014. *Harbour Approach Channels Design Guidelines,* Brussels: PIANC Secrétariat Général.

RÖMISCH, K., 1989. Empfehlungen zur Bemessung von Hafeneinfahrten. *Wasserbauliche Mitteilungen der Universität Dresden*, Band 1, pp. 39-63.

SCHMIECHEN, M., 1997. *Squat-formulae.* Duisburg, s.n.

TERZIEV, M. et al., 2018. Numerical investigation of the behaviour and performance of ships advancing through restricted shallow waters. *Journal of Fluids and Structures*, Band 76, p. 185–215.

TUCK, E. O., 1966. Shallow water flows past slender bodies. In: *Fluid Mechanics.* s.l.:s.n., pp. 81-95.

TUCK, E. O. & TAYLOR, P. J., 1970. *Shallow water problems in ship hydrodynamics.* Washington DC, Office of Naval Research, pp. 627-659.

TUPPER, E. C., 2013. *Introduction to Naval Architecture.* 5 ed. Oxford: Elsevier Butterworth-Heinemann.

ULICZKA, K., 2009. Seeschiffe auf Seeschifffahrtsstraßen am Beipsiel der Unter- und Außenelbe. In: C. OHLIG, Hrsg. *Hamburg - die Elbe und das Wasser sowie weitere wasserhistorische Beiträge.* Siegburg: Deutsche wasserhistorsche Gesellschaft, pp. 97-112.

ULICZKA, K. & KONDZIELLA, B., 2006. Dynamic Response of very large Container Ships in extremly Shallow Water. *Proceedings, 31st PIANC congress*, pp. 1-11.

WEHAUSEN, J. V. & LAITONE, E. V., 1960. *Surface waves. Handbuch der Physik.* 9 ed. Berlin: Springer.

WORTLEY, S., 2013. *CFD Analysis of Container Ship Sinkage, Trim and Resistance,* Bentley: Professor Tilak Chandratilleke, Curtin University, Department of Mechanical Engineering.

ZHOU, M.-g., ZOU, Z. & YAO, J.-x., 2013. Prediction of ship squat in restricetd waters. *Journal of Ship Mechanics*, 06, 17(6).

Additional sources

Student theses

Under the supervision of the author, student research assistants have performed student theses to support the measurement campaigns and the data analysis. The student theses are in German language. They are not published but available on-demand at the Institute of River and Coastal Engineering at the Hamburg University of Technology.

BARTHEL, B. F., 2014: Analyse des Einflusses ausgewählter Parameter auf den Schiffsquat am Beispiel der C335-Klasse auf Unter- und Außenelbe, Master Thesis (in German, not published)

BOCKELMANN, A., 2015: Anwendbarkeit der multiplen Regression zur Analyse gewässerspezifischer Parameter auf die dynamische Tiefertauchung von Fahrzeugen der C335 Klasse, Master Thesis (in German, not published)

KOCH, A., 2016: Entwurf eines Verfahrens zur Berechnung der Tiefgangsänderung von Großcontainerschiffen auf der Schifffahrtsstraße Elbe, Master Thesis (in German, not published)

HARTMUT, G., 2017: Analyse und Bewertung international gebräuchlicher Berechnungsansätze für die dynamische Tiefertauchung von Containerschiffen auf der Unter- und Außenelbe, Student Research Thesis (in German, not published)

SCHWEBE, M. F., 2014: Analyse des Einflusses von Schiffsbegegnungen auf den Schiffsquat am Beispiel der C335 Klasse auf Unter- und Außenelbe, Bachelor Thesis (German, not published)

STRUBE, S., 2015: Analyse des Krängungseinflusses auf den Tiefgang von Großcontainerschiffen auf Unter- und Außenelbe, Bachelor Thesis (in German, not published)

Appendix

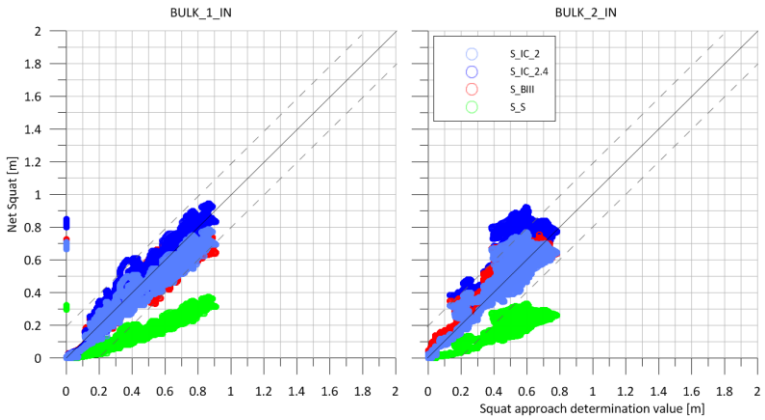

Figure 8.3: Net squat and squat estimation comparison for BULK

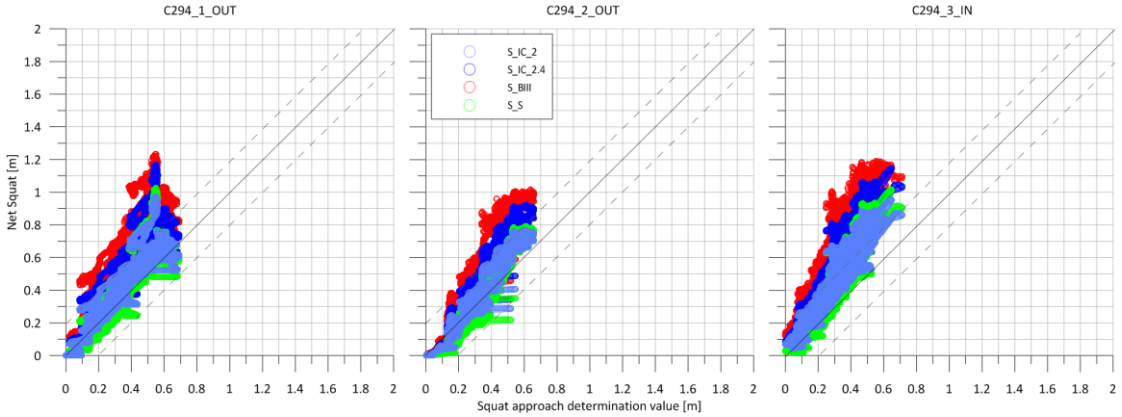

Figure 8.4: Net squat and squat estimation comparison for all C294

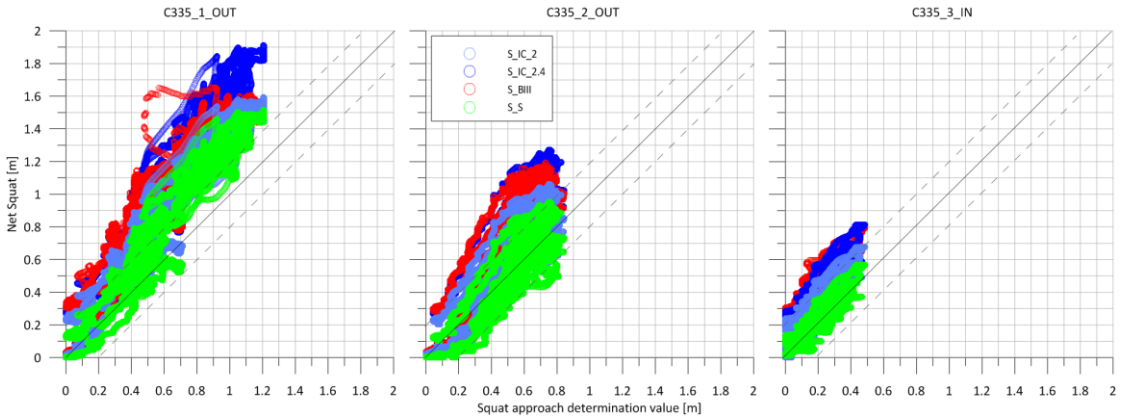

Figure 8.5: Net squat and squat estimation comparison for all C335

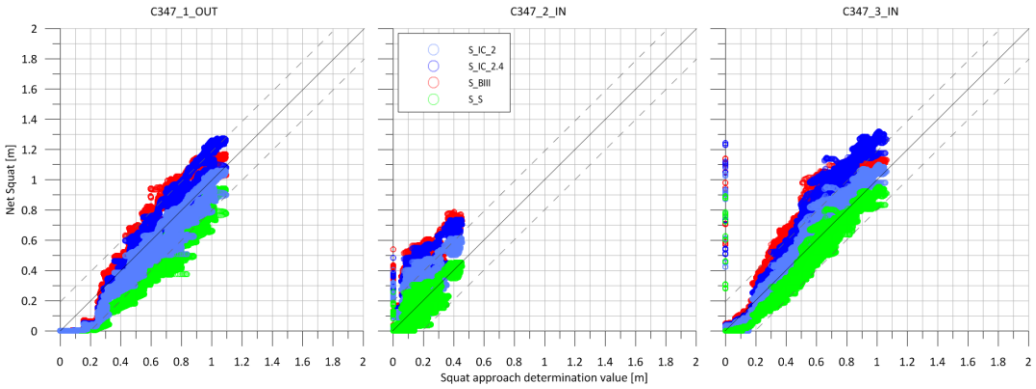

Figure 8.6: Net squat and squat estimation comparison for C347

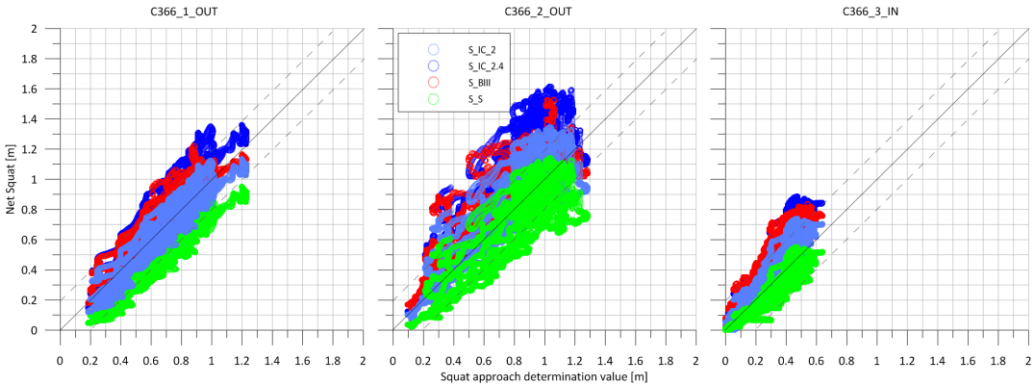

Figure 8.7: Net squat and squat estimation comparison for C366

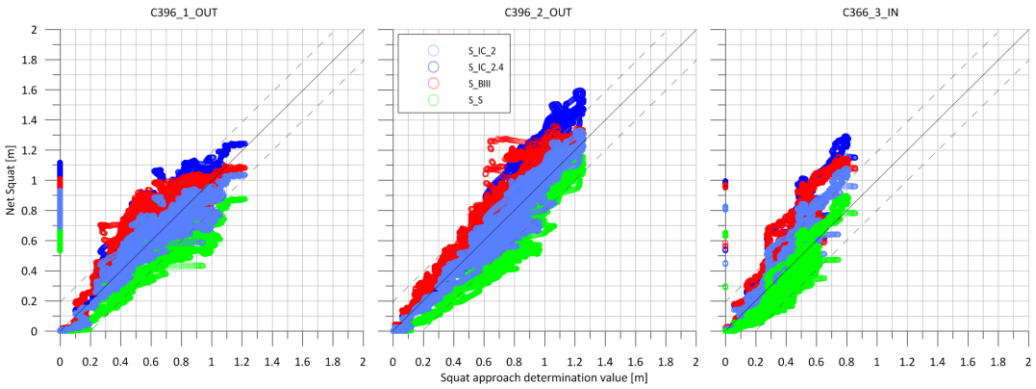

Figure 8.8: Net squat and squat estimation comparison for C396

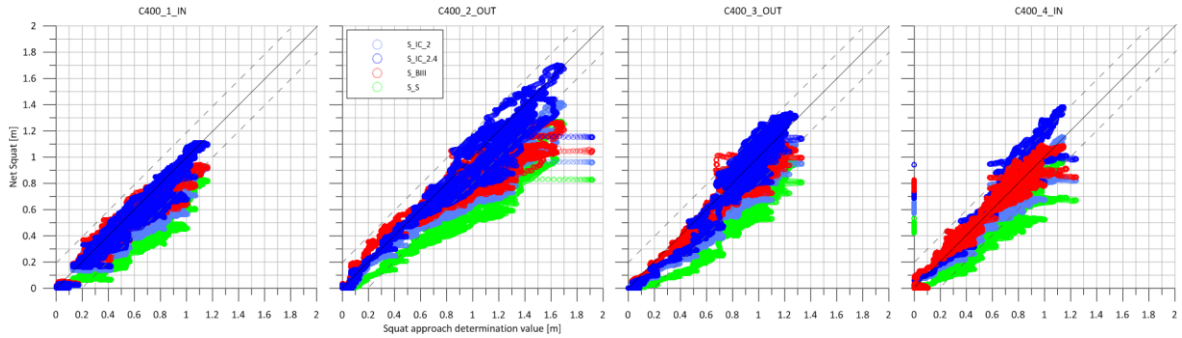

Figure 8.9: Net squat and squat estimation comparison for C400

List of Figures

List of Tables

List of Formulae

List of Factors

Parameter / Factor	Unit	Description
A_C	m^2	*Channel cross-section area*
A_s	m^2	*Underwater cross-section area of the ship*
A_{WP}	m^2	*Water-plane area*
B	m	*Beam of the vessel*
C_B	$-$	*Block coefficient*
C_F	$-$	*Form factor*
C_S	$-$	*Sinkage factor*
C_V	$-$	*Velocity factor*
C_{WP}	$-$	*Water plane coefficient*
C_θ	$-$	*Dynamic trim coefficient*
F_B	N	*Force of buoyancy*
F_G	N	*Gravitational force*
F_{nh}	$-$	*Depth Froude number*
g	m/s^2	*Gravitational acceleration*
h	m	*Channel depth*
h_T	m	*Trench height*
K_P^S	$-$	*Coefficient for propeller effects*
K_S	$-$	*Blockage correction factor*
$K_{\Delta T}$	$-$	*RÖMISCH factor*
L_{PP}	m	*Length between perpendiculars*
n	$-$	*Bank slope run factor*
PAR_CH	$-$	*Coefficient for effects of channel geometry*
PAR_F_{nh}	$-$	*Coefficient for effects of depth Froude number*
PAR_Hulls	$-$	*Coefficient for hull effects*
PAR_H/T	$-$	*Coefficient for depth-draft ratio effects*
R_{hT}	$-$	*Depth to draft ratio*
R_{Lh}	$-$	*Length to depth ratio*
R_{Th}	$-$	*Trench height to depth ratio*
S	m	*Hydrostatic sinkage, Squat*
S_2	$-$	*Blockage factor*
S_b	m	*Bow squat*
S_BIII	m	BARRAS III squat approach

S_{GROSS}	m	*Gross squat*
S_IC_2	m	ICORELS squat approach with pre-factor 2.0
S_IC_2.4	m	ICORELS squat approach with pre-factor of 2.4
S_S	m	SCHMIECHEN squat approach marked in green
S_{max}	m	*Maximum squat*
S_{NET}	m	*Net squat*
T	m	*Draft*
T_R	m	*Draft under consideration of keel radius*
V_C	m/s	*Wave propagation velocity*
V_{Cr}	$kts\ v.\ m\ /\ s$	*Critical vessel speed*
V_S	$kts\ v. m/s$	*Vessel speed*
W	m	*Channel width*
W_{eff}	m	*Effective width*
Δh_S	m	*Uncertainty in bottom soundings*
ΔT_D	m	*Draft increase due to density*
ΔT_M	m	*Uncertainty in draft meter reading*
ΔT_R	m	*Draft increase due to roll*
ΔT_S	m	*Draft increase due to squat*
ΔT_W	m	*Vertical motion due to waves*
ΔW_{MLT}	m	*Allowance of unfavorable deviations from low water*
ΔW_U	m	*Uncertainty in water level forecast*
ρ_{FW}	kg/m^3	*Freshwater density*
ρ_{SW}	kg/m^3	*Seawater density*
Φ	$-$	*Small disturbance velocity potential*
φ	$^\circ$	*Heel angle*
∇	m^3	*Deplacement, Displacement*

List of Abbreviations

ADCP	*Acoustic Doppler Current Profiler*
AIS	*Automatic Identification System*
AP	*Aft Perpendicular*
ASCII	*American Standard Code for Information Interchange*
BAW	*German Federal Waterway Engineering and Research Institute*
BNT	*Numerical squat prediction program by BECK, NEWMAN & TUCK*
CADET	*Channel Analysis and Design Evaluation Tool*
CFD	*Computational Fluid Dynamics*
CTA	*Container Terminal Altenwerder*
CTD	*Conductivity, Temperature & Depth Probe*
DCU	*Data Collection Unit of VDR*
DRU	*Data Recording Unit of VDR*
DTC	*Duisburg Test Case*
DTM	*Digital Terrain Model*
ECDIS	*Electronic Chart Display and Information System*
ETRS89	*European Terrestrial Reference System with GRS89 ellipsoid*
FWD	*Freshwater Draft*
FP	*Fore Perpendicular*
GA	*General Arrangement Plan*
GLONASS	*Global'naya Navigatsionnaya Sputnikovaya Sistema*
GNSS	*Global Navigation Satellite System*
GPPS	*Geodetic Post-processing Positioning Service*
GPS	*Global Positioning System*
GUKC	*Gross Under Keel Clearance*
HPA	*Hamburg Port Authority*
IB	*Inbound*
ICORELS	*International Commission on the Reception of Extraordinary Large Ships*
IMO	*International Maritime Organization*
KSC	*KRISO Container Ship*
LCB	*Longitudinal Centre of Buoyancy*
LCF	*Longitudinal Centre of Flotation*
LCG	*Longitudinal Centre of Gravity*

LOA	*Length over All*
LPP	*Length between Perpendiculars*
MCT	*Moment to Change Trim*
NHN	*Normal Height Null*
NMEA	*National Marine Electronics Association*
MP	*Perpendicular Amidships*
NUKC	*Net Under Keel Clearance*
OB	*Outbound*
PDGPS	*Precise Differential Global Positioning System*
PIANC	*World Association for Waterborne Transport Infrastructure*
PN	*Gauging zero*
PM	*Panamax Container Ship Size*
PPM	*Post Panamax Container Ship Size*
PS	*Port Side*
PSU	*Practical Salinity Unit*
RANSE	*Reynolds Averaged Navier-Stokes Equation*
RG	*Radar Gauge*
RLP	*Relative Longitudinal Position*
RINEX	*Receiver Independent Exchange Format*
ROT	*Rate of Turn*
SAPOS	*Satellite Positioning Service of the German National Survey*
SKN	*Seekartennull, Chart Datum*
SOLAS	*International Convention for Safety of Life at Sea*
SOTDMA	*Self-Organizing Time Division Multiple Access*
STB	*Starboard Side*
STW	*Speed through Water*
TEU	*Twenty Foot Equivalent Unit*
TPC	*Tons per Centimeter Immersion*
UKC	*Under Keel Clearance*
ULCV	*Ultra Large Container Vessel*
UNESCO	*United Nations Educational, Scientific and Cultural Organization*
USB	*Universal Serial Bus*
UPS	*Uninterrupted Power Supply Unit*
UTC	*Coordinated Universal Time*
VC	*Video Camera*

VHF	*Very High Frequency Radio*
VDR	*Voyage Data Recorder*
WSA	*German Federal Waterway and Shipping Office*
WSV	*German Federal Waterways and Shipping Administration*

24

WASSERBAU
River and Coastal Engineering

DOI: 10.15480/882.3080

TUHH
Technische Universität Hamburg